

# BIOMECHANIKA KRĘGOSŁUPA



*Folie prof. M. Dietricha*



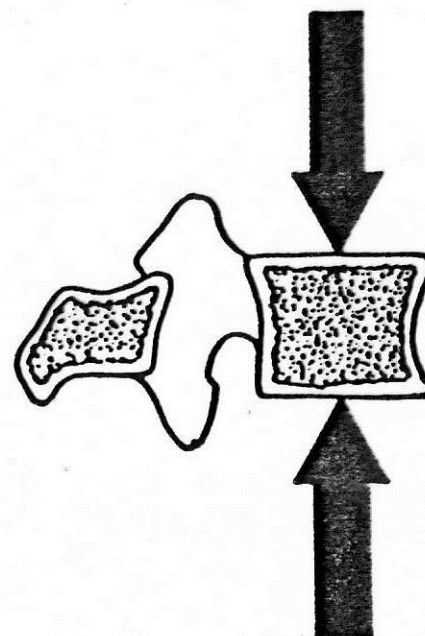
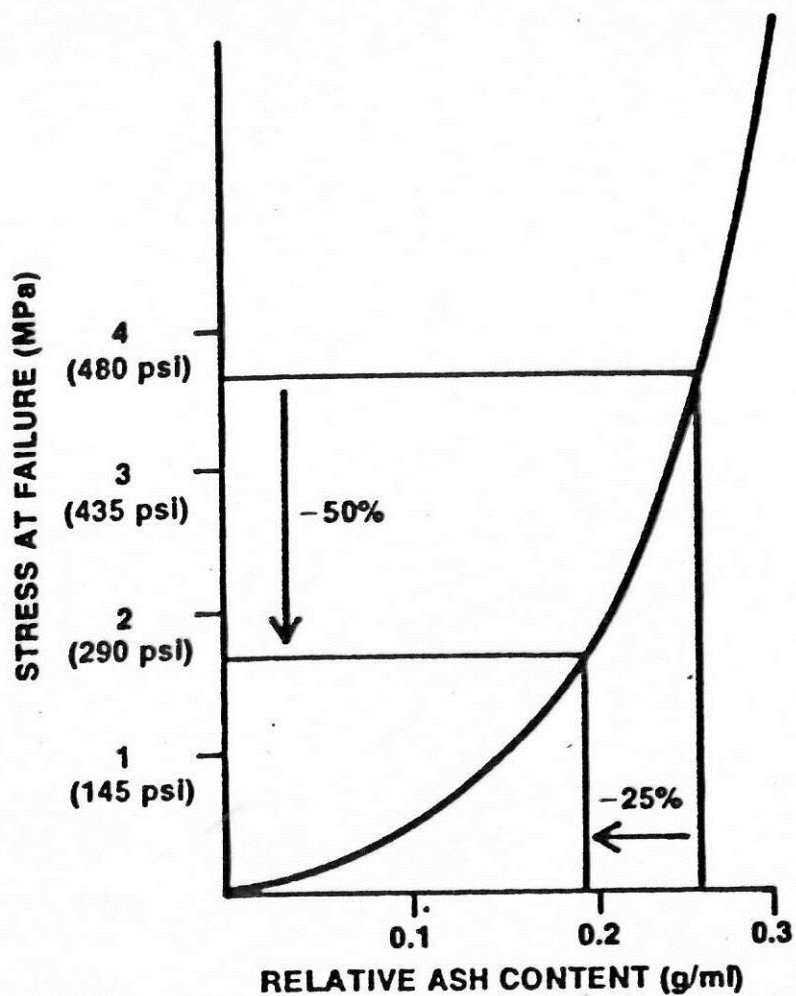


# METHODS OF PREDICTION OF INTERNAL FORCES

- Experimental, i.e. direct *in situ measurements*; invasive and therefore their application should be limited.
- Theoretical, based on mathematical modelling and computer simulation; commonly used.



# Zawartość popiołów





# Własności więzadeł

**Table 1-2. Physical Properties of Spine Ligaments**

<b>Ligamentum Flavum*</b>		
	<b>YOUNG† (<math>&lt; 20</math> years)</b>	<b>OLD† (<math>&gt; 70</math> years)</b>
Resting force	18 N	5 N
Failure stress	10 MPa	2 MPa
Extension at failure	70%	30%
<b>Anterior and Posterior Longitudinal Ligaments†</b>		
	<b>ANTERIOR†</b>	<b>POSTERIOR†</b>
Pretension (non-degenerated)	1.8 N	3.0 N
Pretension (degenerated)	1.2 N	1.8 N
Failure load	340 N	180 N
Failure stress	21 MPa	20 MPa





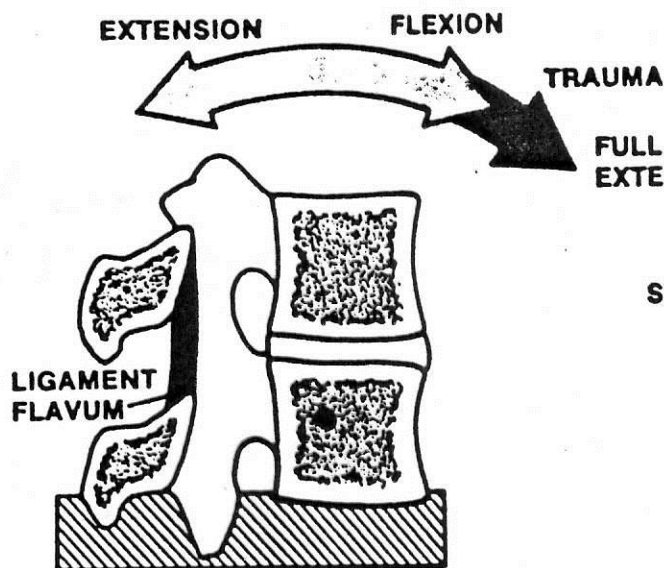
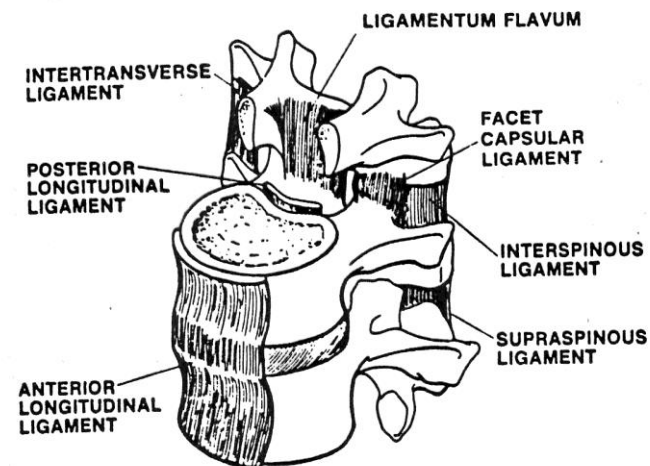
# Własności kości gąbczastej

*Table 1-4. Compressive Strength Properties of Cancellous Bone of Vertebrae*

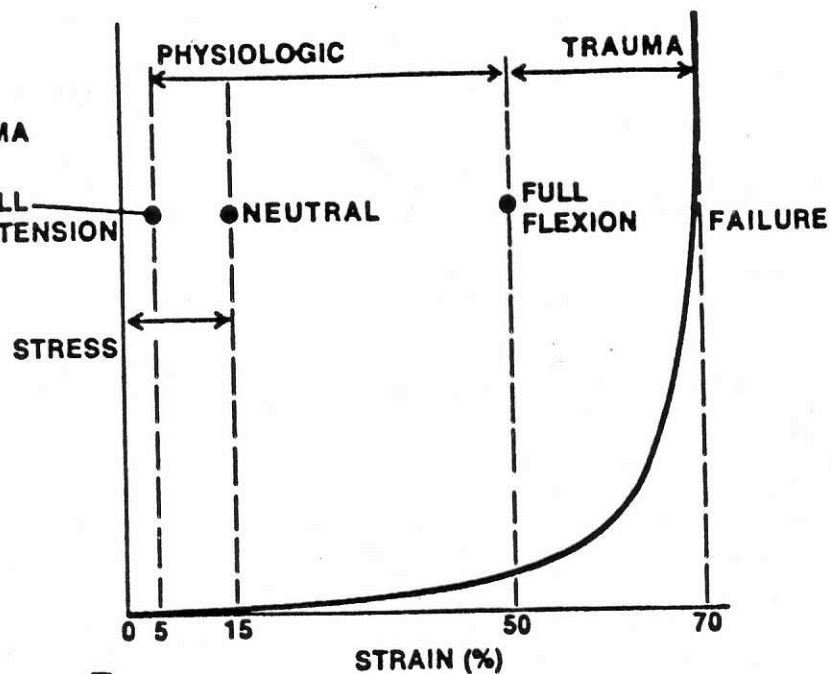
PHYSICAL PROPERTY	MAGNITUDE
Proportional-limit stress†	4.0 MPa
Compression at proportional limit	6.7%
Modulus of elasticity	55.6 MPa
Failure stress	4.6 MPa
Compression at failure	9.5%



# Wiązadła żółte



A



B



# Model Chaffina

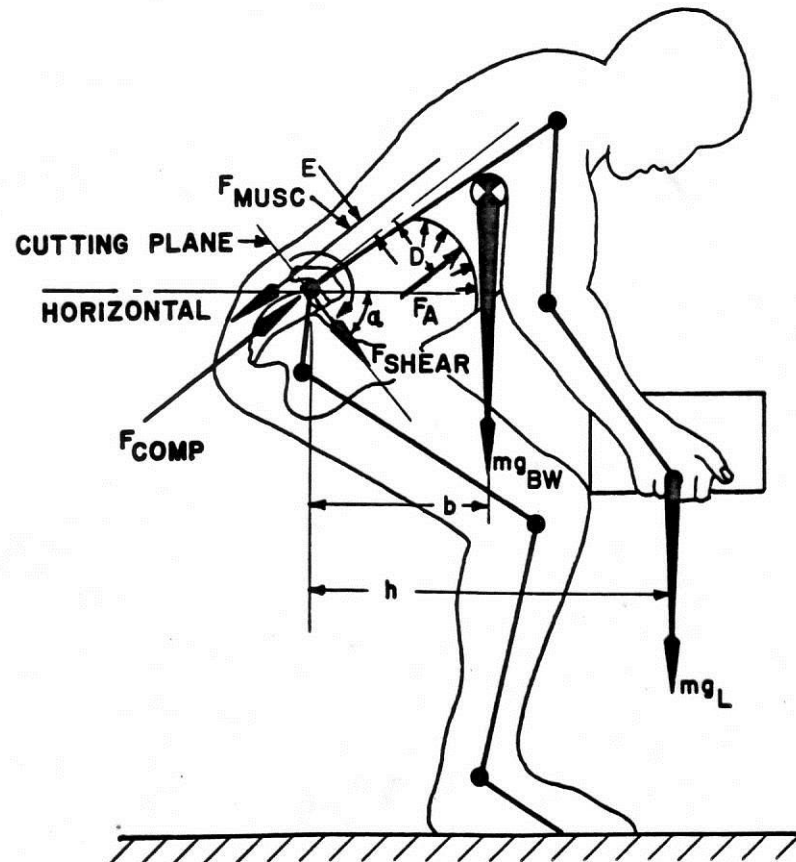


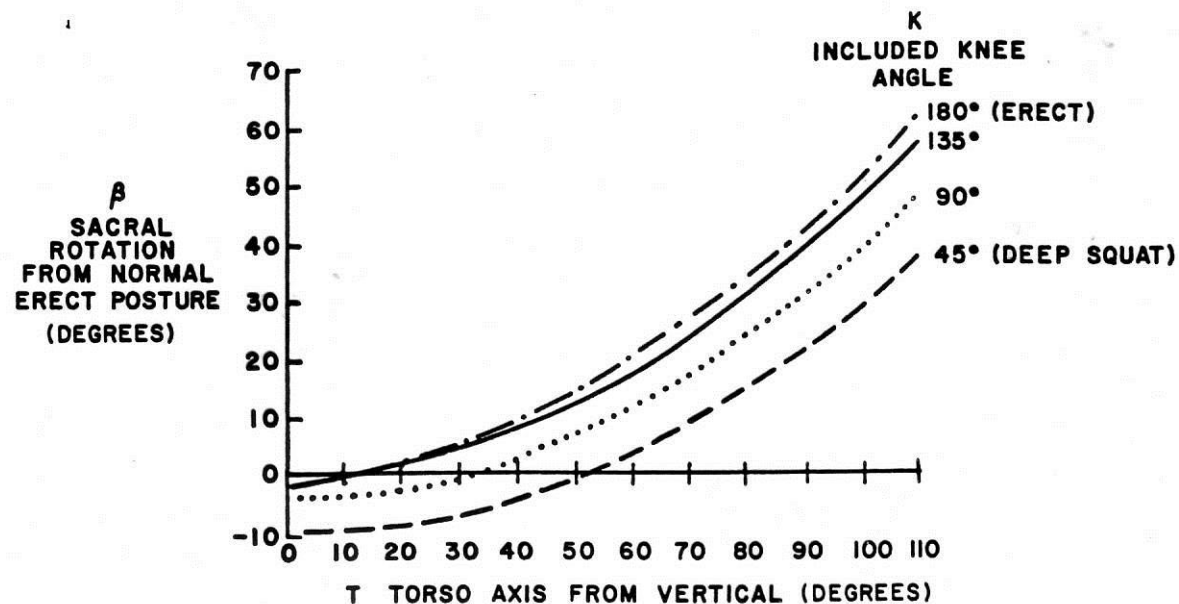
**Figure 6.24** Simple cantilever low-back model of lifting as adapted by Chaffin (1975) for static coplanar lifting analyses.



# Kąt pochylenia miednicy

218

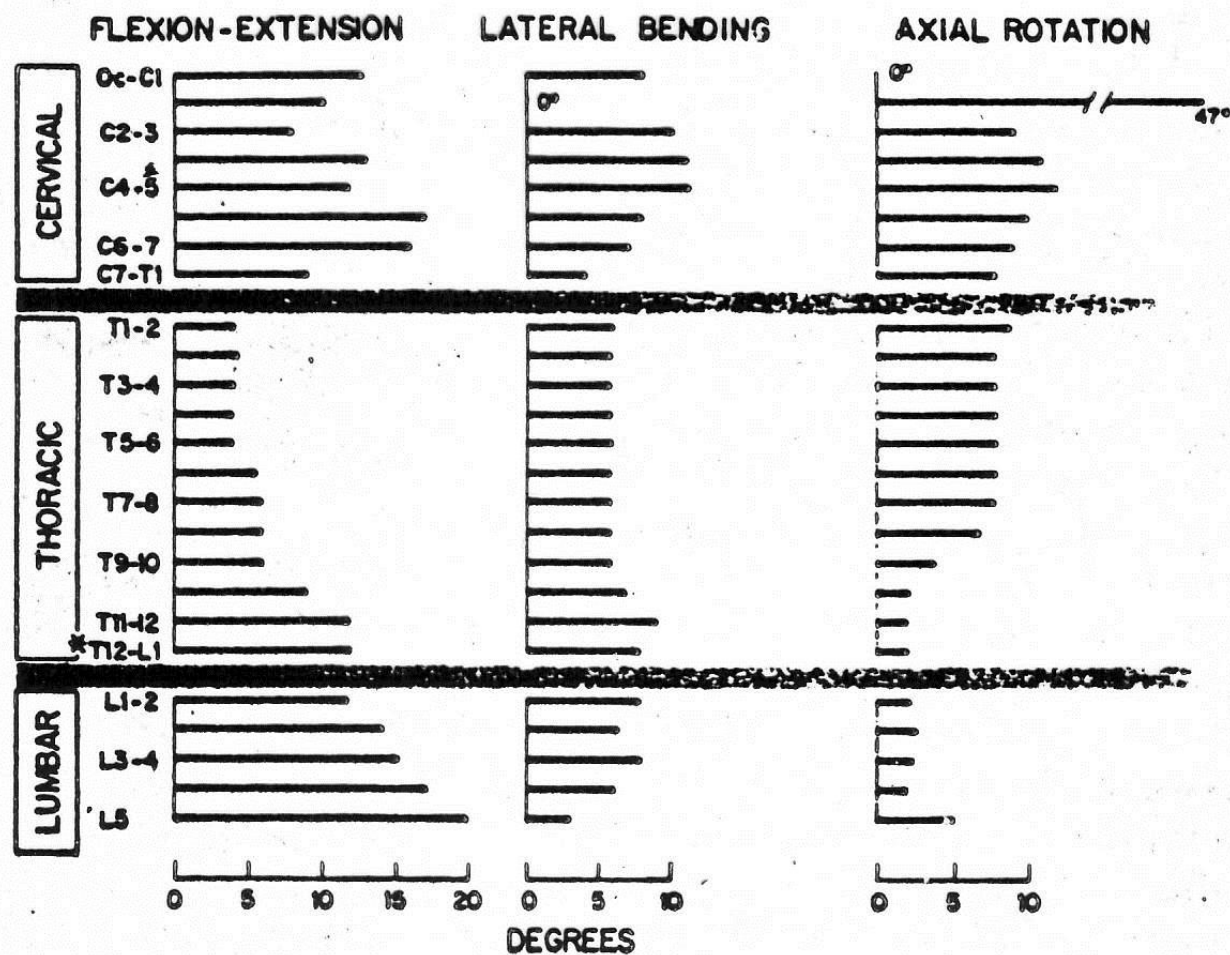
## OCCUPATIONAL BIOMECHANICAL MODELS



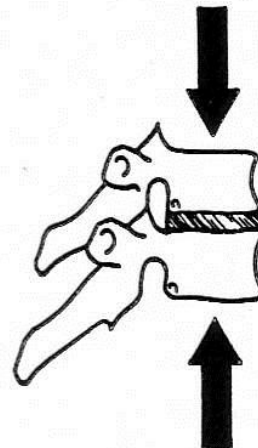
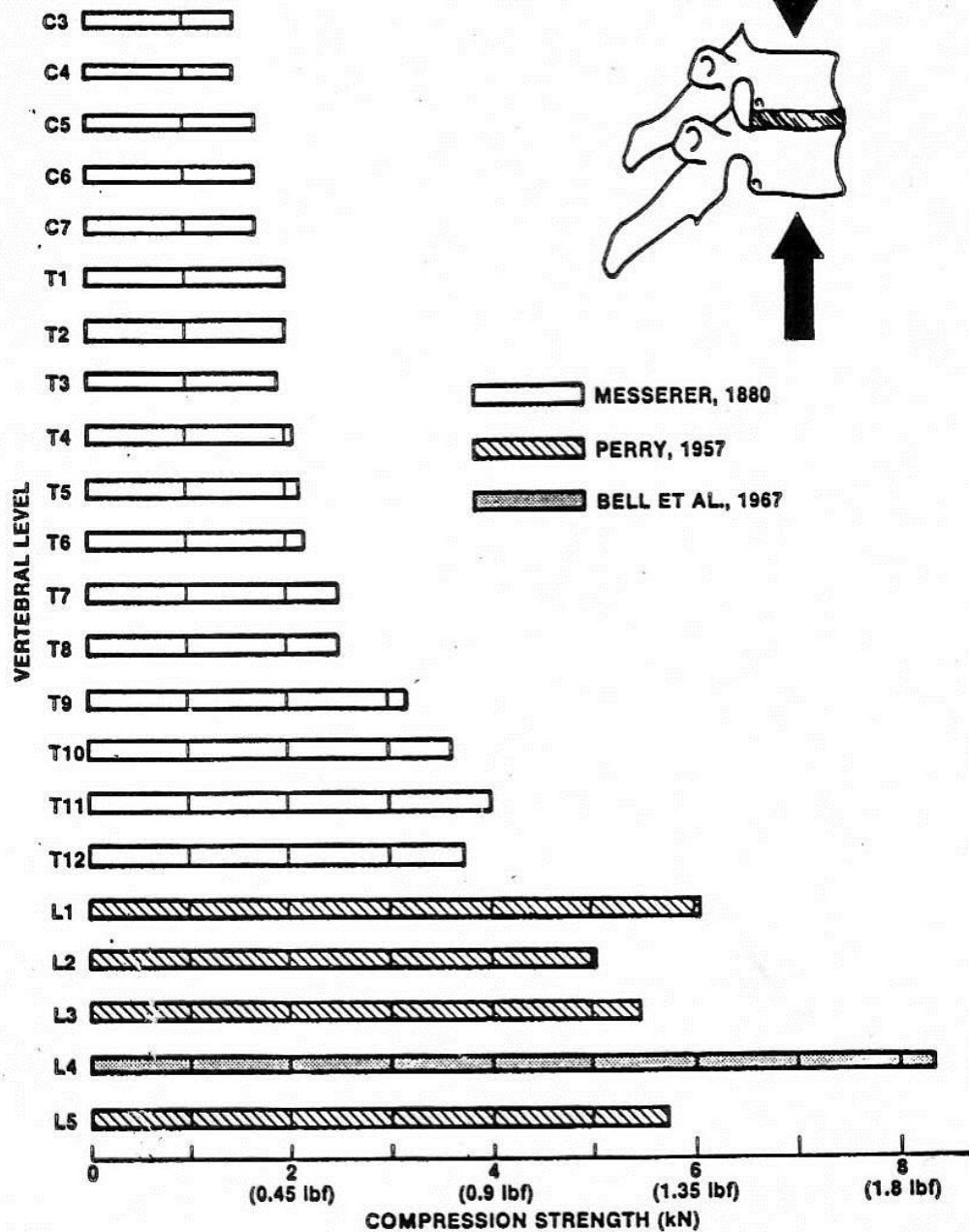
**Figure 6.23** Pelvic angle  $\beta$  changes as a function of torso flexion  $T$  and knee flexion included angle  $K$  (from Anderson et al., 1986).



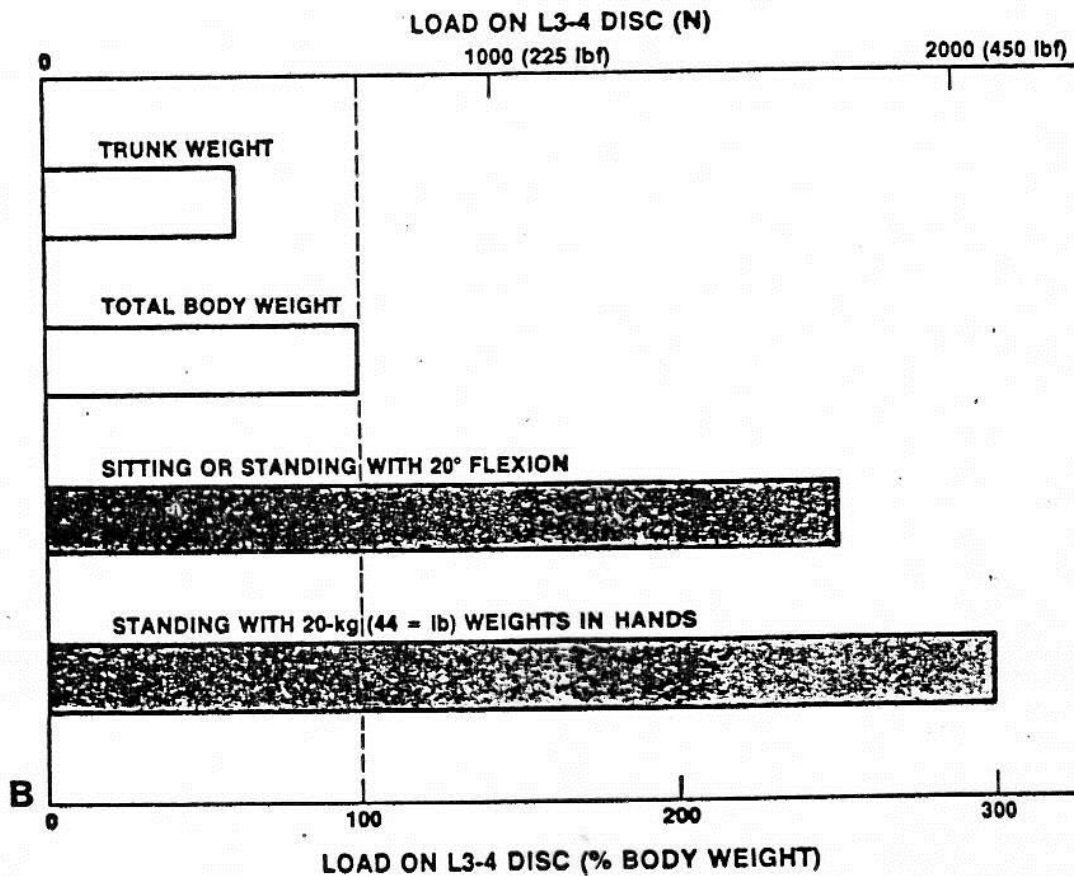
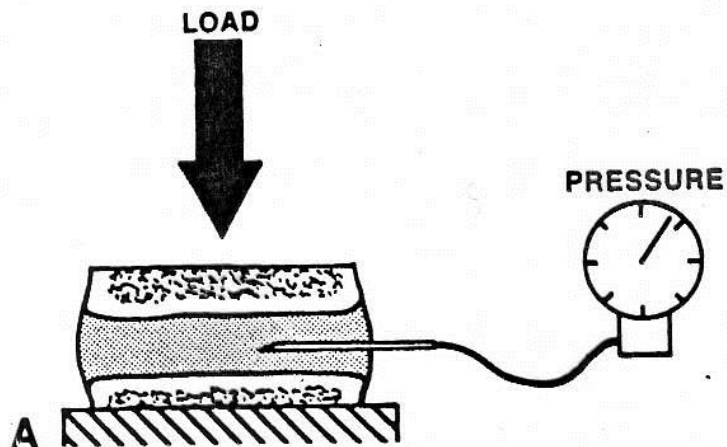
# Zakresy ruchu kregoslupa





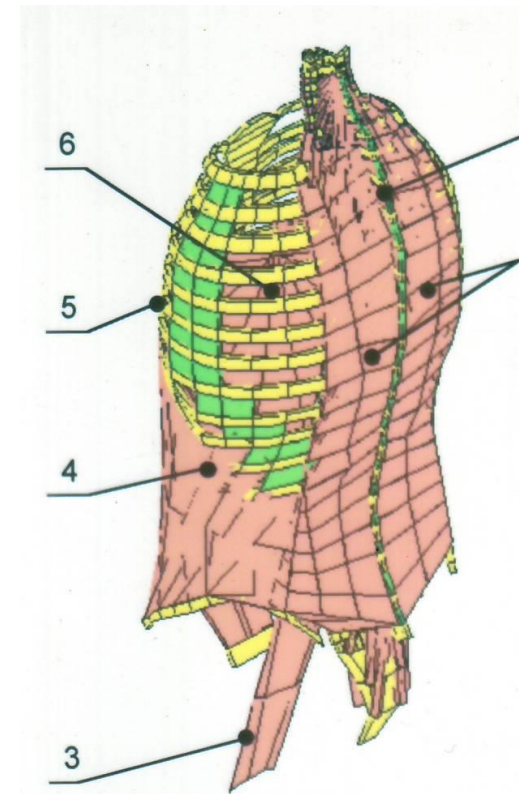






# BIOMECHANIKA KRĘGOSŁUPA

## MODEL TUŁOWIA CZŁOWIEKA

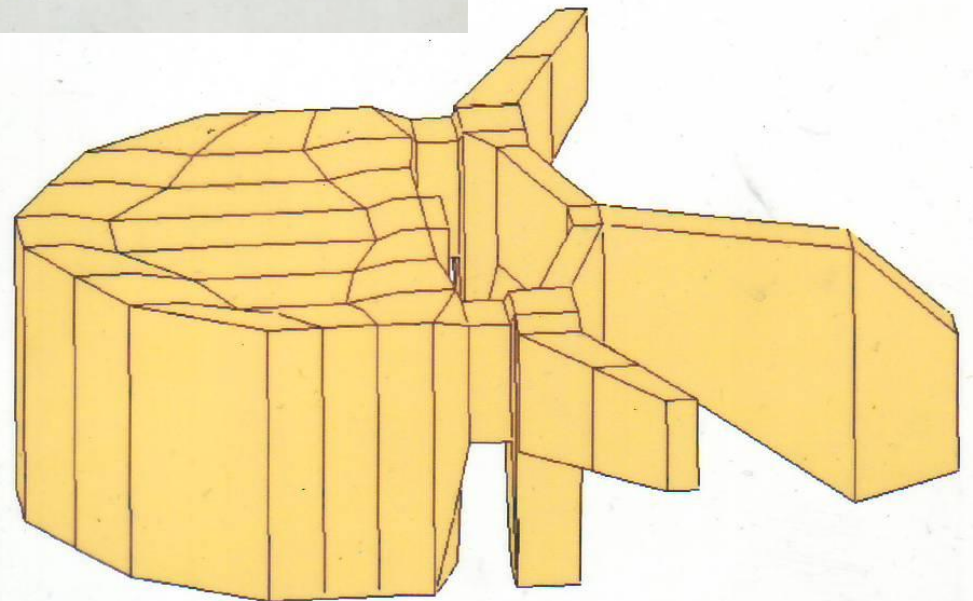


*M. Dietrich, K. Kędzior, T. Zagrajek*



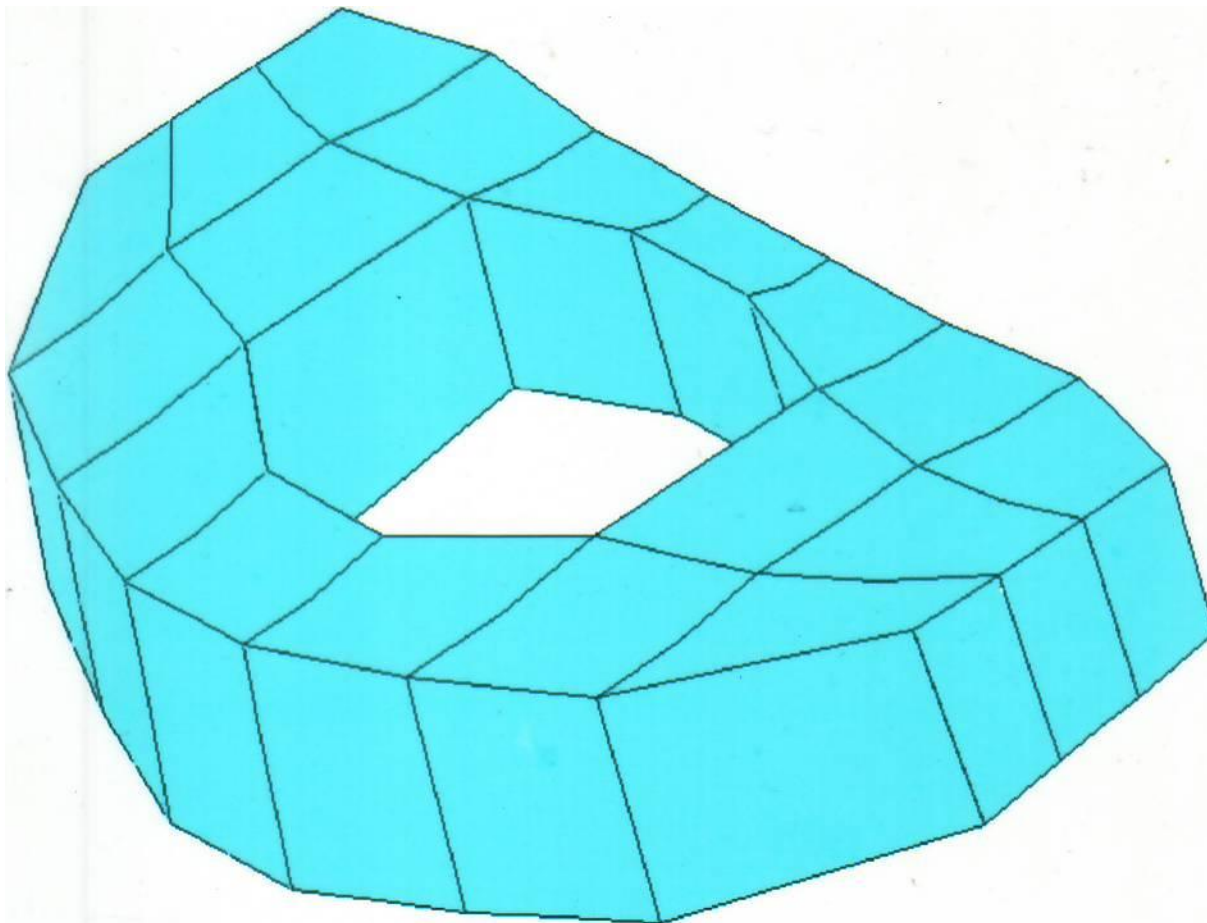
# Spine model

**The model of torso represents precisely anatomy of the human spinal system. It includes vertebrae, ribs, pelvis elements, sternum, intervertebral discs, ligaments, muscles, gas appearing in the abdominal cavity and incompressible fluid presence in nucleus pulposus of intervertebral discs. The fact that muscles are controlled by the central nervous system has been also taken into account.**



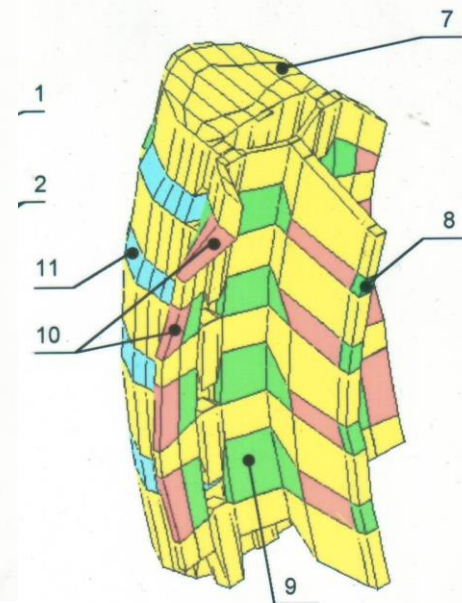
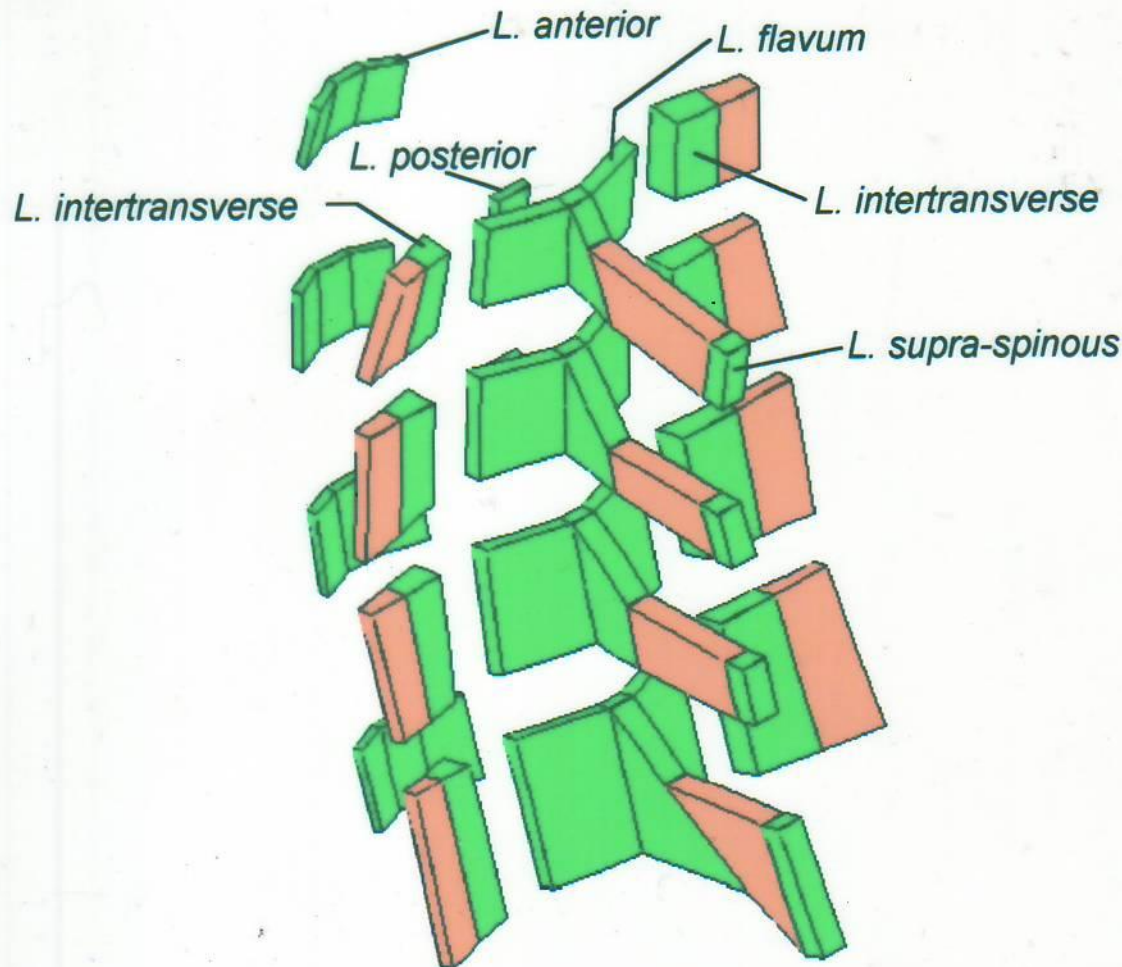
FEM mesh of intervertebral disc L3-L4

# Siatka MES krążka międzykręgowego L3-L4





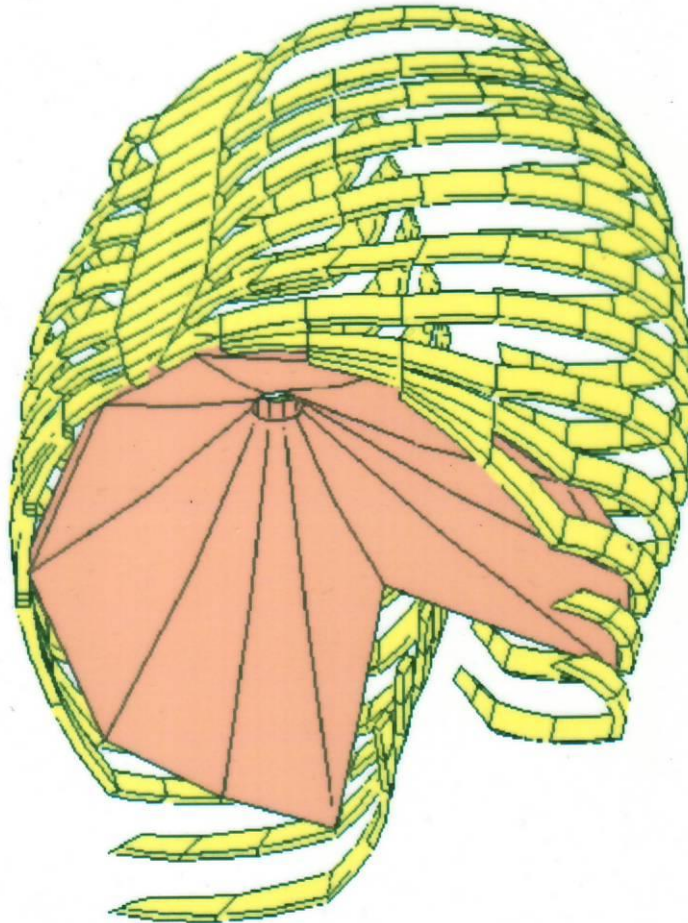
# Siatka MES więzadeł – odcinek L1–L5





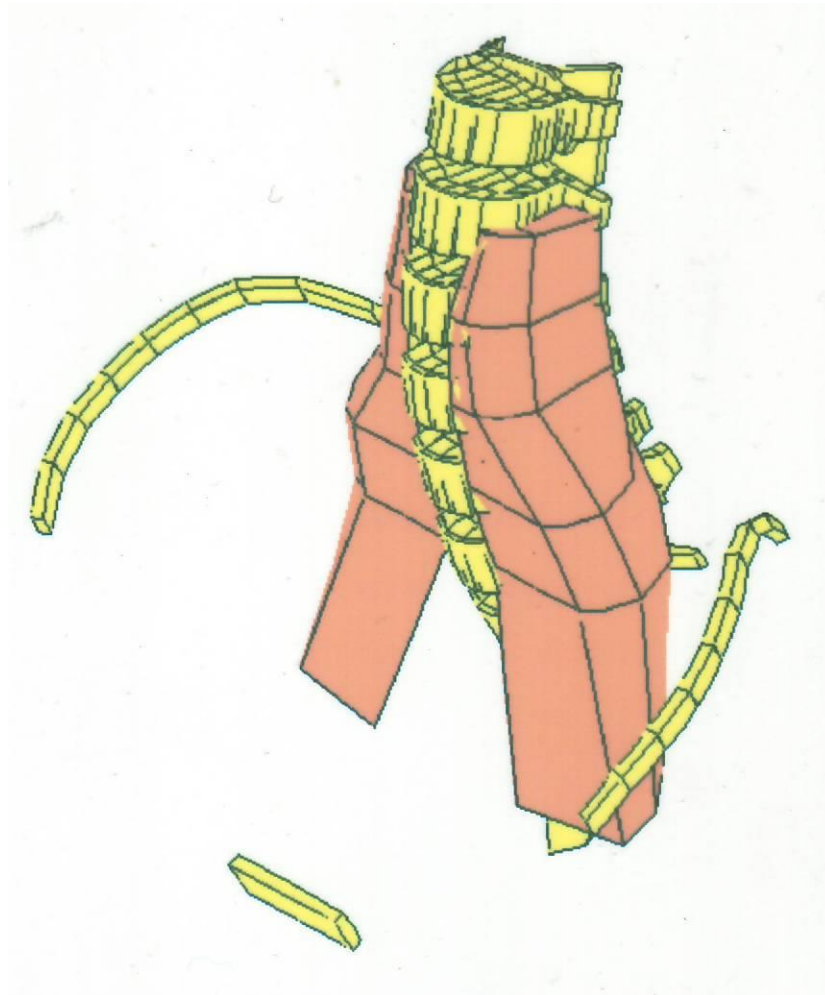
FEM mesh of rib-cage and diaphragm

# Siatka MES klatki piersiowej i przepony

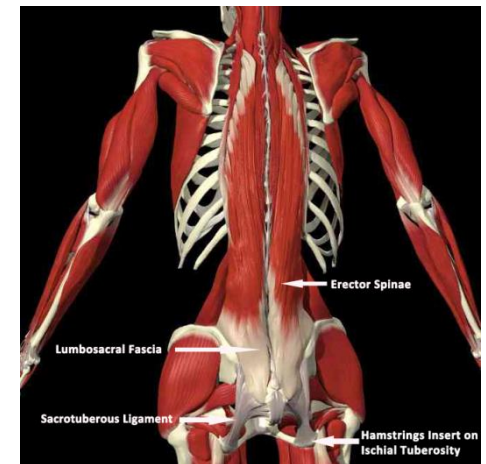
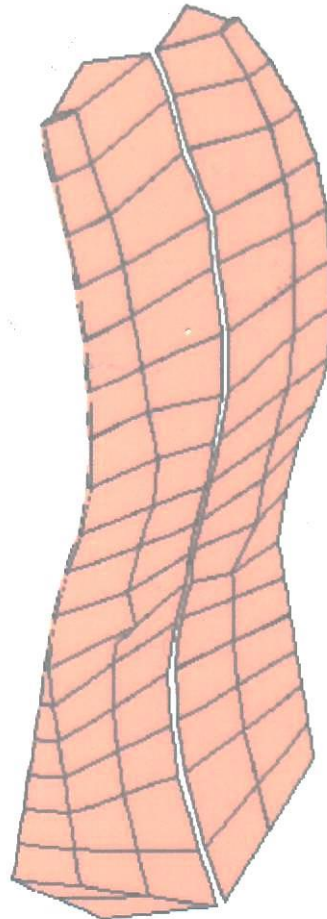


FEM mesh of muscle psoas

# Siatka MES mięśnia lędźwiowego większego

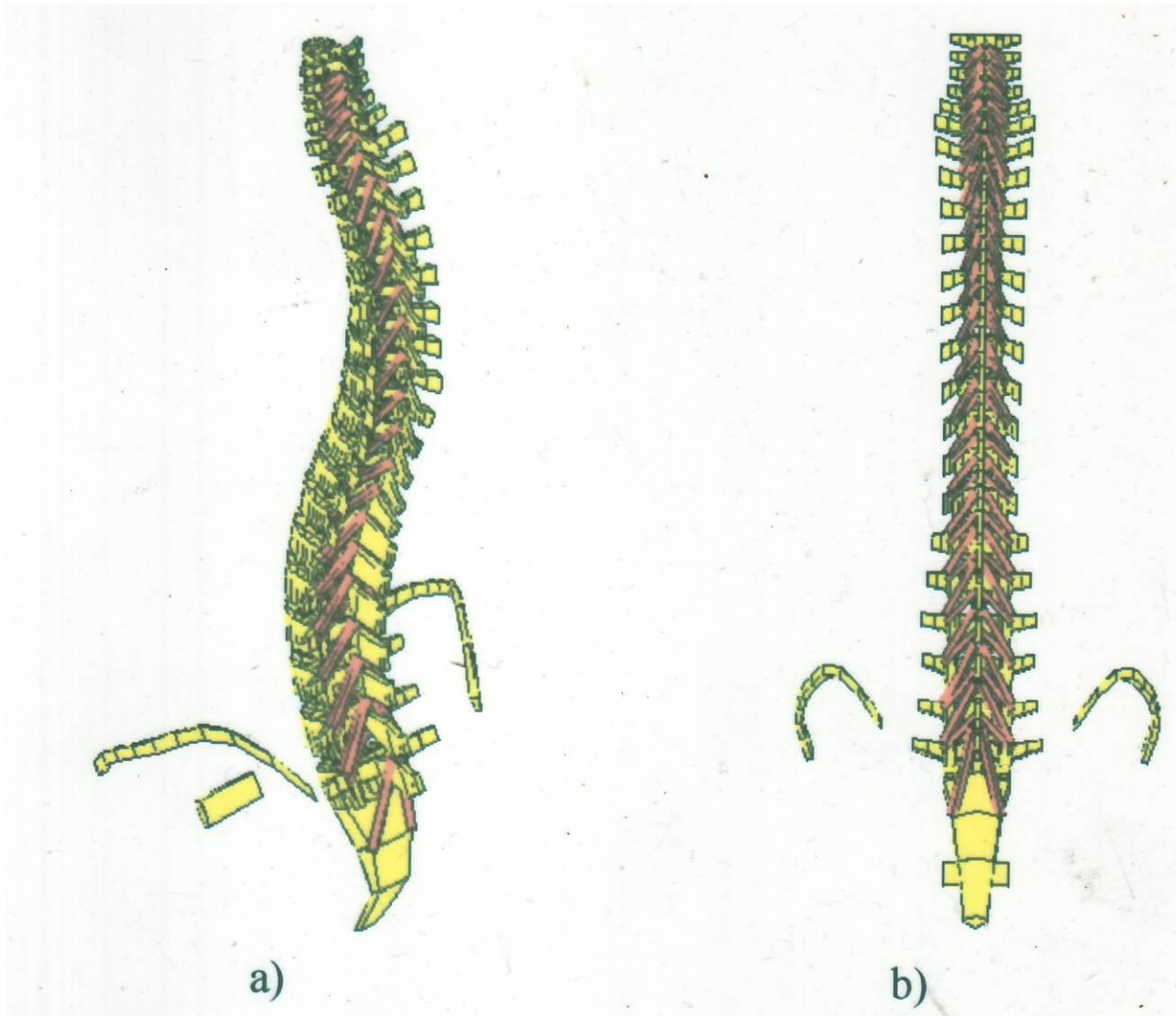


# Siatka MES mięśni prostowników grzbietu





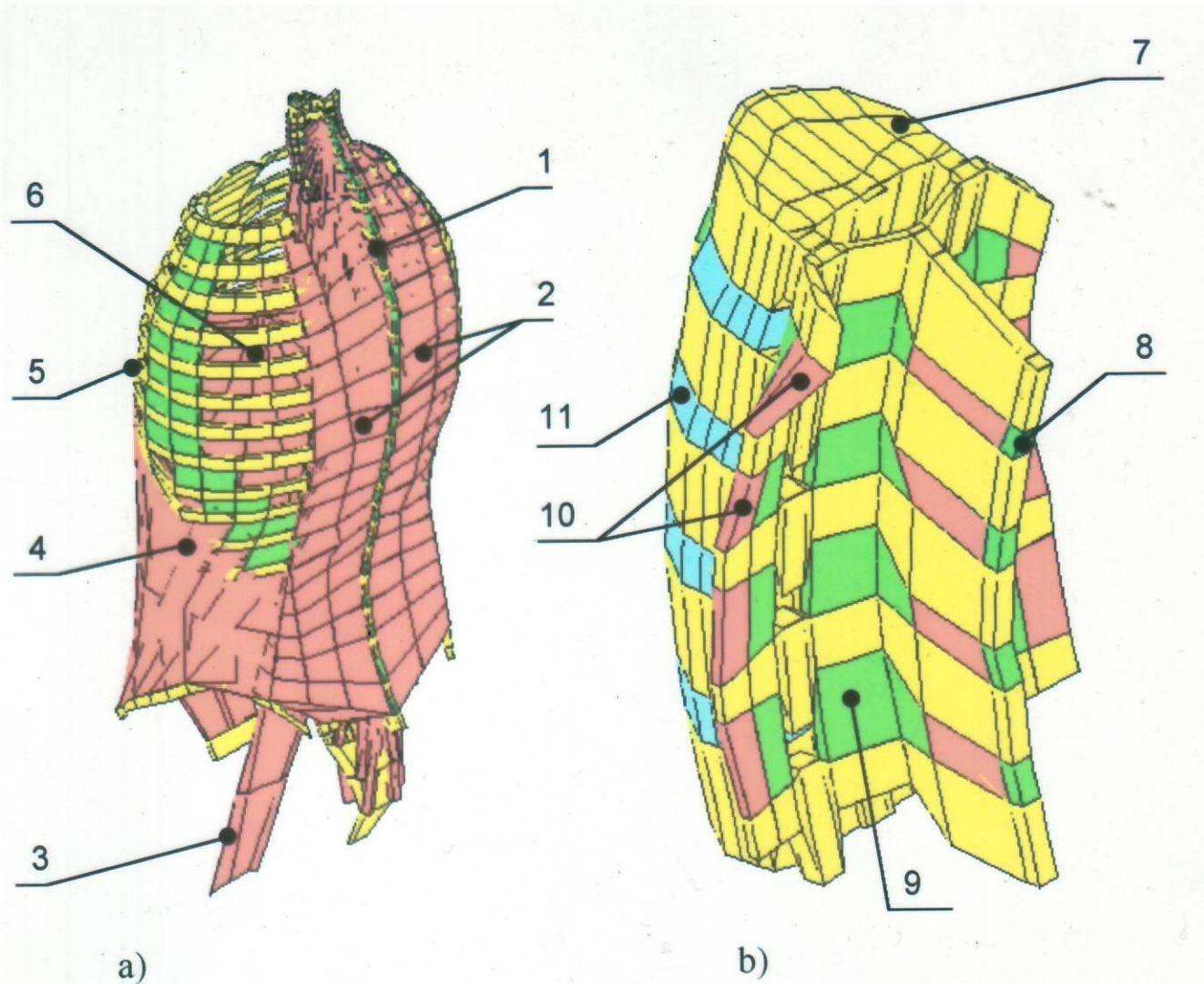
## FEM mesh of rotatores muscle: a) side view, b) back view







FEM mesh of the human spinal system in the straightened position of the body: a) general view, b) lumbar section of the spinal column; 1 - spinal column, 2- erector spinae muscle, 3 - psoas muscle, 4 - muscles of abdomen, 5 - rib-cage, 6 - diaphragm, 7 - vertebra L1, 8 - ligament supraspinous, 9 - ligament flavum, 10 - rotatores muscle, 11 - disc L2-L3 (only a few elements are marked).





# Optymalizacja

The number of muscle forces in the human body is higher than the number of generalised displacements (it appears also in the present model), the problem, therefore becomes statically indeterminate.

To overcome this obstacle, an additional “merit criterion” is introduced into the mathematical model. The solution to Eq. (6), which satisfies also the adopted (but not necessary true) criterion is sought after.





# Kryteria optymalizacji

## 1. Wykonanie zadania

- maksymalna prędkość
- maksymalny ciężar
- itp.

## 2. Stan normalny

- minimum energii potencjalnej
- łagodnego nasycenia
- 
- Maksymalnej wytrzymałości (bezpieczeństwa)  $\max(\frac{\sigma_i}{\sigma_{mi}})=\min.$   
 $\max(\frac{p_i}{p_{mi}})=\min.$

## 3. Stan patologiczny

- $\sigma_k = \min.$
- łagodnego nasycenia (dotyczące badanego rejonu)



# Kryterium energetyczne

In the present model it has been assumed that muscles satisfy the so-called energetic criterion of the form

$$\frac{1}{2} \sum_{i=1}^m \frac{l_i F_i^2}{E_i A_i} = \min$$

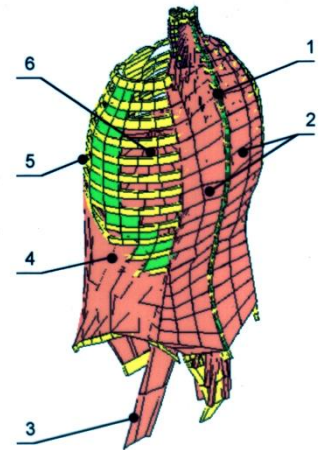
where:

$i = 1, \dots, m$  - index denoting a number of muscle,

$F_i$  - total force (active plus passive components) exerted by the  $i$ -th muscle,

$A_i$  - averaged physiological cross-section of the  $i$ -th muscle,

$E_i$  - Young's modulus of the  $i$ -th spar - 3D element representing the  $i$ -th muscle (passive component only).





# Ograniczenie siły w mięśniu

It is additionally assumed that the magnitude of total force exerted by a given muscle  $F = F_p + F_a$  must be lower than the permissible force  $F_{\max}$ , having the form

$$F_{\max} = A[\text{m}^2] \cdot 10^6 [\text{N}/\text{m}^2] \quad (5)$$

where:

A - averaged physiological cross-section of a given muscle, i.e. the muscle volume divided by the value of  $l_{\text{fib}}$ .

In order to solve the problem of muscle co-operation there were used the following two merit criteria:

energetic criterion (Dietrich et al., 1990), which has been formulated in the form

$$\sum_{i=1}^k \int_{V_i} \frac{\sigma_i^2}{E_i} dV_i = \min$$

and soft saturation criterion (Siemieński, 1992) in the form

$$\sum_{i=1}^k \left( 1 - \sqrt{1 - \left( \frac{\sigma_i}{\sigma_a} \right)^2} \right) = \min$$

where:

$k$  - number of muscle actons (independently stimulated muscle zones),

$\sigma_i$  - tension along muscle fibres ( $\sigma_i \geq 0$ ),

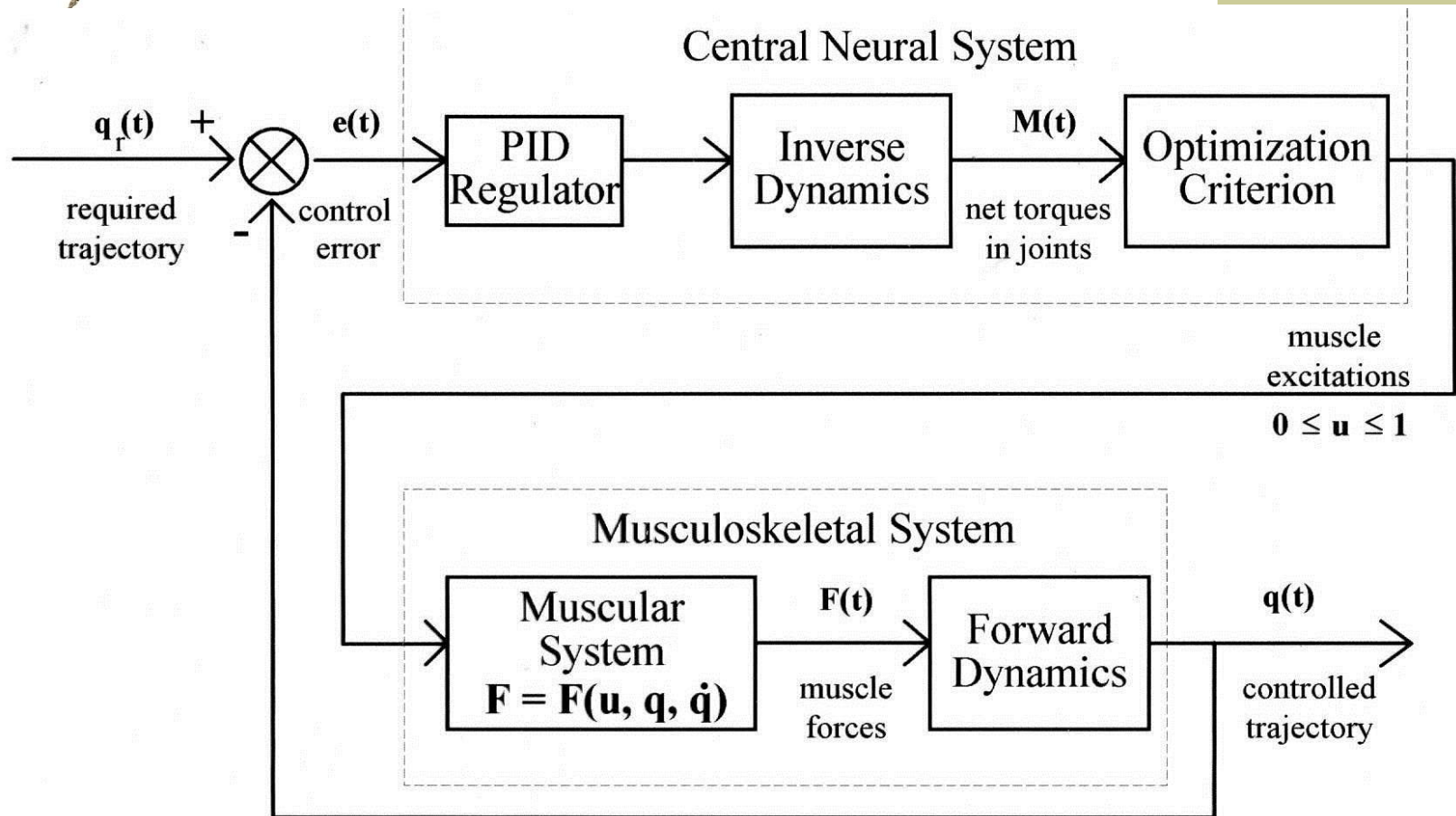
$\sigma_a$  - allowable muscle tension (assumed 1 MPa in this case, averaged value for a given muscle),

$V_i$  - muscle zone volume,

$E_i$  - Young's modulus along muscle fibres.



A block diagram of multidimensional control system of human motion:  $\mathbf{q}_r(t)$ ,  $\mathbf{q}(t)$  - vectors of generalised co-ordinates,  $\mathbf{F}(t)$  - vector of muscular forces,  $t$  - time.

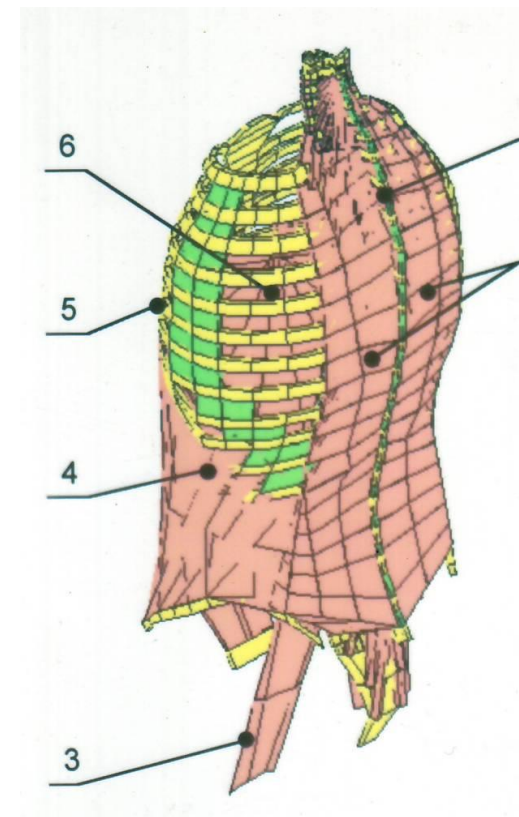





# BIOMECHANIKA KRĘGOSŁUPA



**Wyniki**

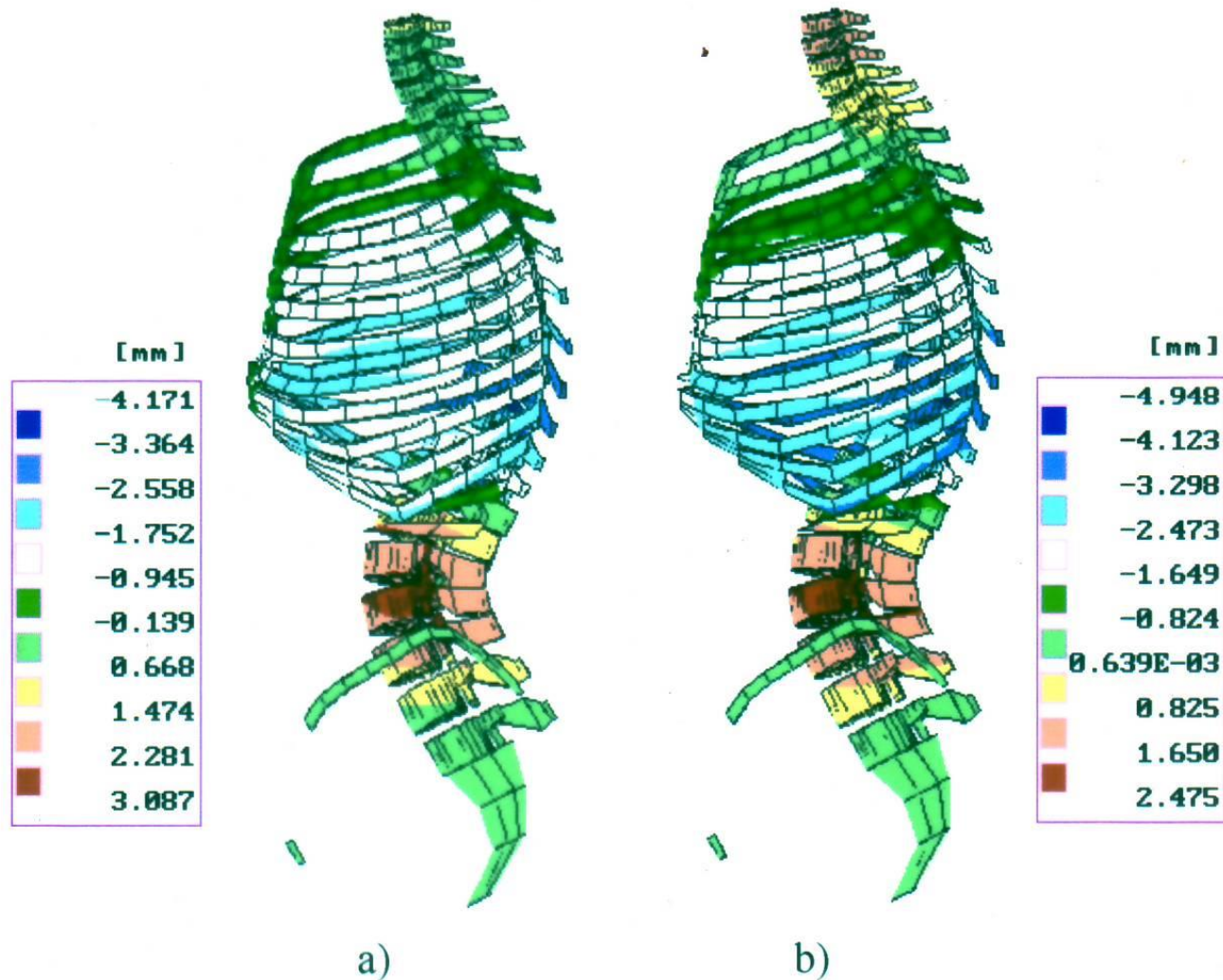






Equation (6) is solved using the step-by-step method with the matrices  $M_0$ ,  $C_0$  and  $K_0$  being changed at successive time steps  $\Delta t$  due to variable configuration of the physical model which represents at successive time steps a corresponding, variable position of the body.

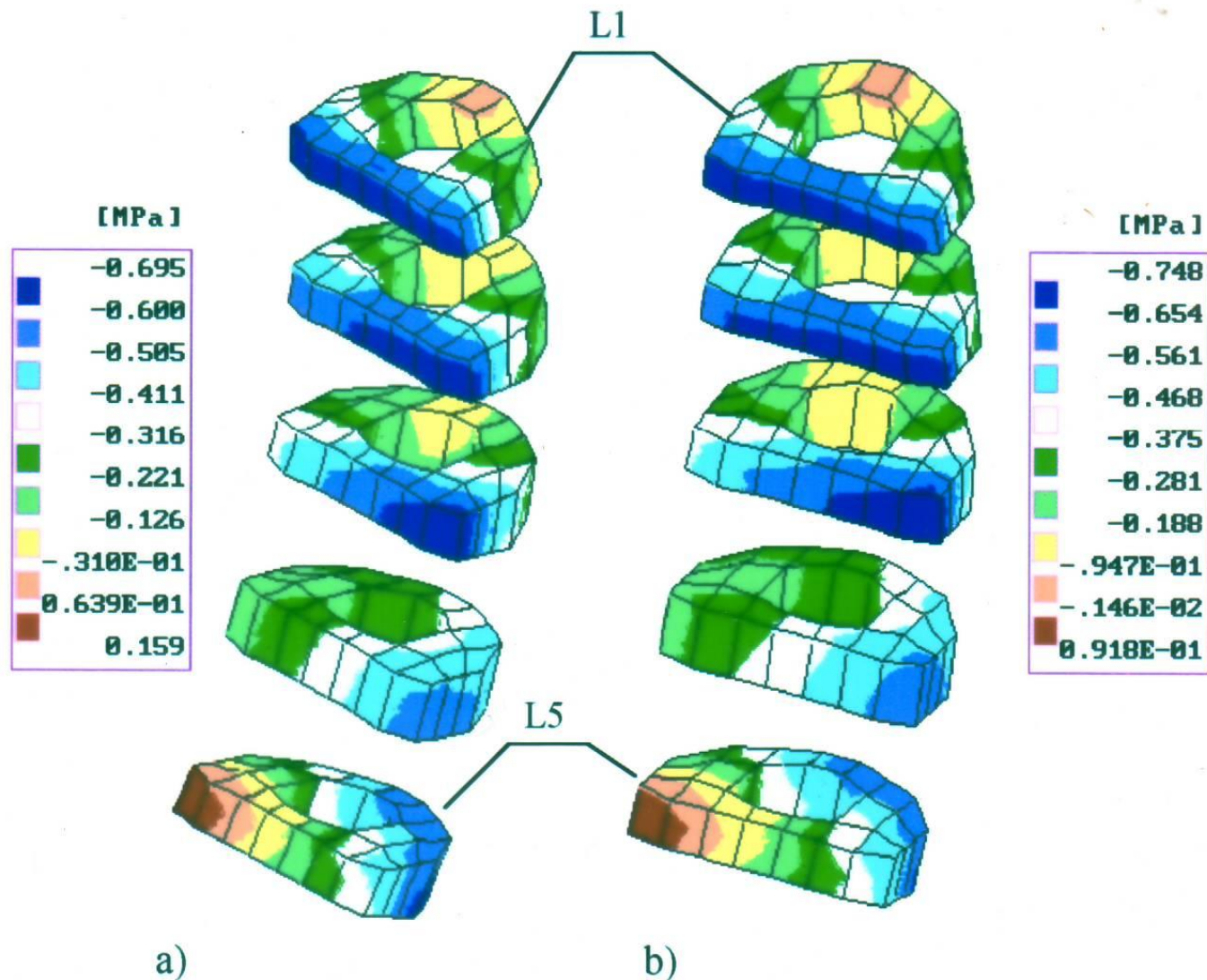
The mass matrix, for example is recalculated at each step. Masses of the elements representing muscles (active spar - 3D), tendons, discs and ligaments (spar - 3D, beam - 3D), respectively, are reduced to the centres of mass of the corresponding rigid bodies, applying the principle that the system energy remains unchanged after the reduction. This approach enables the changes of the human body mass distribution due to motion (i.e. muscles dislocations relative to bones) to be reasonably approximated.



Horizontal dislocations of the ribs and vertebrae in the sagittal plane due to external load of  $1 \times 200\text{N}$  held in the left hand: a) for the energetic criterion, b) for the soft saturation criterion.

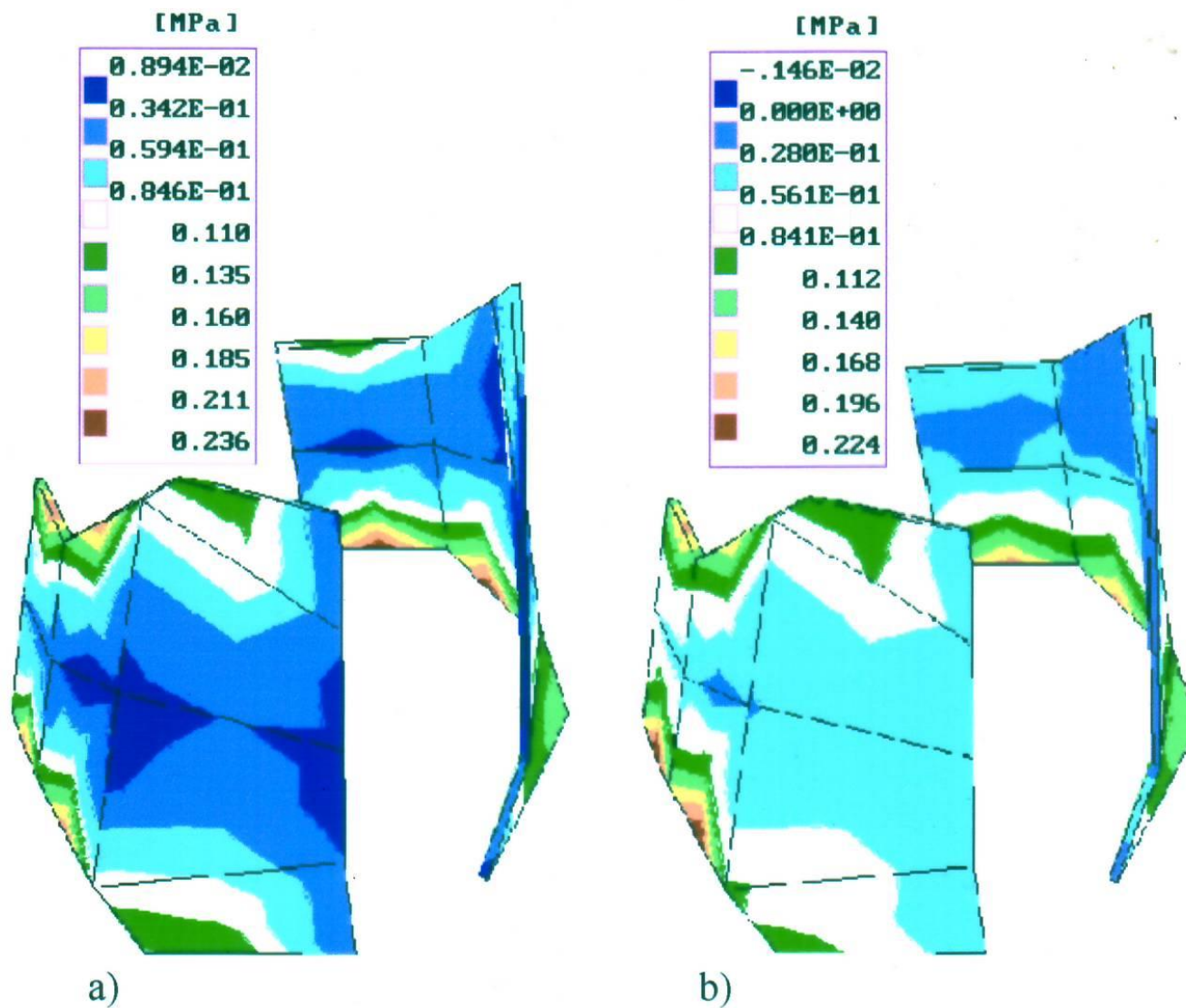
*(Initial position of the body - straightened, linear analysis)*





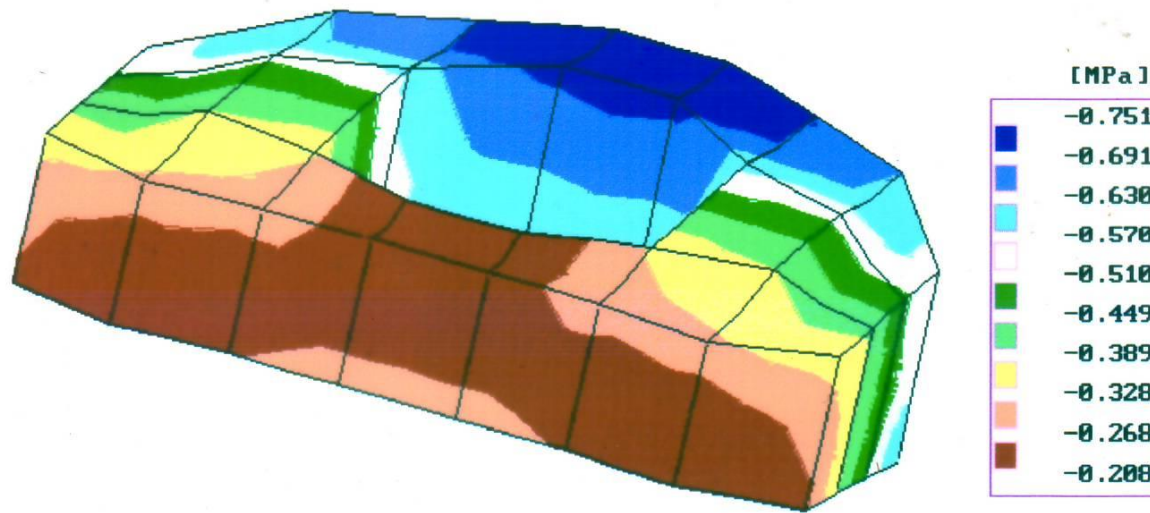
Compressive stress distribution in annuli fibrosi of the intervertebral discs L1 - L5 (lumber section) due to external load of  $1 \times 200\text{N}$  held in the left hand:  
a) for the energetic criterion, b) for the soft saturation criterion.

*(Initial position of the body - straightened, linear analysis)*

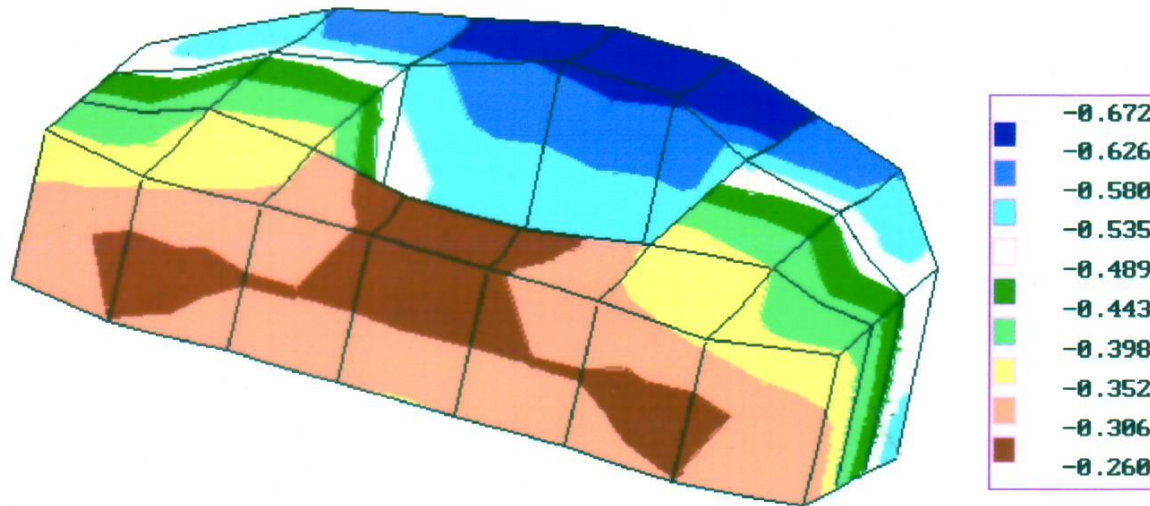


Distributions of tension along muscle fibres in transverse muscle of abdomen due to external load of  $1 \times 200\text{N}$  held in the left hand: a) for the energetic criterion, b) for the soft saturation criterion.

*(Initial position of the body - straightened, linear analysis)*



a)

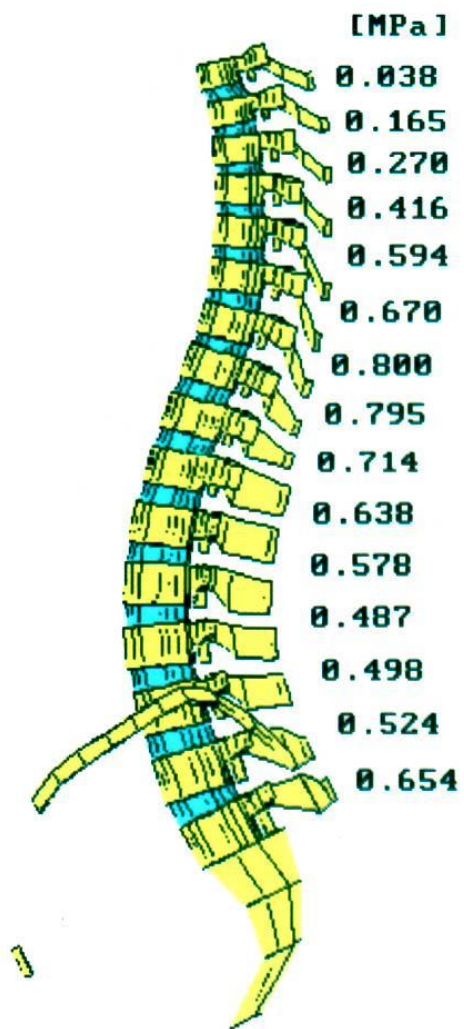


b)

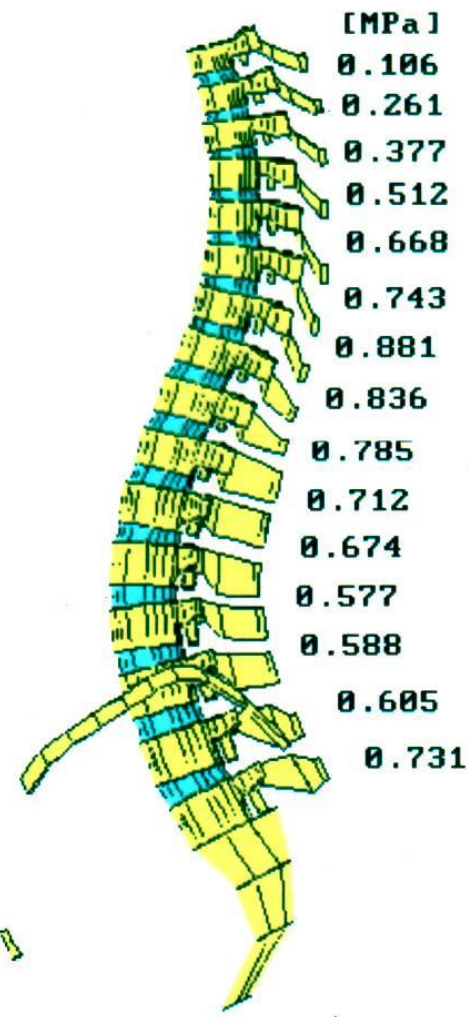
Compressive stress distributions in annuli fibrosi of the intervertebral disc L5 - S1 due to external load of  $2 \times 200\text{N}$  held in hands: a) for the energetic criterion, b) for the soft saturation criterion.

*(Initial position of the body - straightened, linear analysis)*





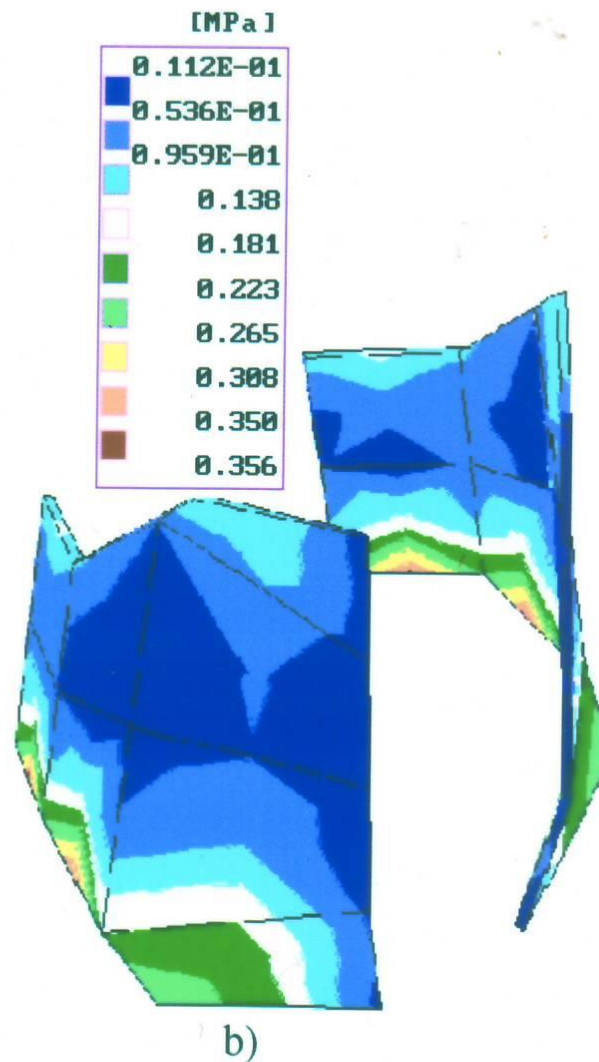
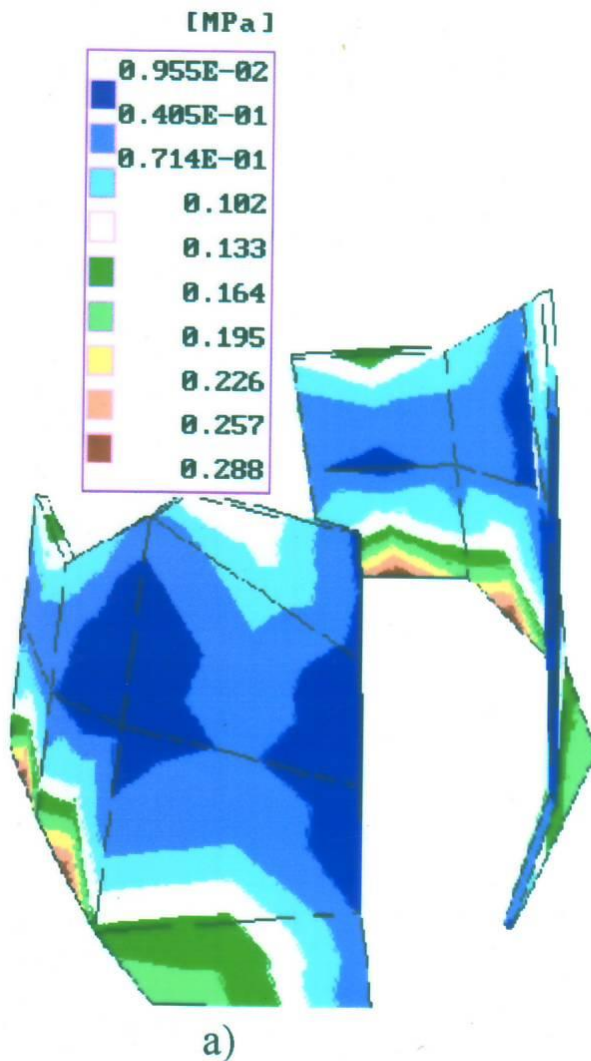
a)



b)

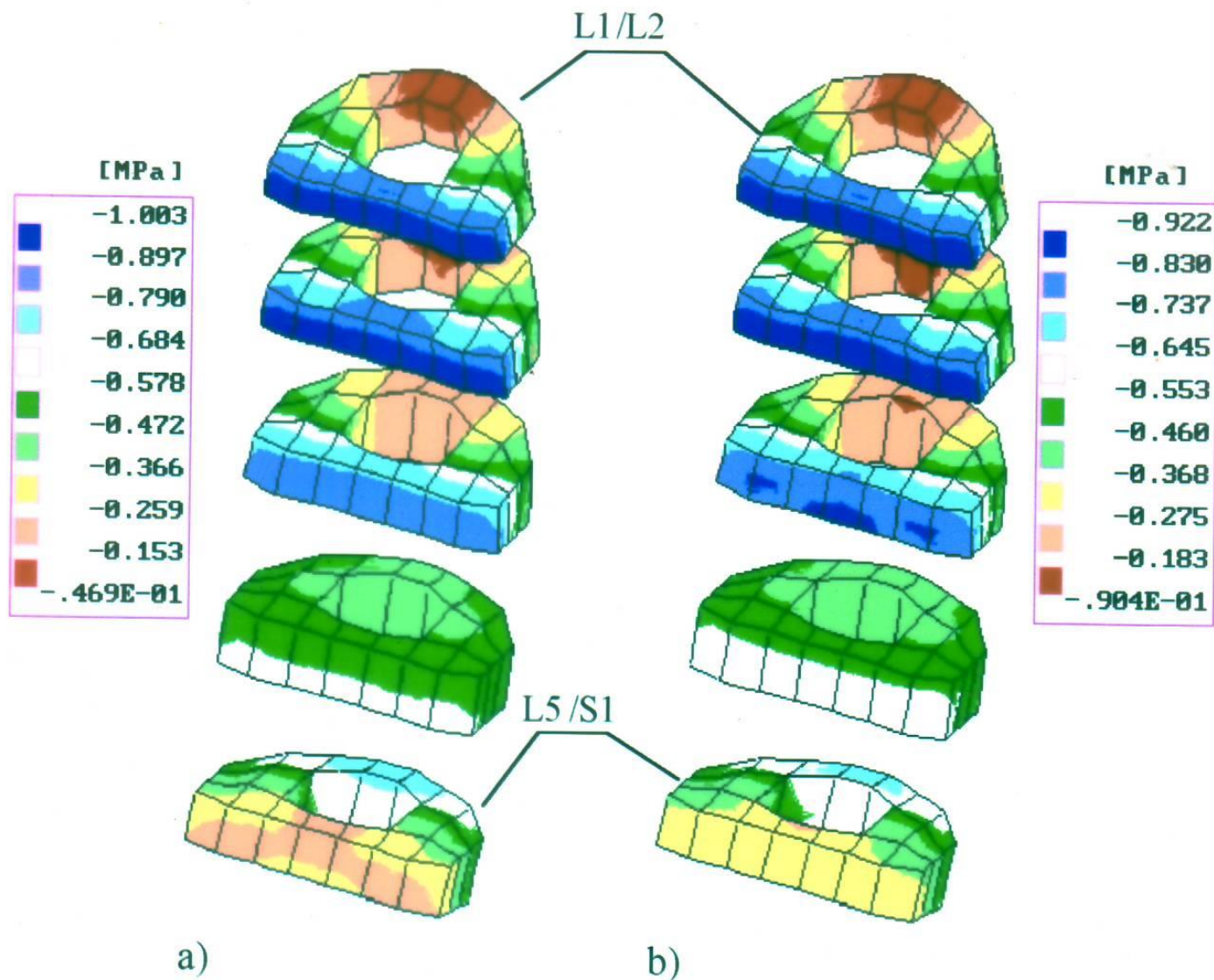
Pressure distribution along the spinal column in nuclei pulposi of the intervertebral discs due to external load of  $1 \times 200\text{N}$  held in the left hand: a) for the energetic criterion, b) for the soft saturation criterion.

*(Initial position of the body - straightened, linear analysis)*



Distributions of tension along muscle fibres in transverse muscle of abdomen due to external load of  $2 \times 200\text{N}$  held in hands: a) for the energetic criterion, b) for the soft saturation criterion.

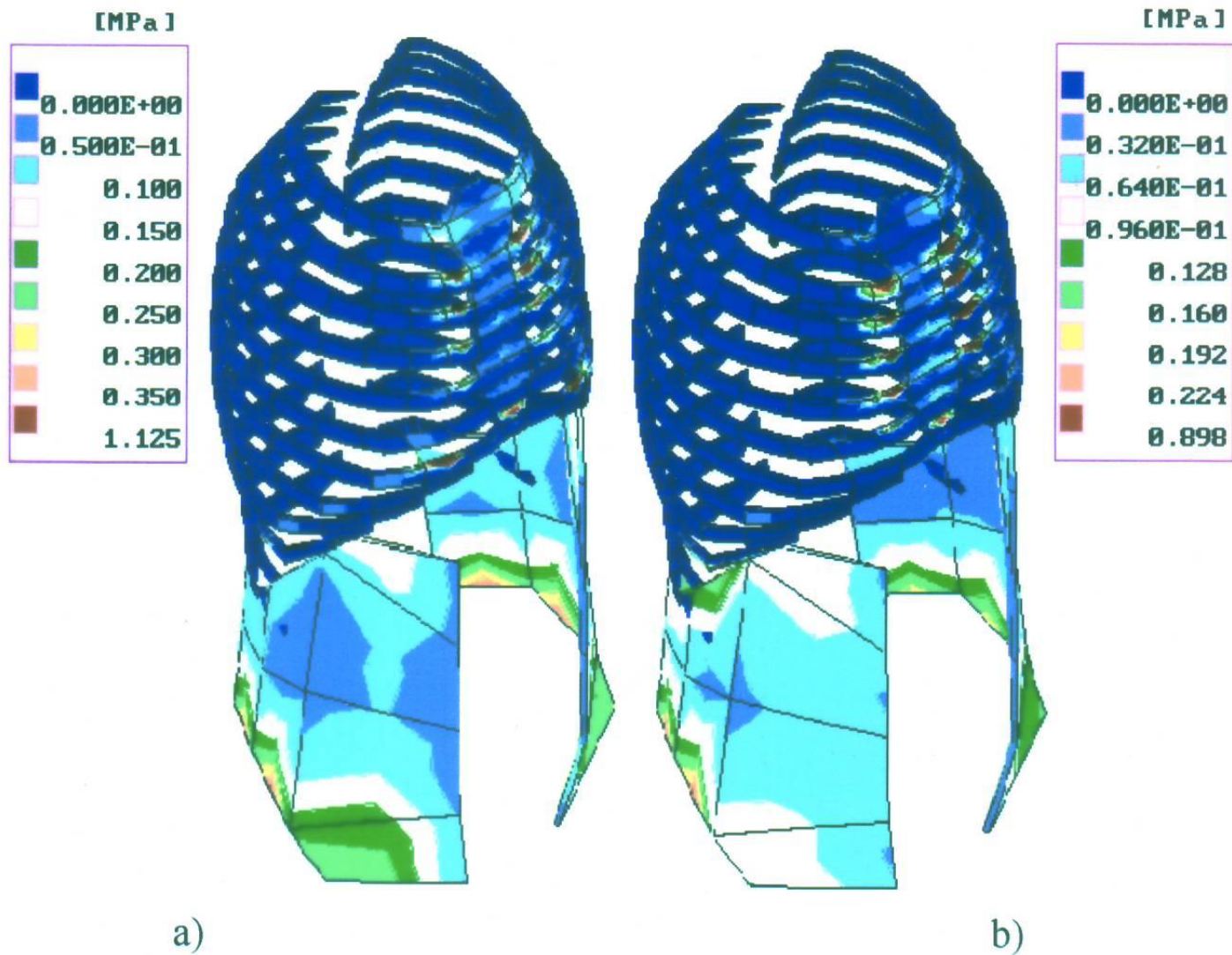
*(Initial position of the body - straightened, linear analysis)*



Compressive stress distribution in annuli fibrosi of the intervertebral discs L1 - L5 (lumbar section) due to external load of  $2 \times 200\text{N}$  held in hands: a) for the energetic criterion, b) for the soft saturation criterion.

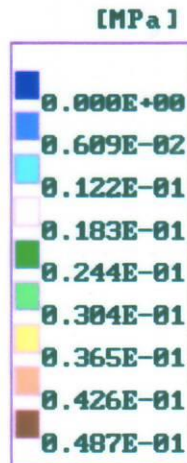
*(Initial position of the body - straightened, linear analysis)*





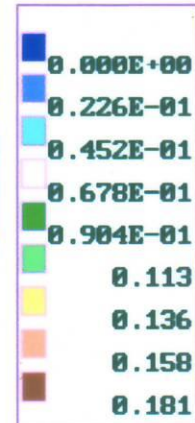
Distributions of tension along muscle fibres in transverse muscle of abdomen:  
a) due to external load of  $2 \times 200\text{N}$  held in hands; b) due to 200N held in the left hand.

*(Initial position of the body - straightened, soft saturation criterion, linear analysis)*



a)

[MPa]



b)

Distributions of tension along muscle fibres in straight muscle of abdomen:  
a) due to external load of  $2 \times 200\text{N}$  held in hands; b) due to  $200\text{N}$  held in the left hand.

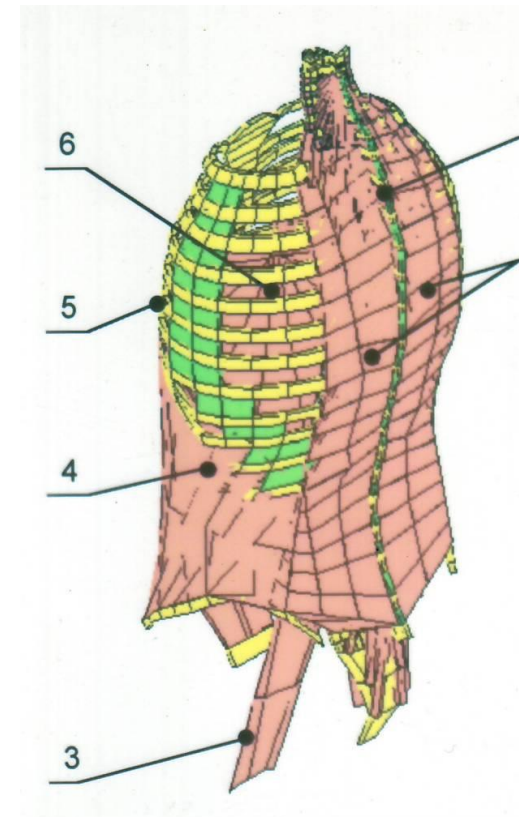
*(Initial position of the body - straightened, soft saturation criterion, linear analysis)*

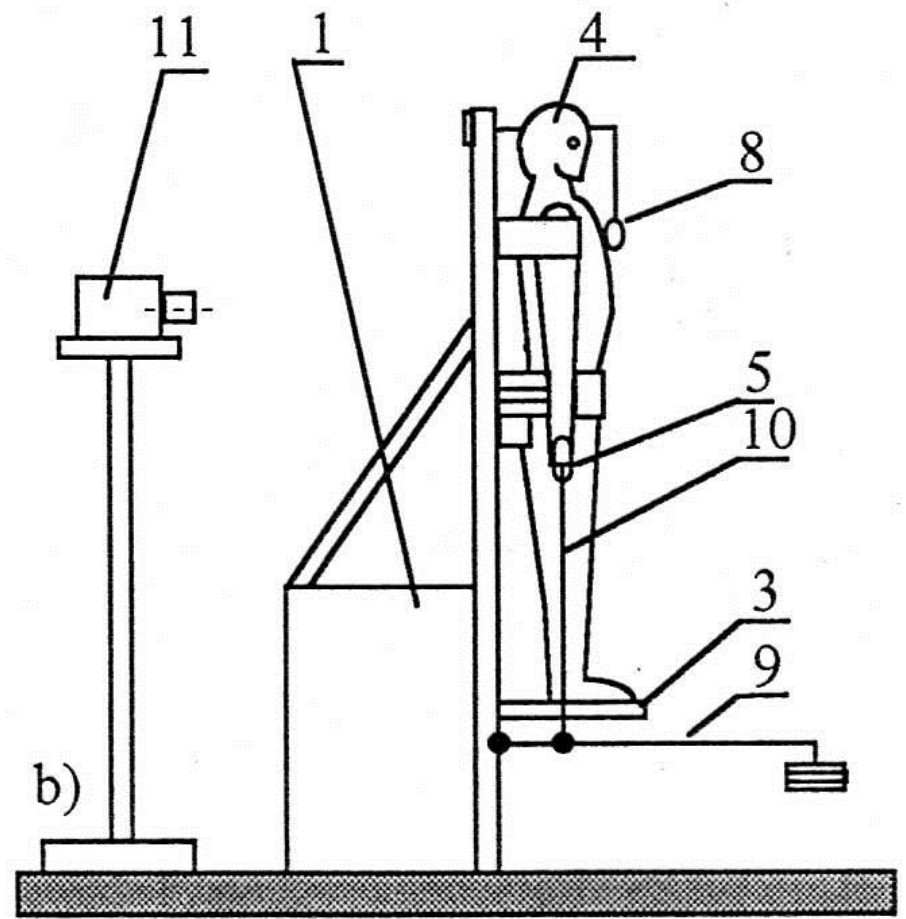
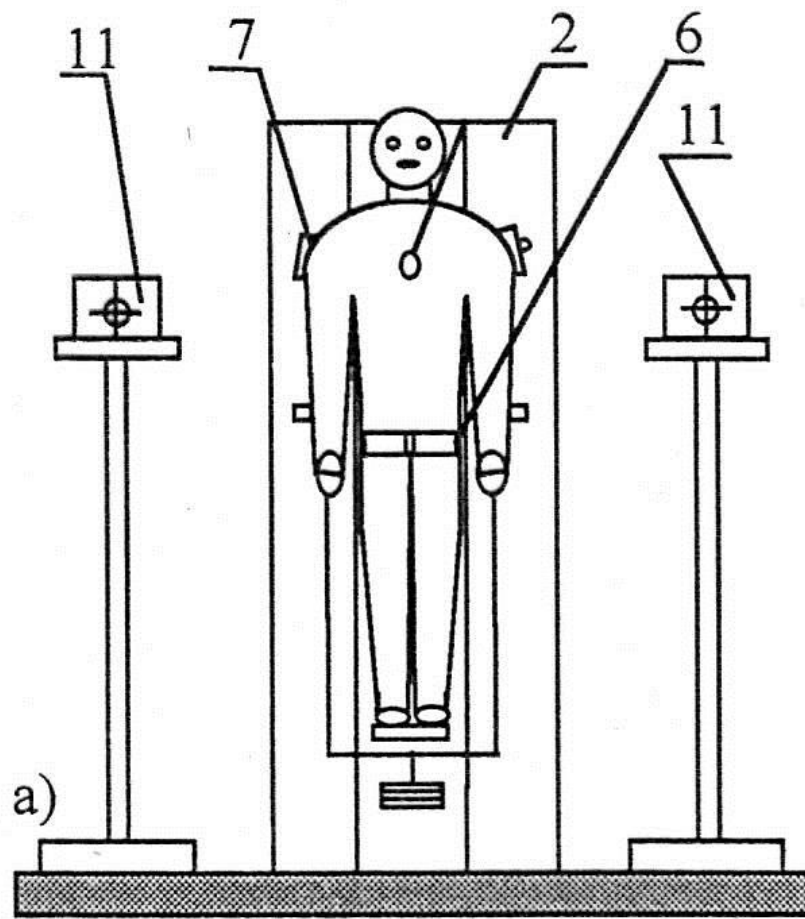


# BIOMECHANIKA KRĘGOSŁUPA

## MODEL TUŁOWIA CZŁOWIEKA

weryfikacja





### Experimental stand:

a - front view, b - side view; 1 - sturdy base, 2 - vertical frame, 3 - dais, 4 - examined subject, 5 - handle, 6, 7 and 8 - limiters of pelvis, sternum and shoulders movements respectively, 9 and 10 - levers, 11 - camera.



## Experimental stand - back view







## Experimental stand - the load held in the left hand

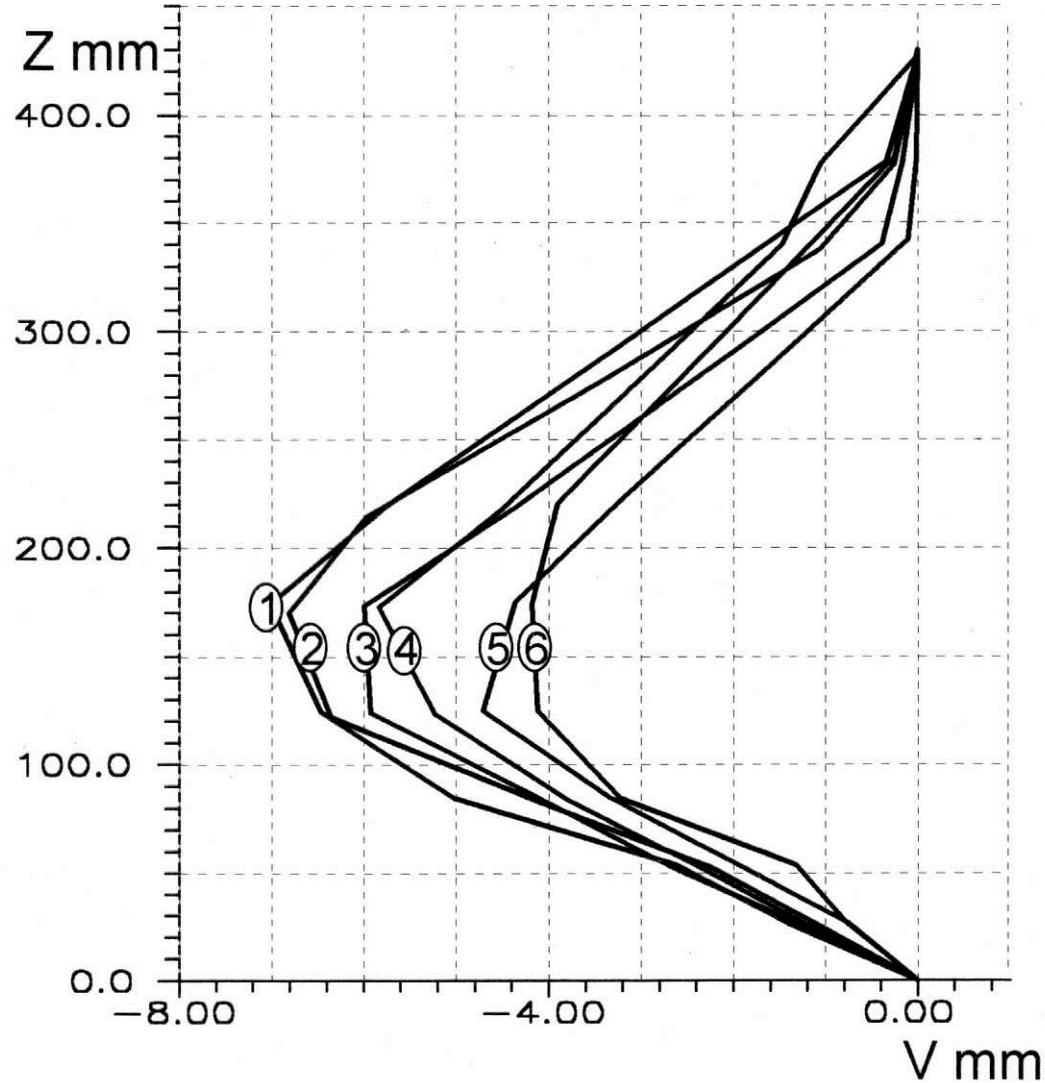




## Experimental stand - immobilisation in the area of the pelvis



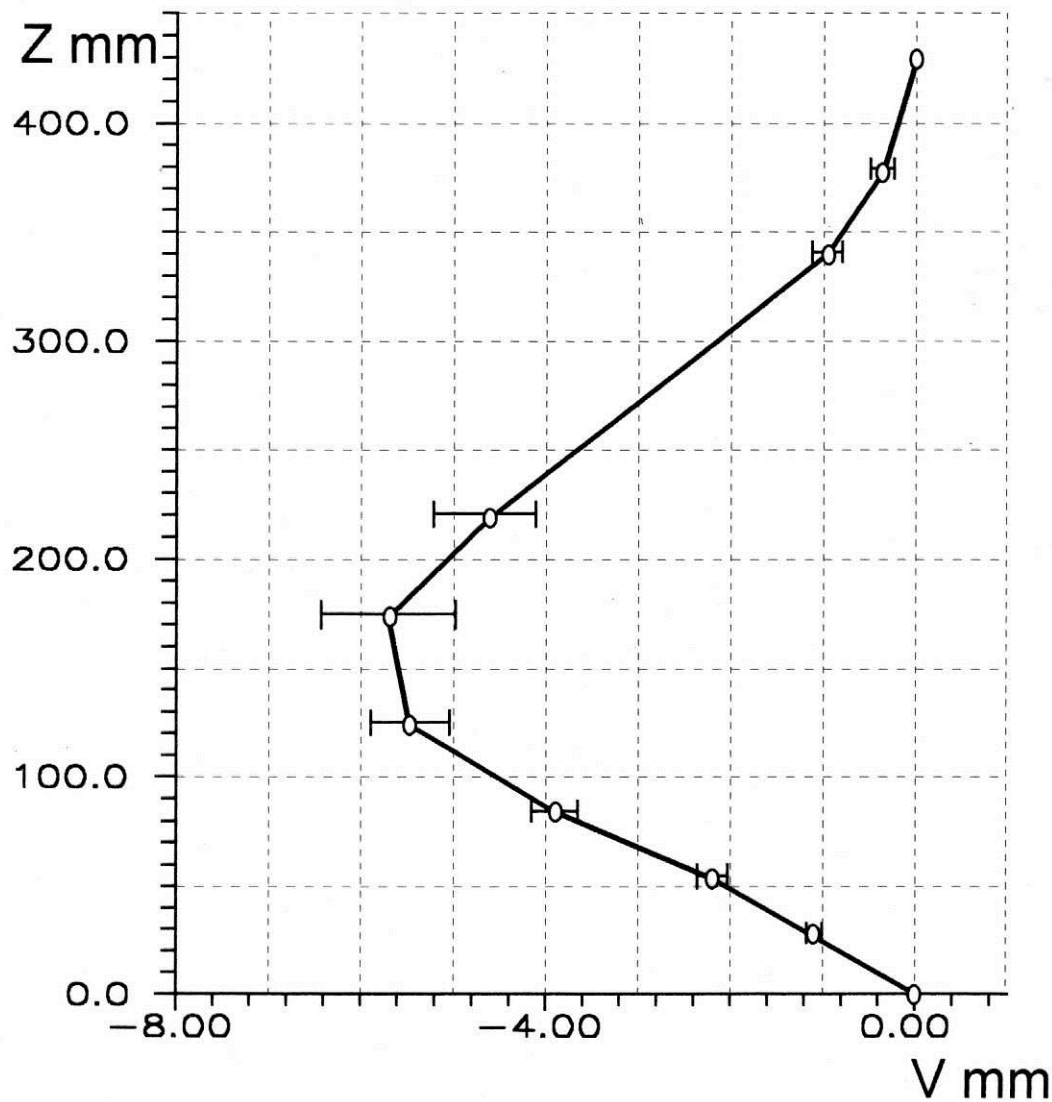




### Experimental results:

V - dislocations in the sagittal plane of the markers stuck on the skin above the spinal processes, Z - height of the trunk measured from level L5/S1; ①÷⑥ - results of succeeding experiments.

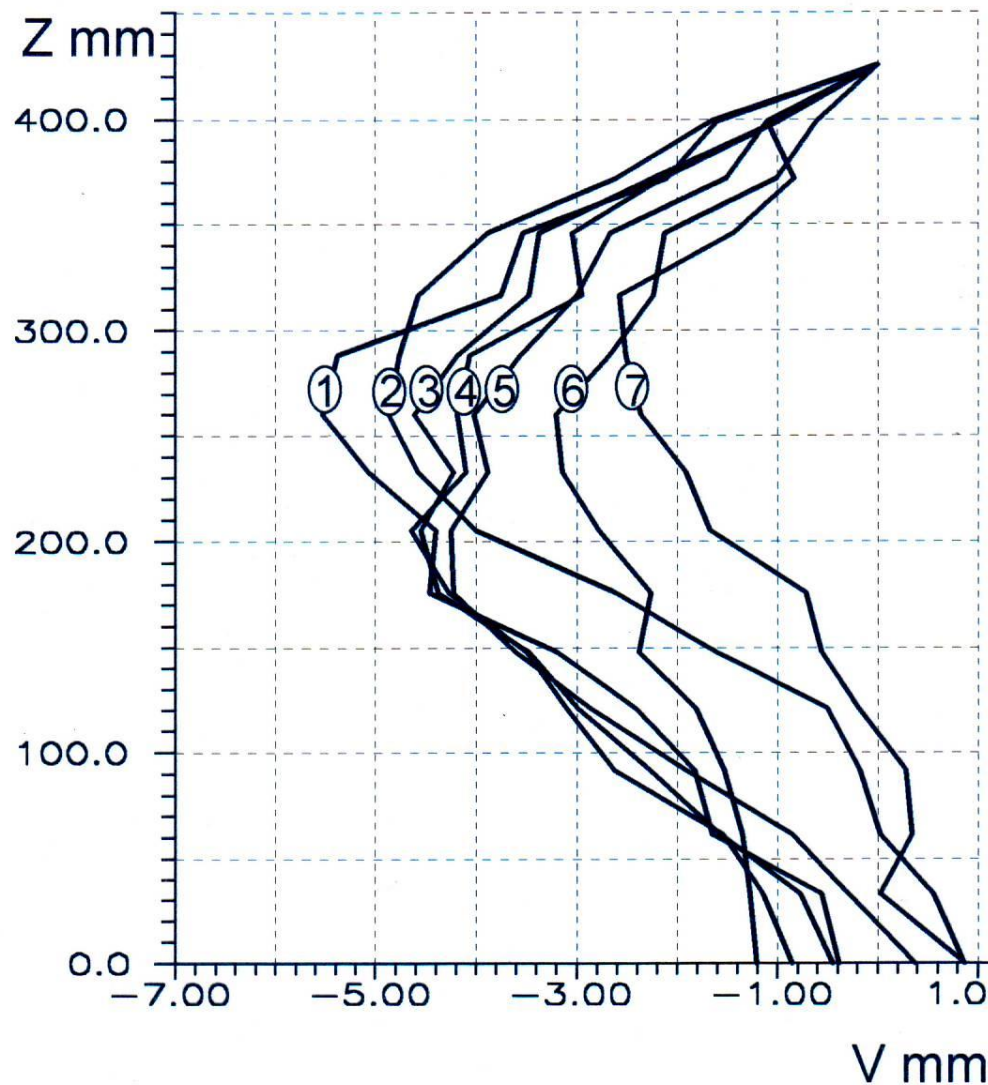
(Subject S.B., *asymmetric* external load  $1 \times 200N$  held in the left hand.)



**Averaged experimental results of subsequent six measurements:**

V - dislocations in the sagittal plane of the markers stuck on the skin above the spinal processes, Z - height of the trunk measured from level L5/S1.

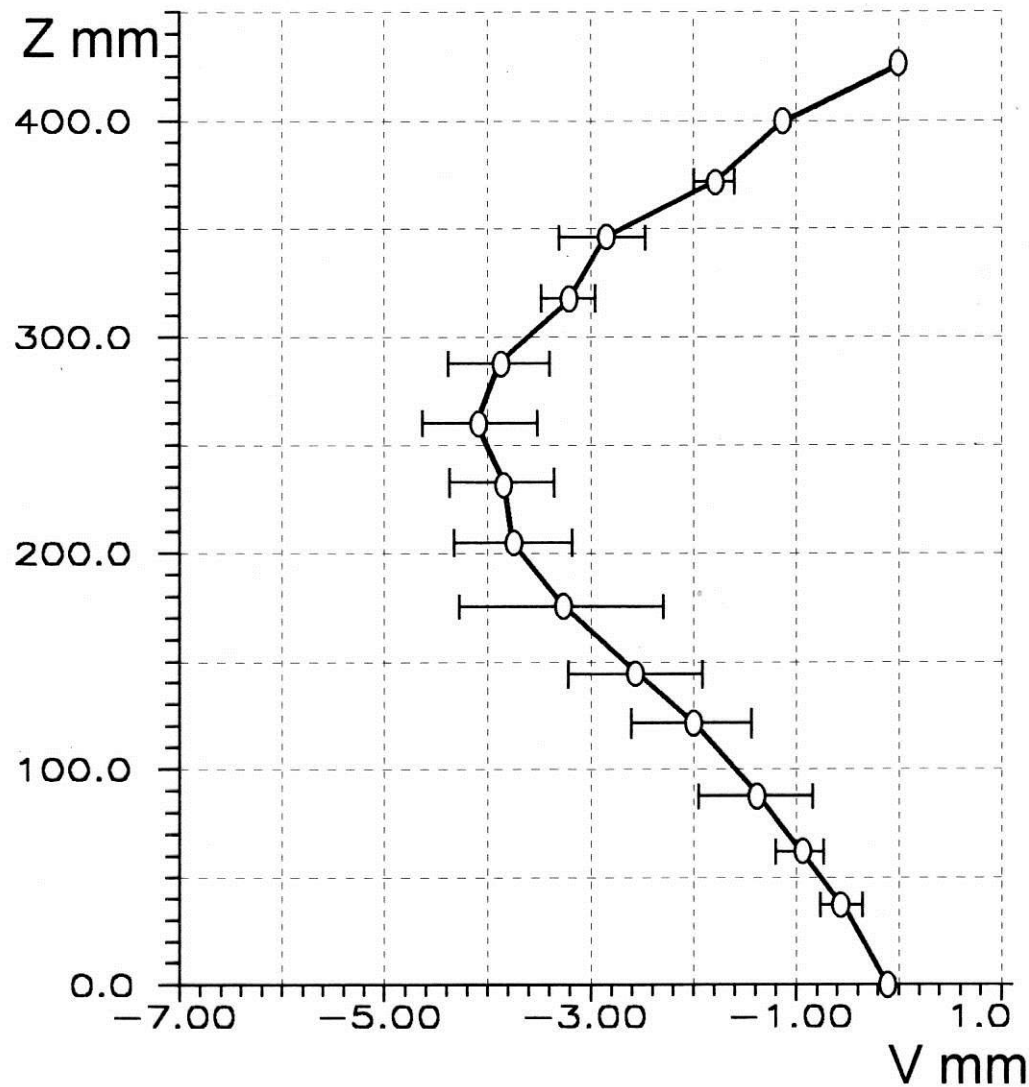
*(Subject S.B., asymmetric external load  $1 \times 200\text{N}$  held in the left hand.)*



### Experimental results:

V - dislocations in the sagittal plane of the markers stuck on the skin above the spinal processes, Z - height of the trunk measured from level L5/S1; ①÷⑦ - results of succeeding experiments.

(Subject S.B., *symmetric* external load  $2 \times 200\text{N}$  held in hands.)

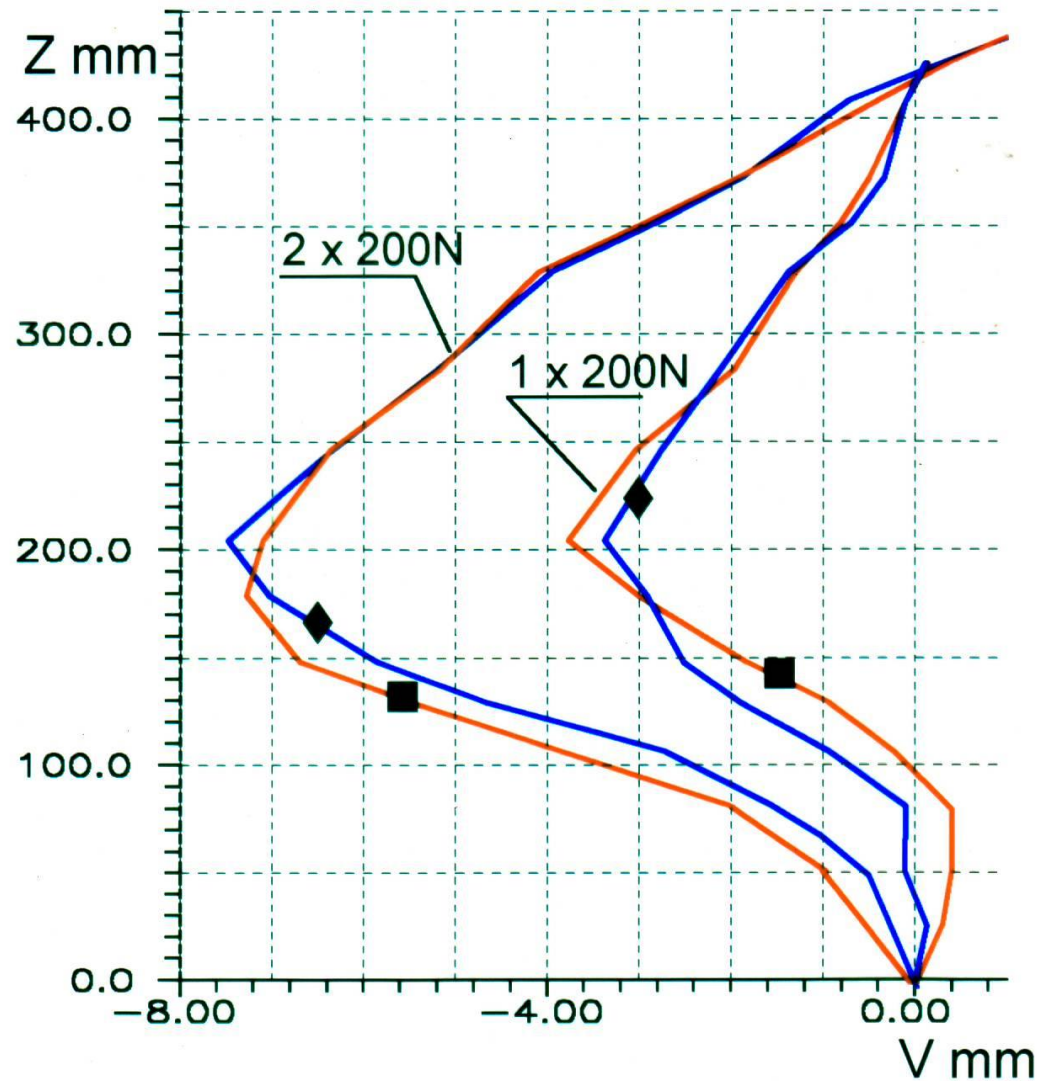


**Averaged experimental results of subsequent seven measurements:**

V - dislocations in the sagittal plane of the markers stuck on the skin above the spinal processes, Z - height of the trunk measured from level L5/S1.

(Subject S.B., *symmetric* external load  $2 \times 200\text{N}$  held in hands.)



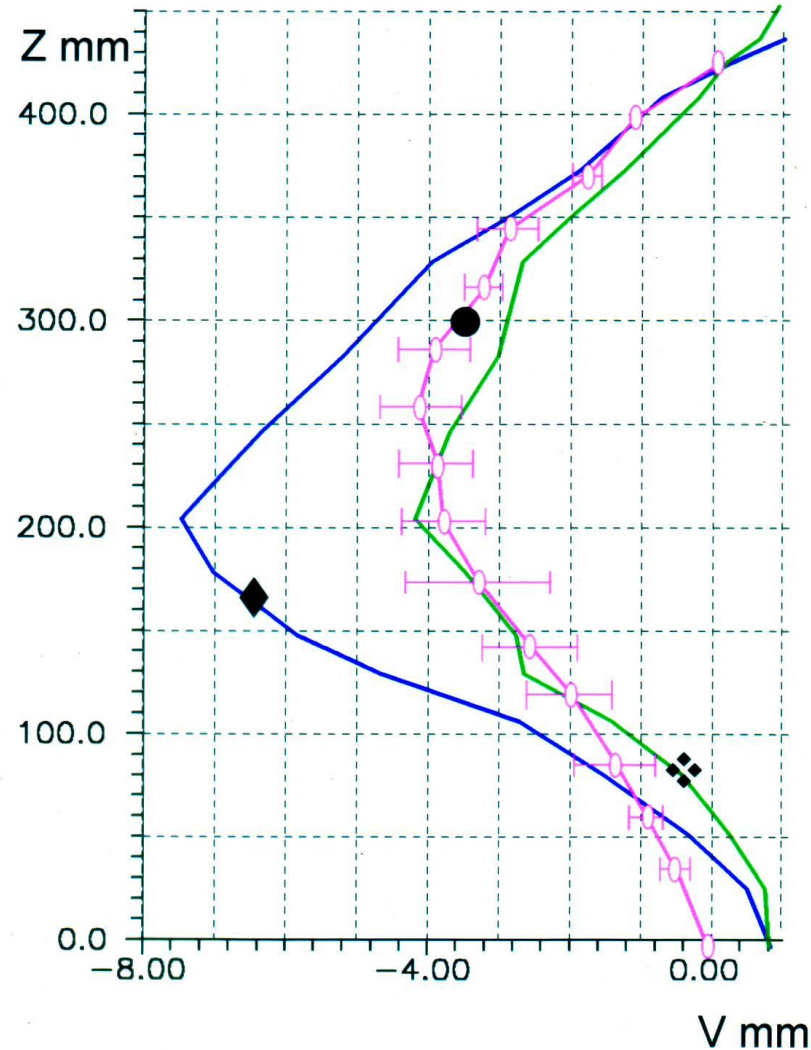


### Theoretical results:

V - dislocations of the spinal processes in the sagittal plane due to external load,  
 Z - height of the trunk measured from level L5/S1; ♦ - **energetic criterion**, ■ - **soft saturation criterion**

(Subject S.B., **symmetric** external load  $2 \times 200\text{N}$  held in hands or **asymmetric** load  $2 \times 200\text{N}$  held in the left hand.)

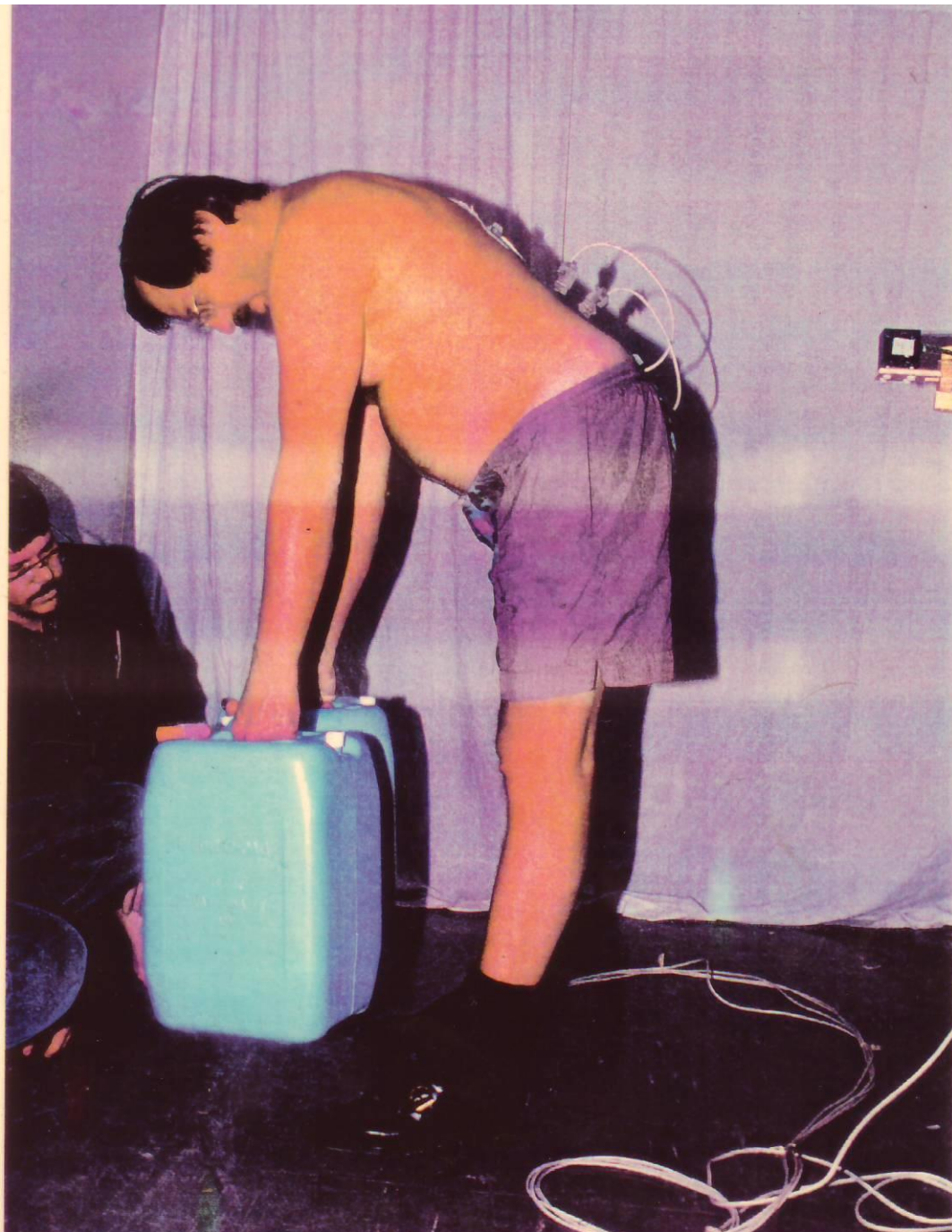


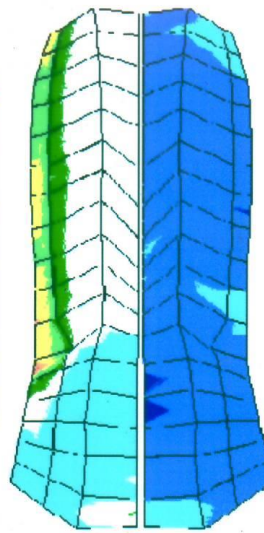
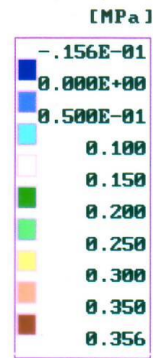


### Comparison of theoretical results and experimental ones:

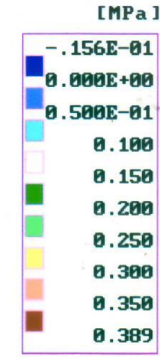
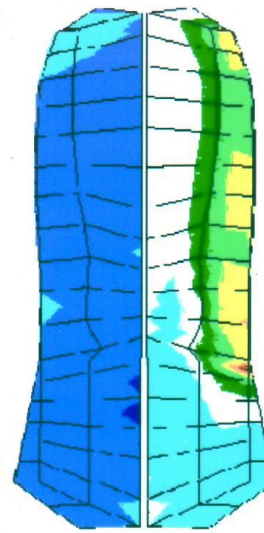
V - dislocations in the sagittal plane of the spinal processes due to external load, Z - height of the trunk measured from level L5/S1, ● - averaged experimental results of subsequent seven measurements, ◆ - theoretical results of linear analysis, ❖ - theoretical results of non-linear analysis.

(Subject S.B., *symmetric* external load  $2 \times 200\text{N}$  held in hands.)

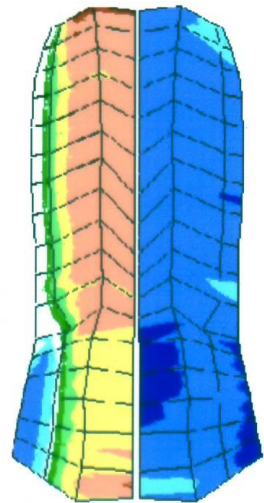
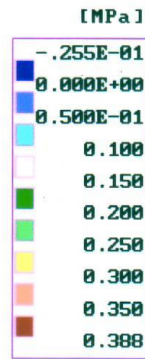




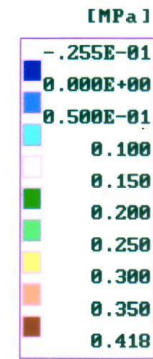
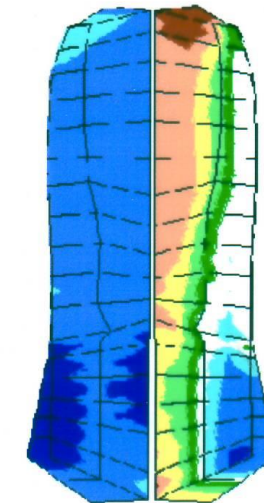
a)



b)



c)

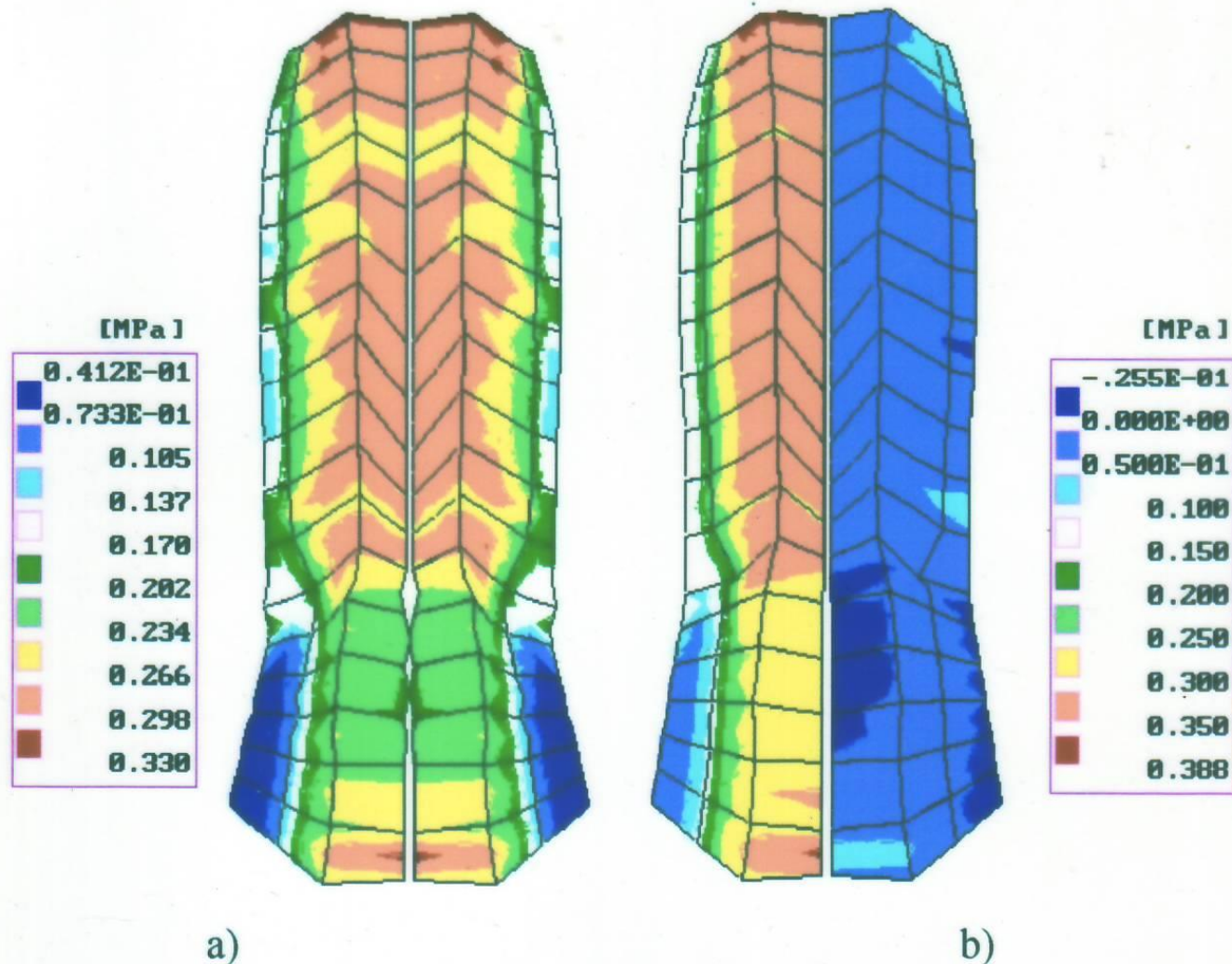


d)

Distributions of tension along muscle fibres in erector spinae muscle due to external load of  $1 \times 200\text{N}$  held in the left hand; for the energetic criterion: a) front view, b) back view; for the soft saturation criterion: c) front view, d) back view.

*(Initial position of the body - straightened, linear analysis)*

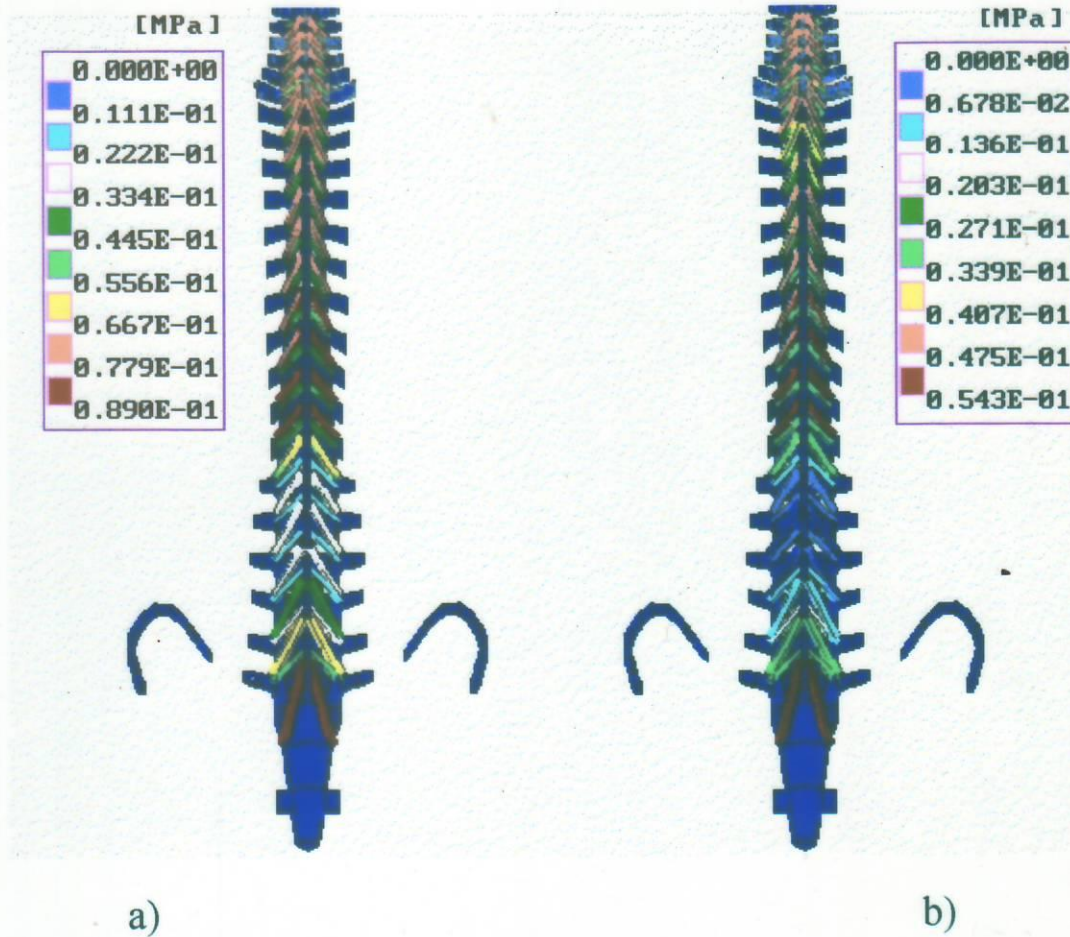




Tension distribution along muscle fibres in erector spinae muscle, front view:  
 a) due to external load of  $2 \times 200\text{N}$  held in hands, b) due to  $200\text{N}$  held in the left hand.

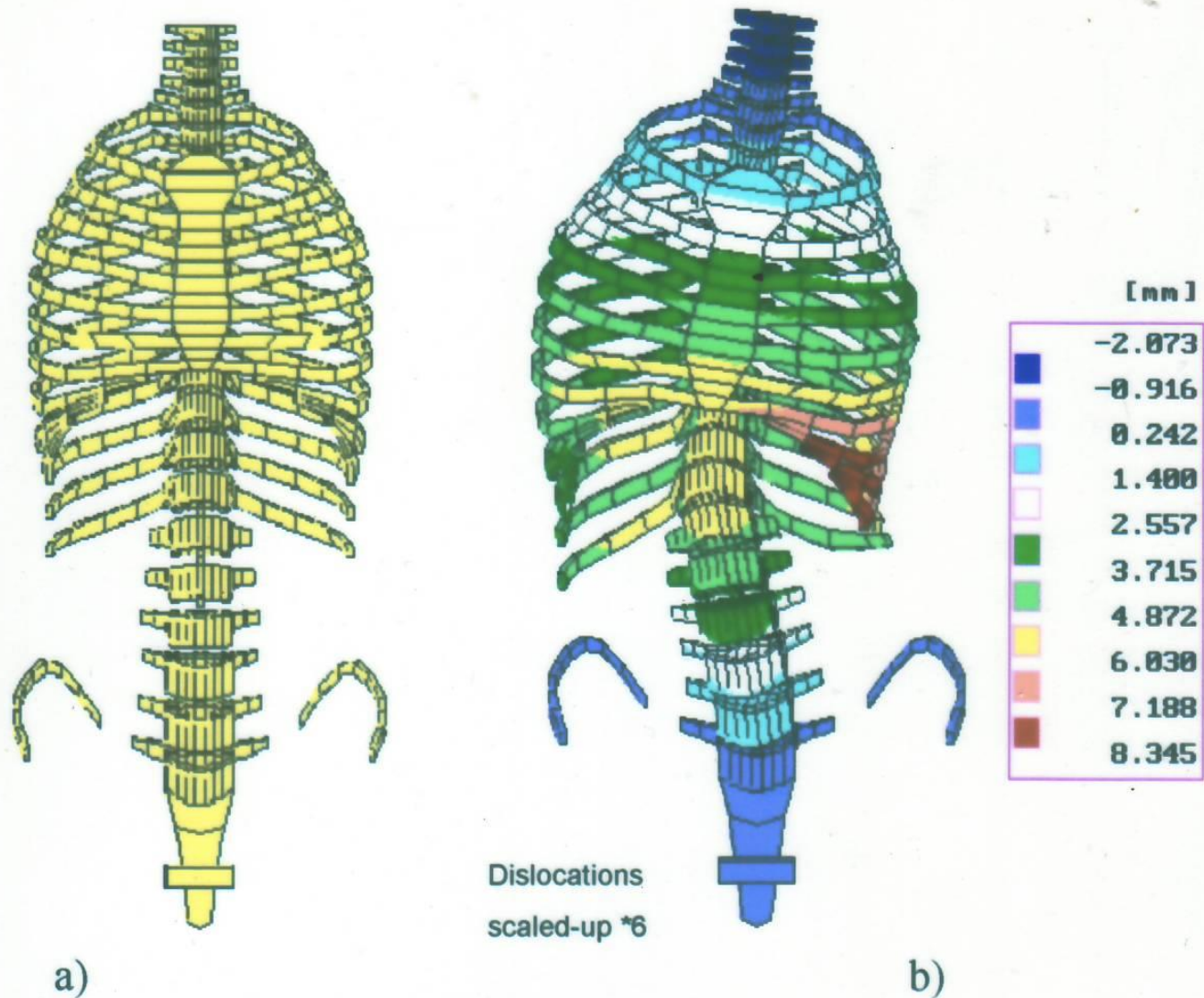
*(Initial position of the body - straightened, soft saturation criterion, linear analysis)*





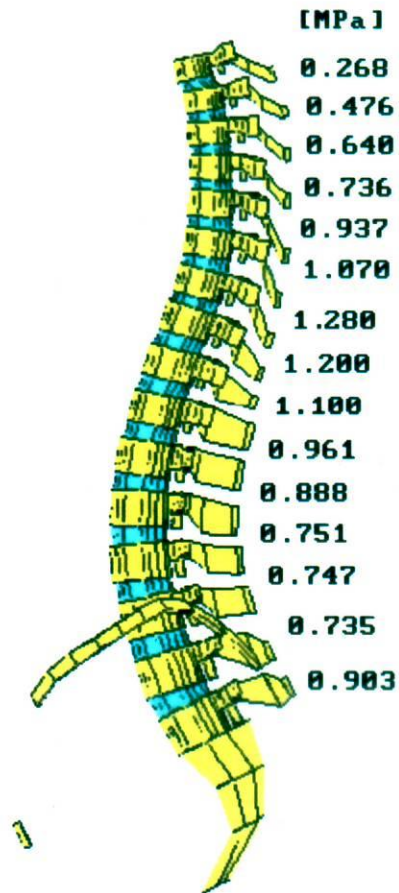
Distribution of tension in rotatores due to external load of  $2 \times 200\text{N}$  held in hands in the straightened position of the body - back view: a) for the energetic criterion, b) for the soft saturation criterion.

*(Initial position of the body - straightened, linear analysis)*

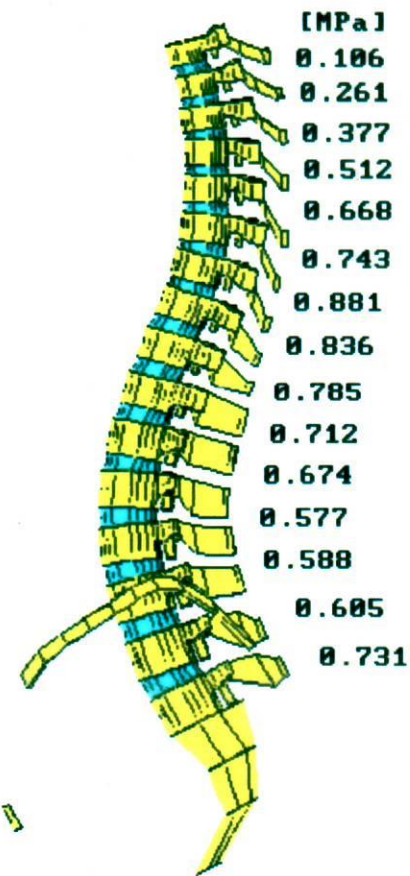


Dislocations of the ribs and vertebrae in the frontal plane: a) due to external load of  $2 \times 200\text{N}$  held in hands; b) due to  $200\text{N}$  held in the left hand.

*(Initial position of the body - straightened, soft saturation criterion, linear analysis)*



a)

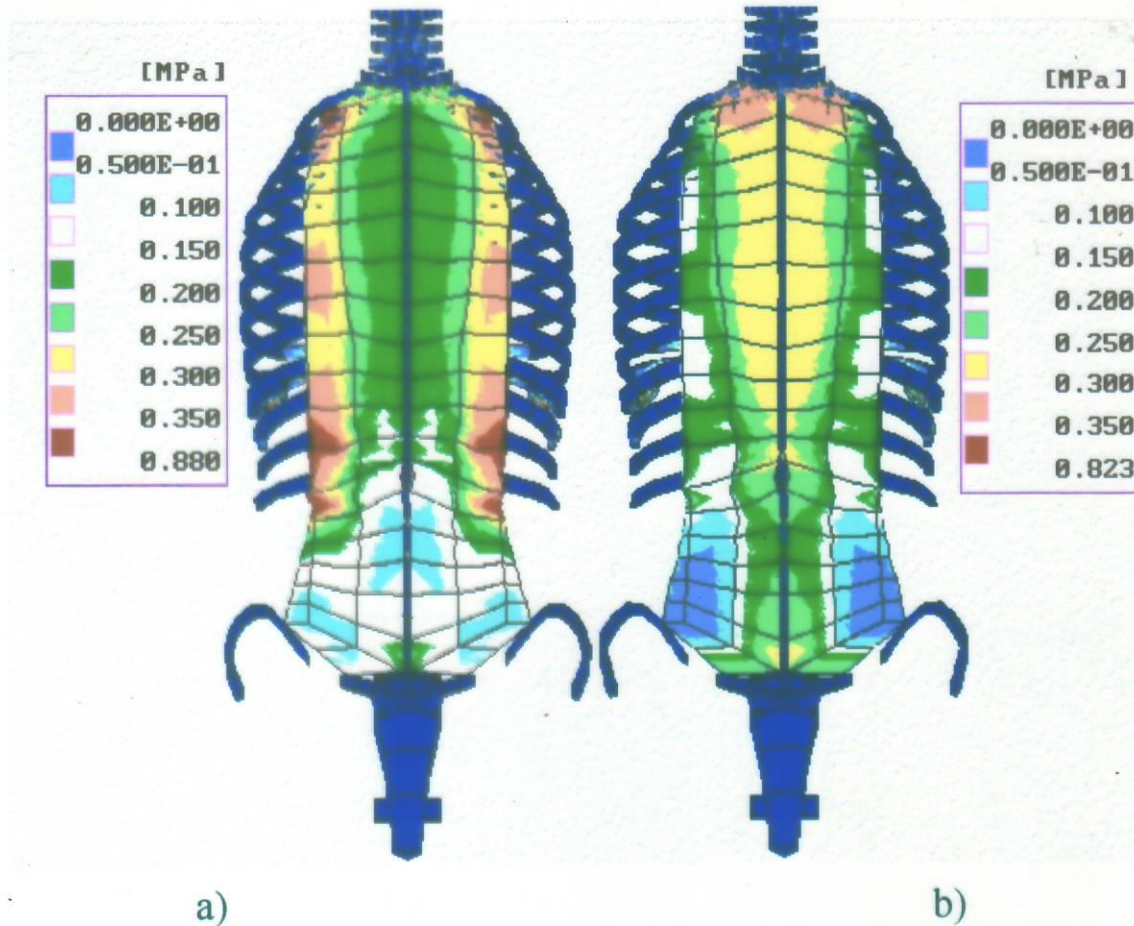


b)

Pressure distribution along the spinal column in nuclei pulposi of the intervertebral discs: a) due to external load of  $2 \times 200\text{N}$  held in hands, b) due to  $200\text{N}$  held in the left hand.

*(Initial position of the body - straightened, soft saturation criterion, linear analysis)*

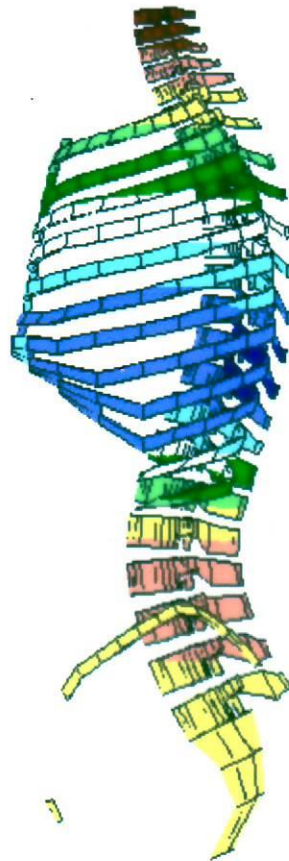
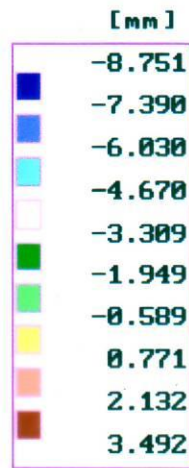




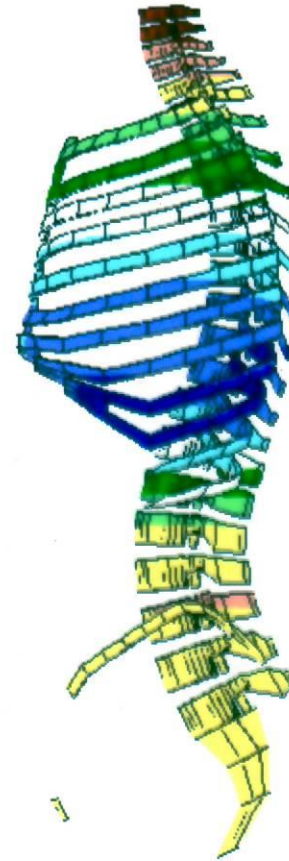
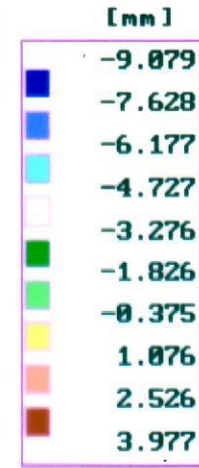
Distribution of tension along muscle fibres in erector spinae muscle due to external load of  $2 \times 200\text{N}$  held in hands in the straightened position of the body  
 - back view: a) for the energetic criterion, b) for the soft saturation criterion.

*(Initial position of the body - straightened, linear analysis)*





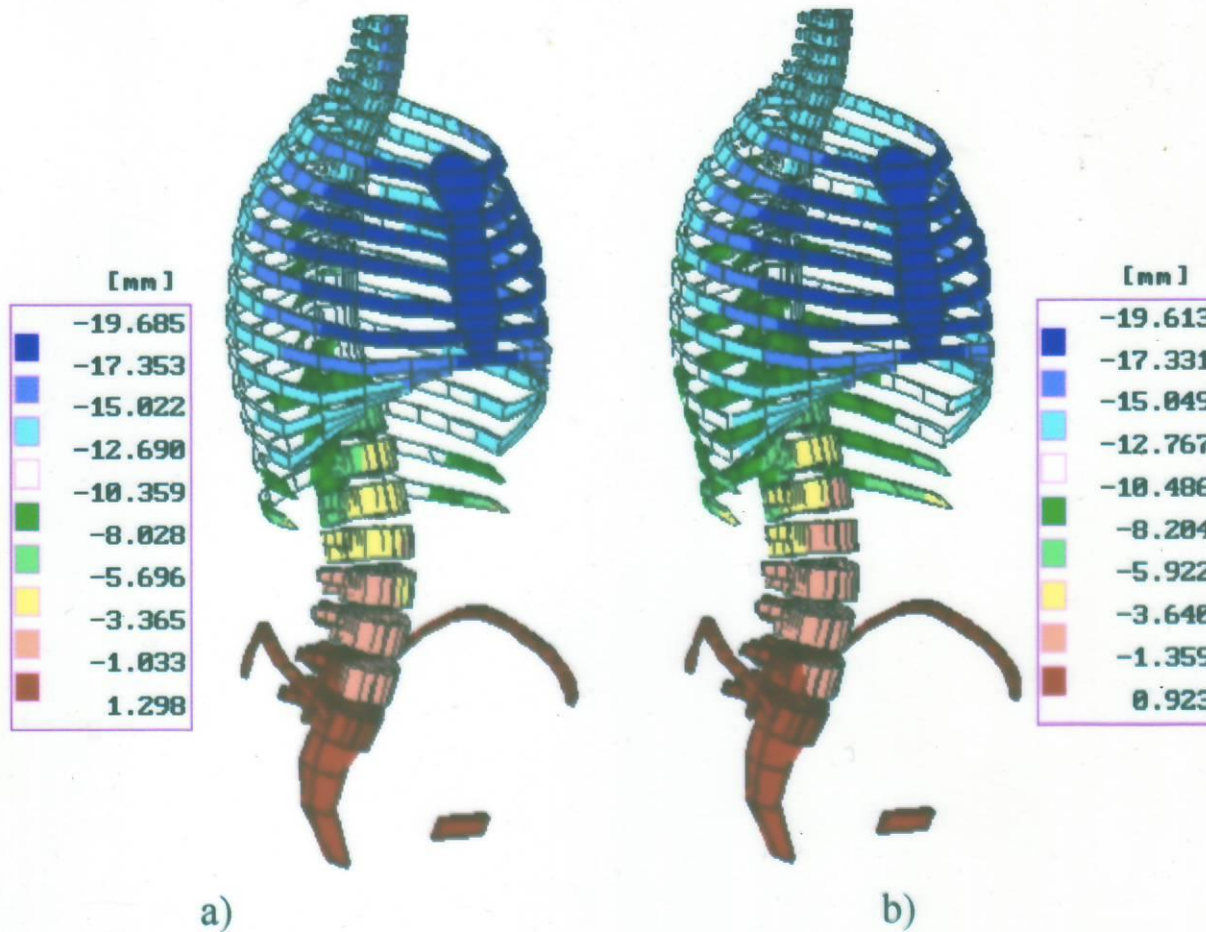
a)



b)

Horizontal dislocations of the ribs and vertebrae in the sagittal plane due to external load of  $2 \times 200\text{N}$  held in hands, a) for the energetic criterion, b) for the soft saturation criterion.

*(Initial position of the body - straightened, linear analysis)*

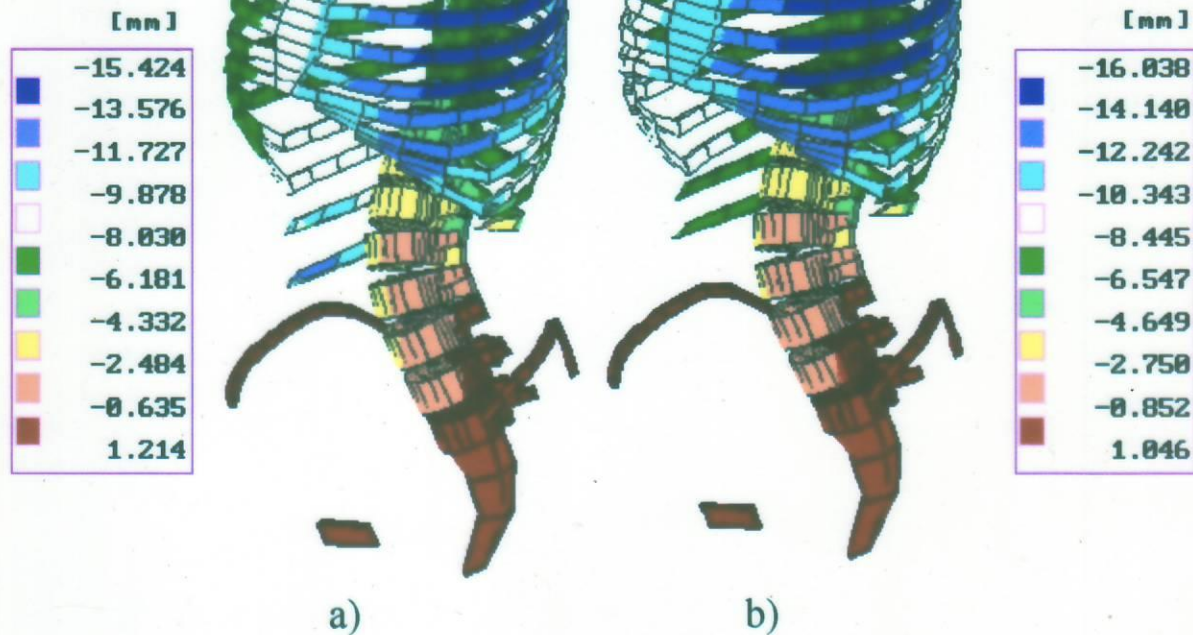


Vertical dislocations of the ribs and vertebrae due to external load of  $2 \times 200\text{N}$  held in hands, a) for the energetic criterion, b) for the soft saturation criterion.

*(Initial position of the body - straightened, linear analysis)*



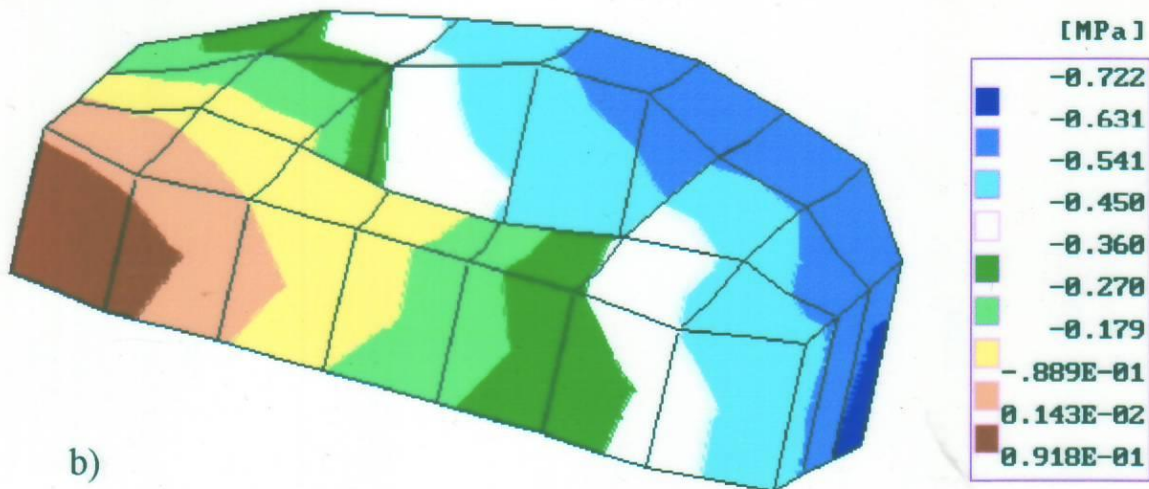
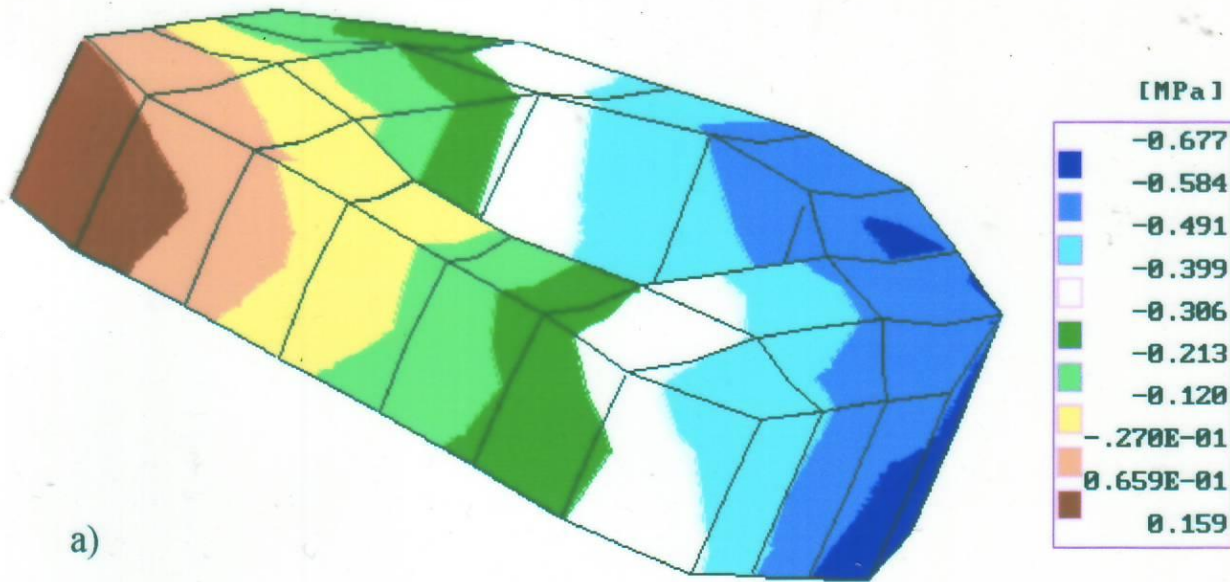
(Dislocations scaled-up \*6)



Vertical dislocations of the ribs and vertebrae due to external load of  $1 \times 200\text{N}$  held in the left hand: a) for the energetic criterion, b) for the soft saturation criterion.

*(Initial position of the body - straightened, linear analysis)*

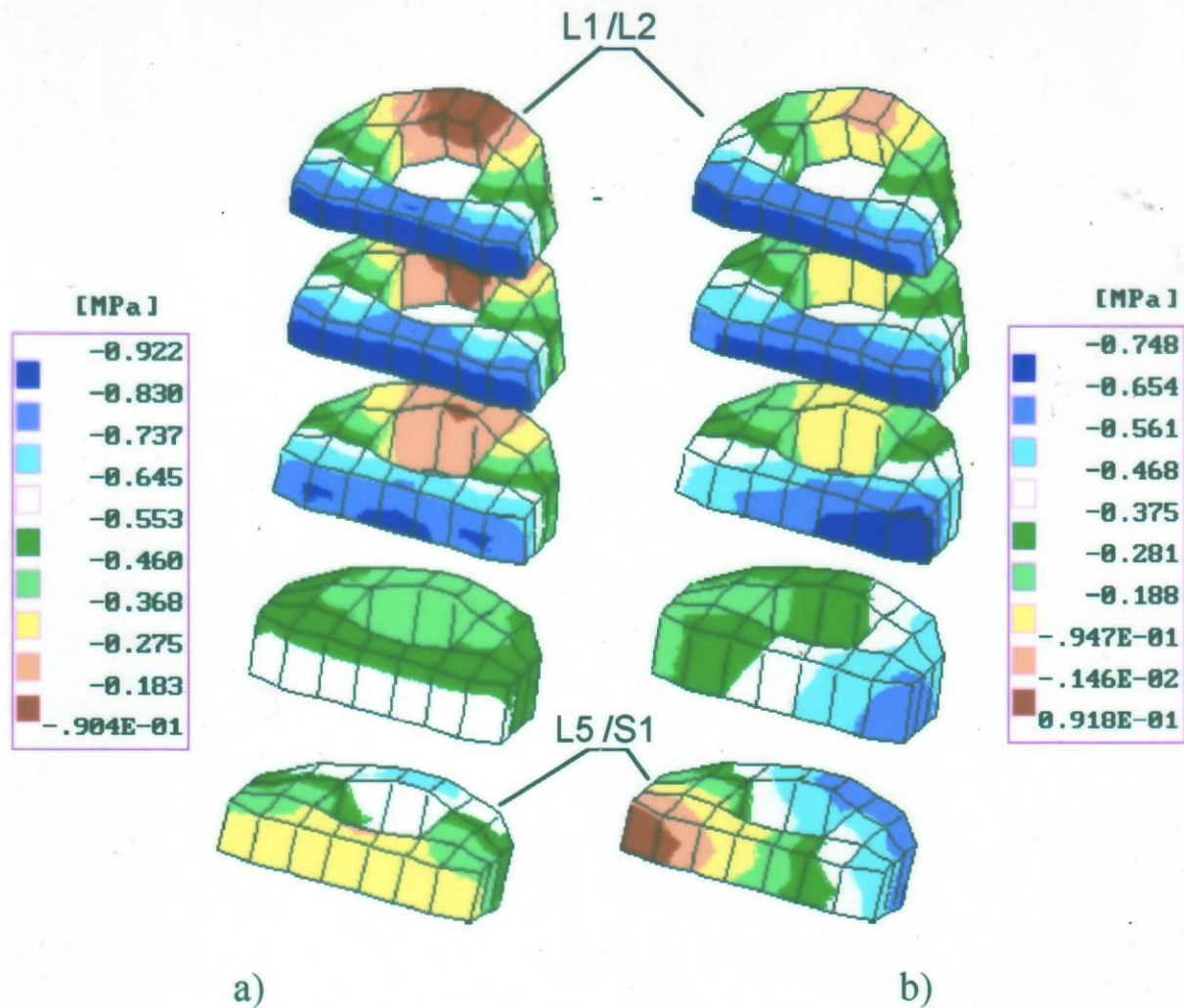




Compressive stress distribution in annuli fibrosi of the intervertebral disc L5 - S1 due to external load of  $1 \times 200\text{N}$  held in the left hand: a) for the energetic criterion, b) for the soft saturation criterion.

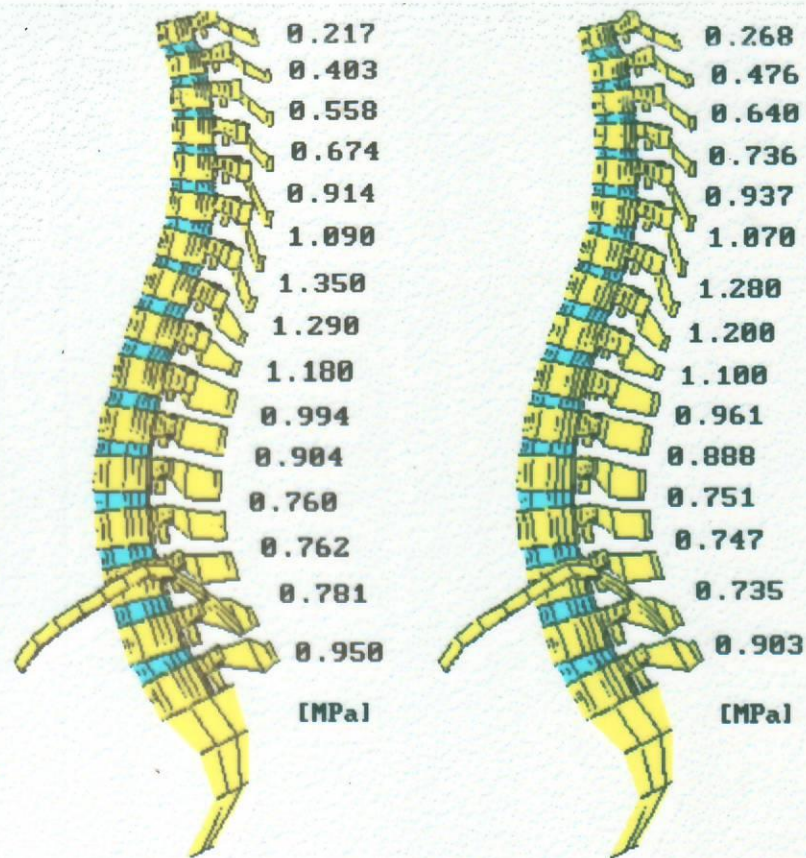
*(Initial position of the body - straightened, linear analysis)*





Compressive stress distribution in annuli fibrosi of the intervertebral discs L1-L5 (lumbar section): a) due to external load of  $2 \times 200\text{N}$  held in hands, b) due to  $200\text{N}$  held in the left hand.

*(Initial position of the body - straightened, soft saturation criterion, linear analysis)*



a)

b)

Pressure distribution along the spinal column in nuclei pulposi of the intervertebral discs due to external load of  $2 \times 200\text{N}$  held in hands in the straightened position of the body: a) for the energetic criterion, b) for the soft saturation criterion.

*(Initial position of the body - straightened, linear analysis)*

# BIOMECHANIKA KRĘGOSŁUPA



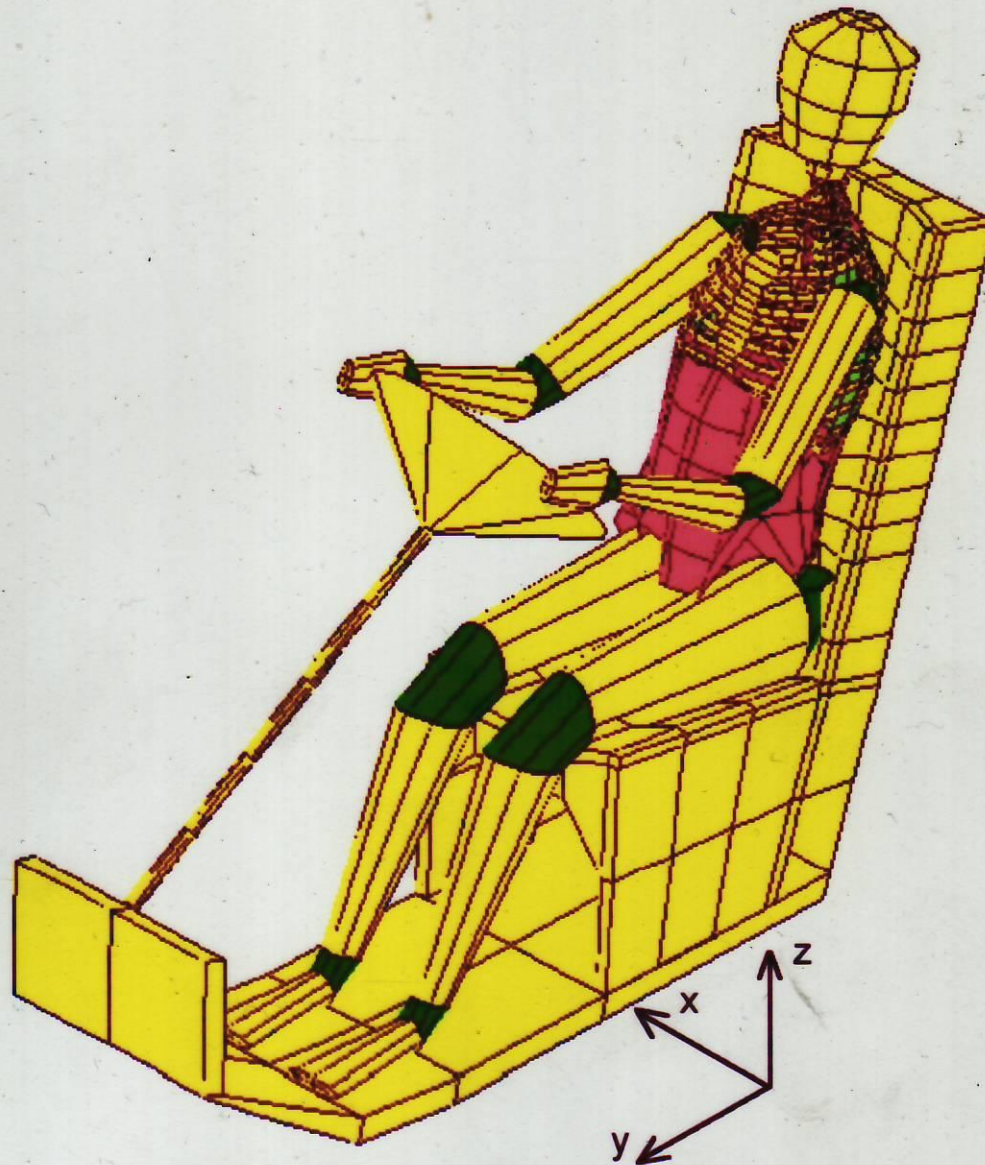
## DRGANIA CZŁOWIEKA







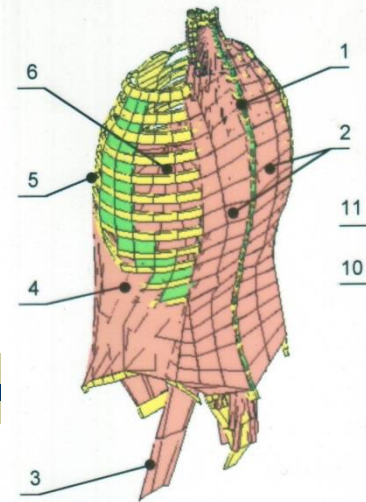
## FEM model of a man-operator under vibration.





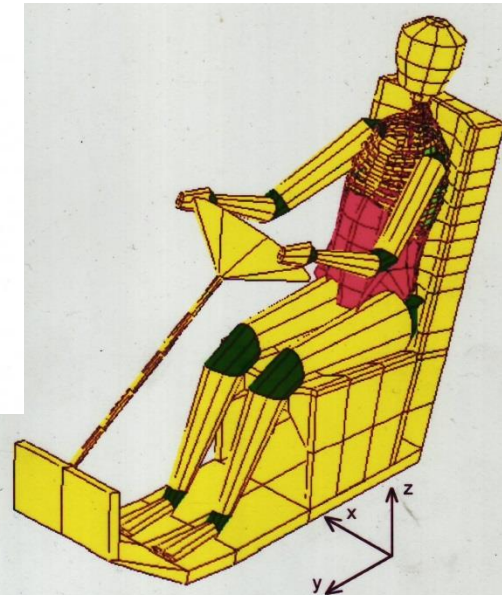


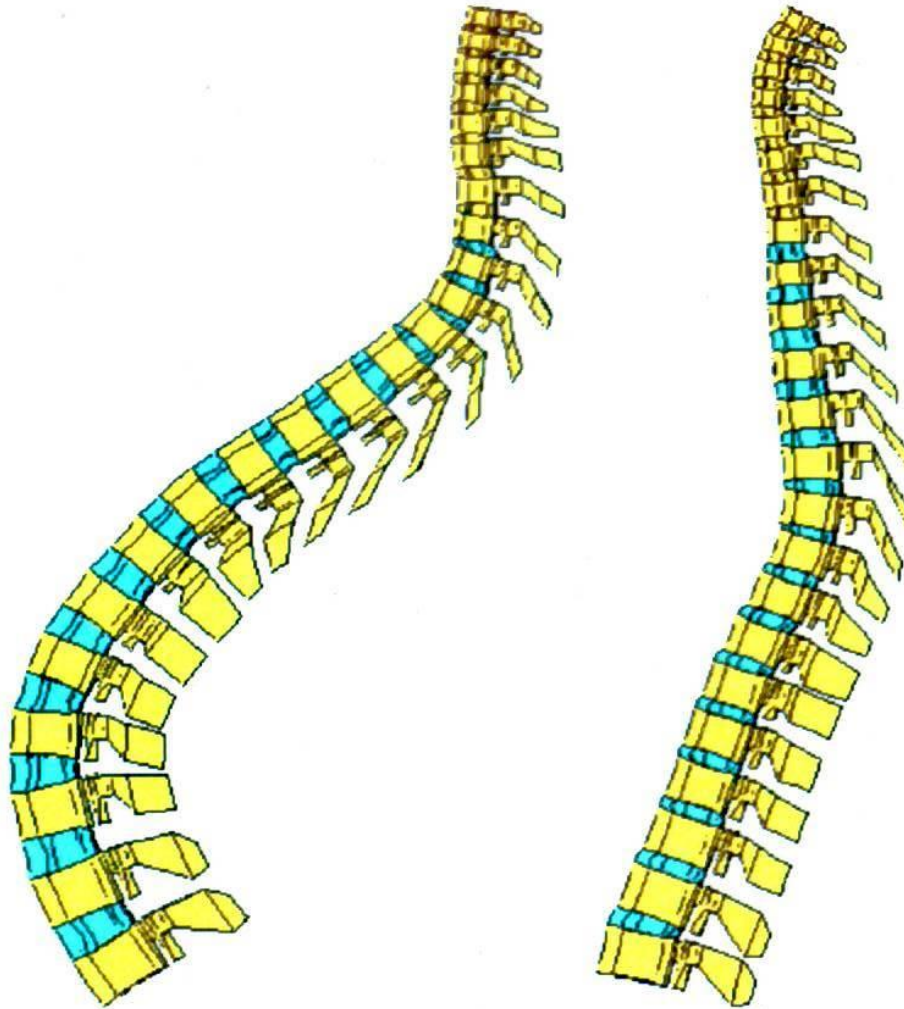
# Model tułowia



The three-dimensional FEM model of man-vehicle system used in this study is composed of 2936 rigid and flexible three-dimensional finite elements. The model is symmetric to the sagittal plane. The main part of the model is the structure of human spinal system (torso) built of 2640 finite elements.

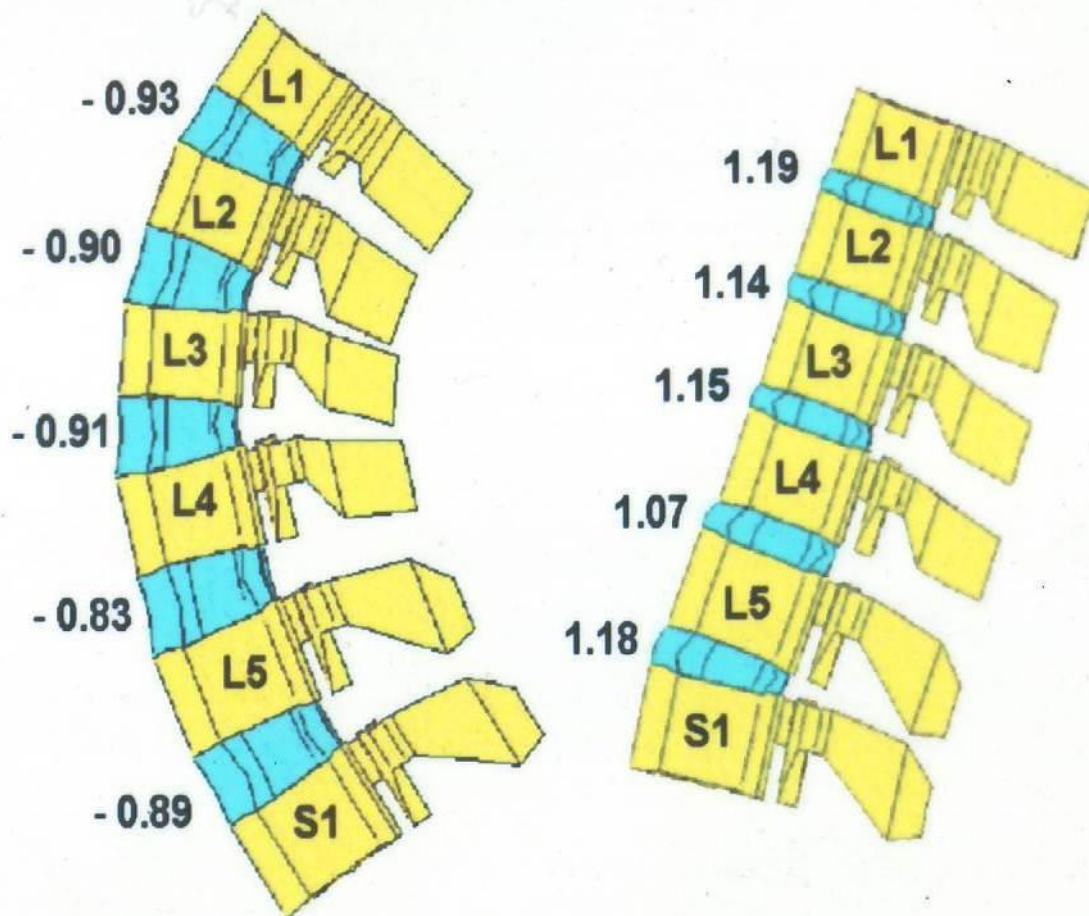
Limbs and head were divided into rigid finite elements regardless of their anatomical structure. The joints (i.e. elbows, wrists, knees, ankles) were modelled using flexible elements. The vehicle structure was modelled using rigid elements. The seat and backrest surface was modelled using flexible elements; a number of finite elements nodes of the seat-backrest surface and the body surface (thighs and back) are common (so called “back-on” position of the operator’s body).



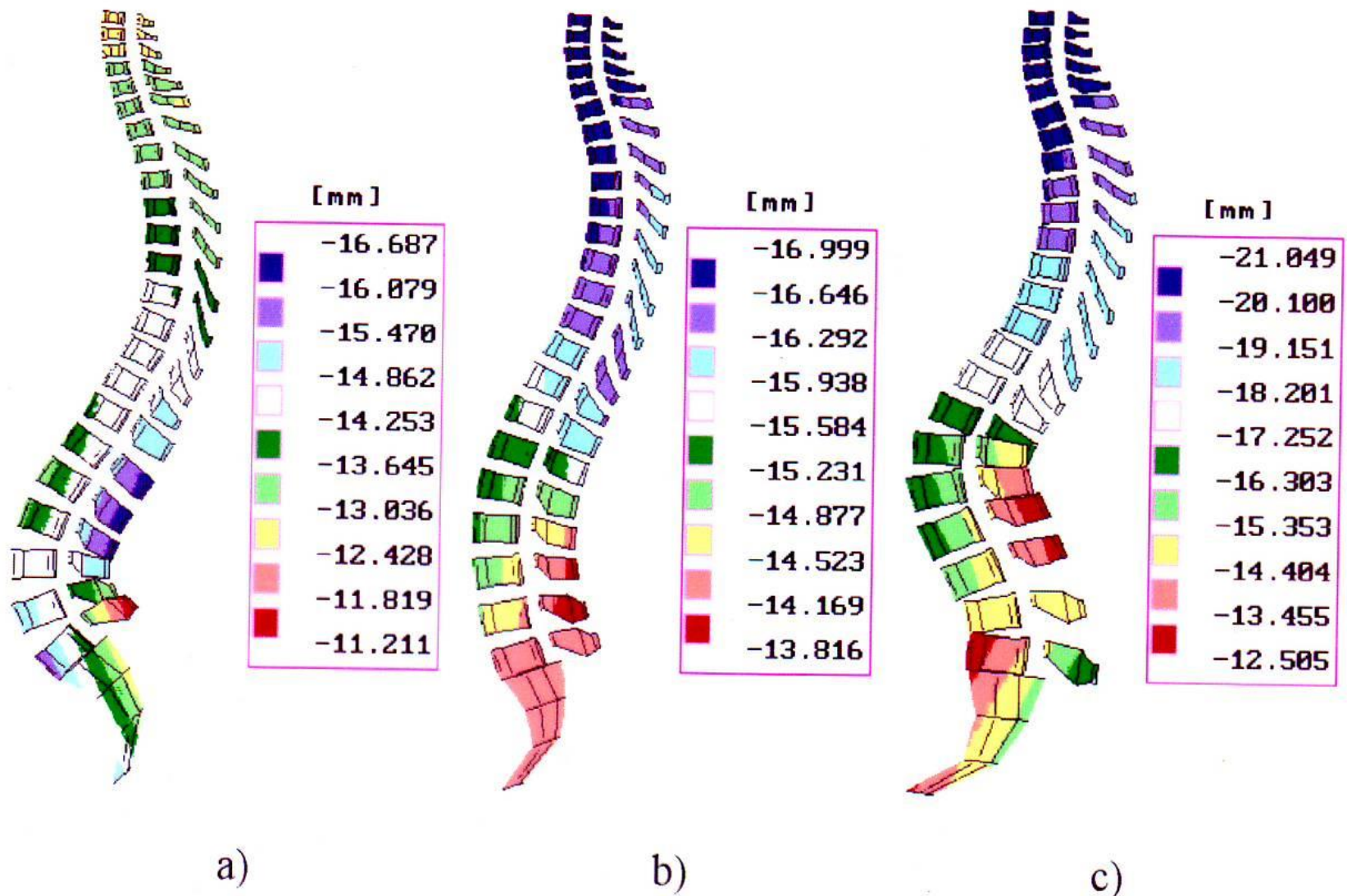


Extreme positions of the spinal column (vertebrae and intervertebral discs) for one cycle of vibration at the frequency 23,2 Hz; displacements are scaled up  $\times 5$ .





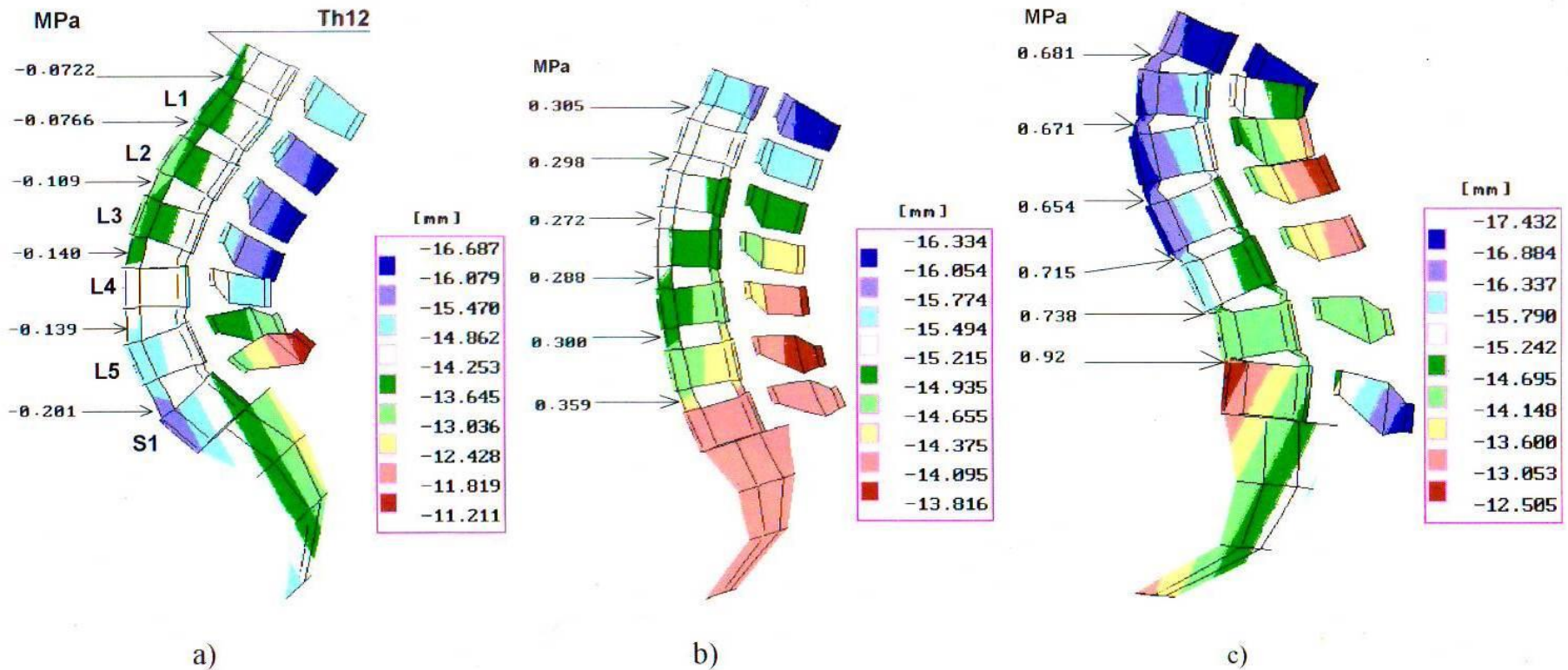
Extreme positions of the lumbar section of spinal column for one cycle of vibration at the frequency 23,2 Hz; pressure values in nuclei pulposi of the intervertebral discs are marked, in MPa (negative pressure means hypotension in nucleus).



Extreme positions (vertical displacements) of the spinal column (vertebrae and intervertebral discs) for one cycle of vibration at the frequency 15.75 Hz (theoretical results): a) and c) - extreme positions, b) neutral position; displacements scaled up  $\times 10$ .

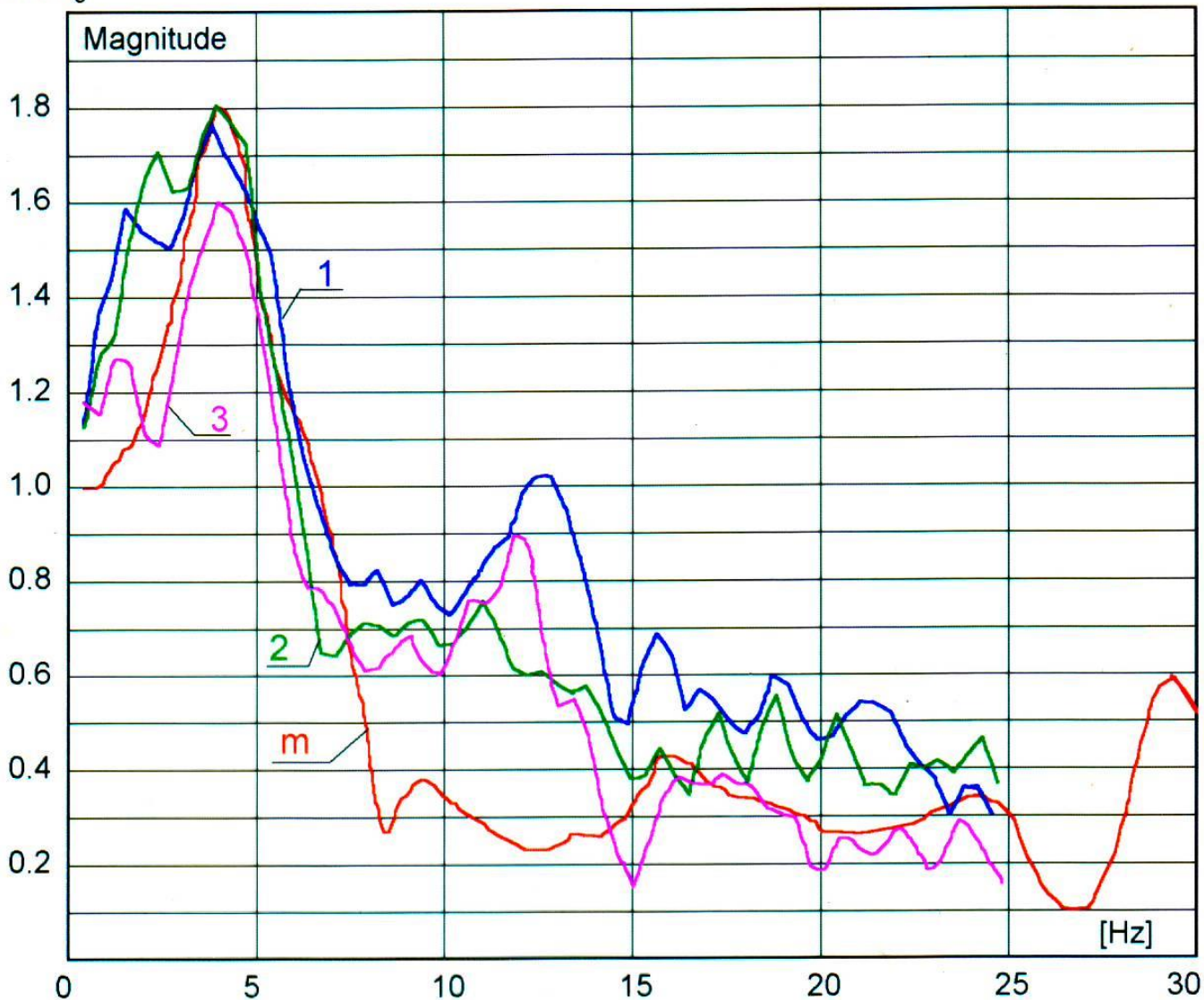


# Częstość drgań 15,75 Hz



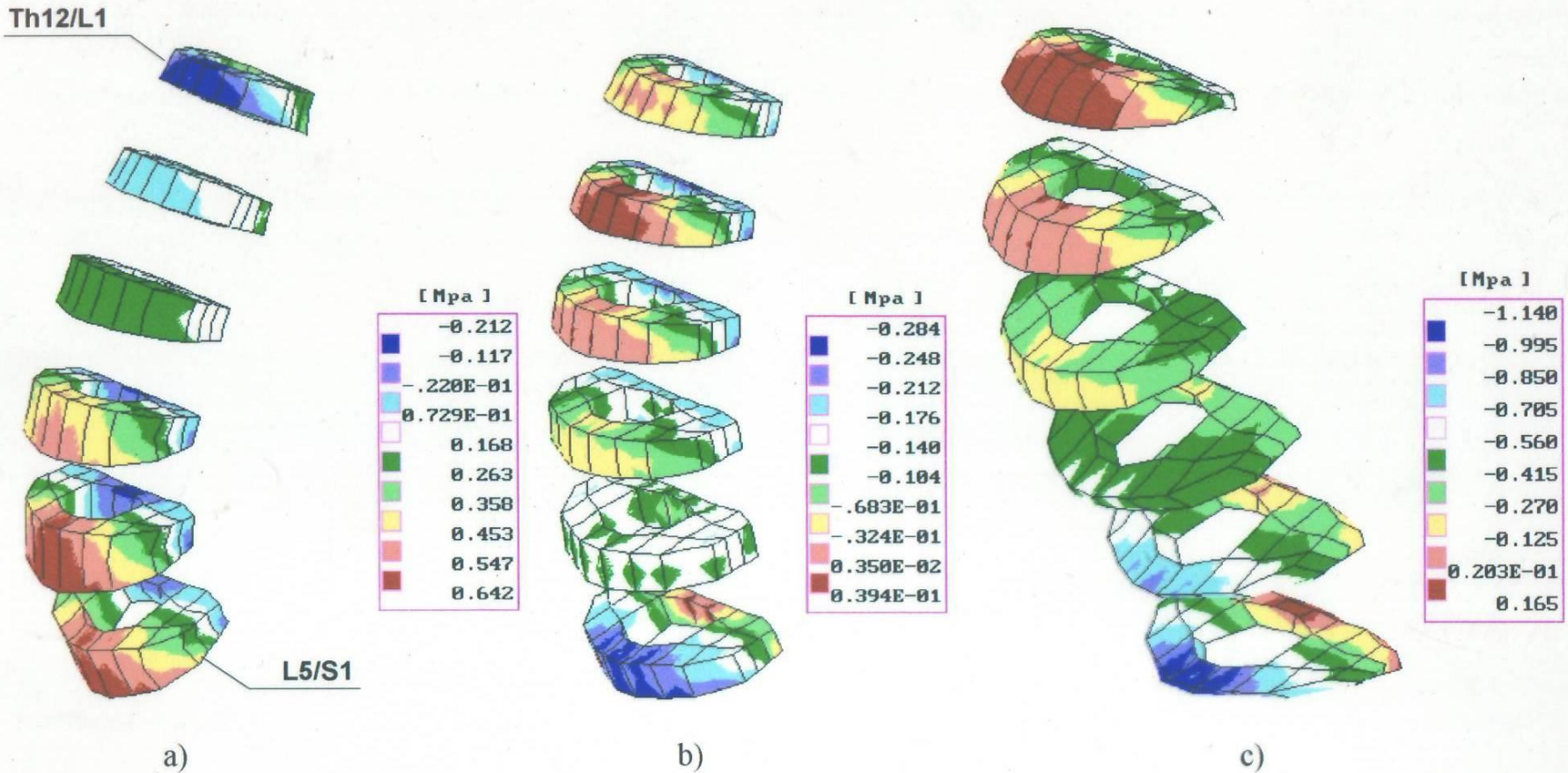
Extreme positions (vertical displacements) of the lumbar section of the spinal column for one cycle of vibration at the frequency 15.75 Hz (theoretical results); pressure values in nuclei pulposi of intervertebral discs are marked in MPa (negative pressure means hypotension); a) and c) - extreme positions, b) neutral position; displacements scaled up  $\times 10$ .



$A/A_0$ 

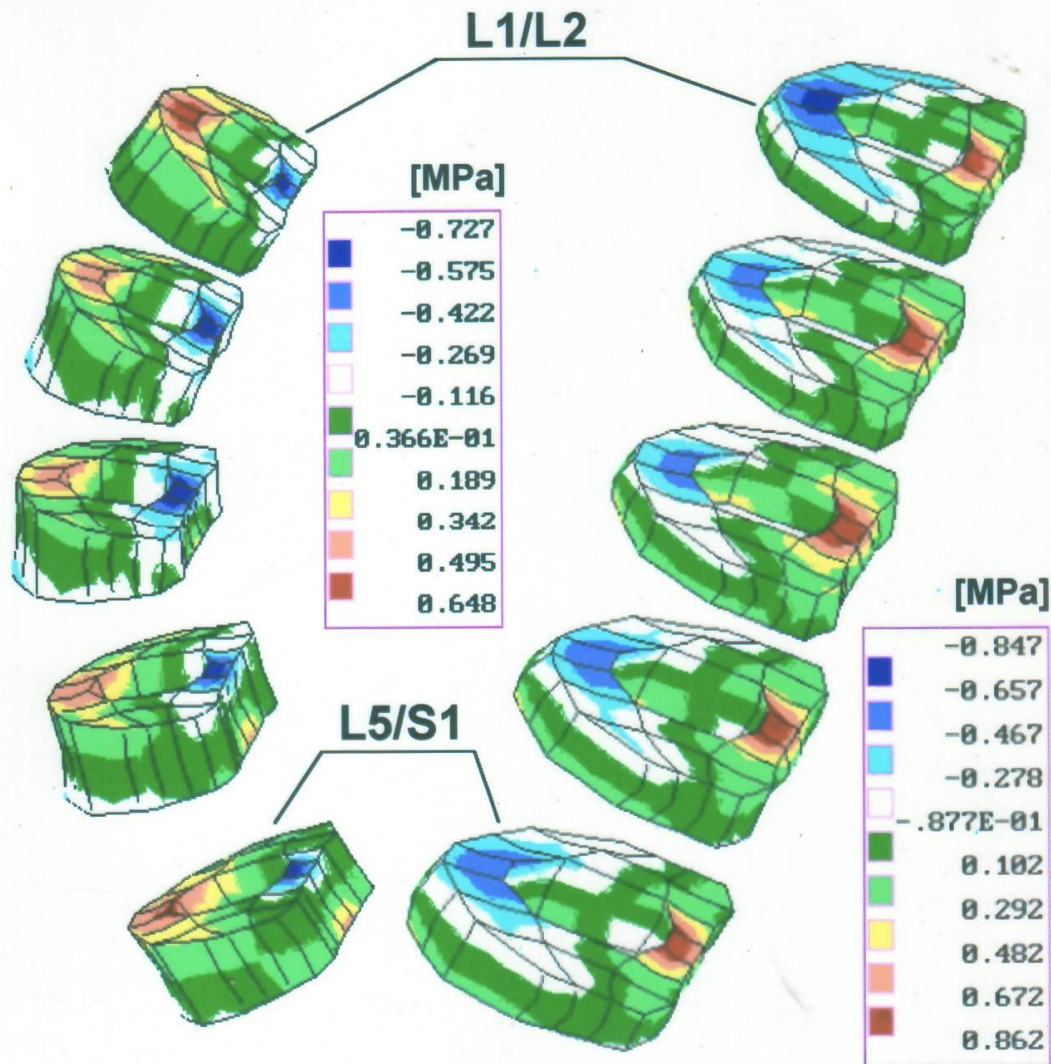
Transfer function magnitude, i.e. vertical amplitude ratios of output (head) amplitude  $A$  divided by input (seat) amplitude  $A_0$  as a function of frequency: 1, 2, 3 - number of test (experimental results), m - theoretical curve based on FEM model.

# Naprężenia ściskające



Compressive stress distributions in annuli fibrosi of the intervertebral disc of the lumbar section for extreme positions for one cycle of vibration at the frequency 15.75 Hz (theoretical results); negative stress means compressing, positive - stretching; a) and c) - extreme positions, b) neutral position; deformations scaled up  $\times 10$ .





Shear stress distributions in annuli fibrosi of the intervertebral discs of the lumbar section of the spine for the extreme positions for one cycle of vibration at the frequency 23,2 Hz.



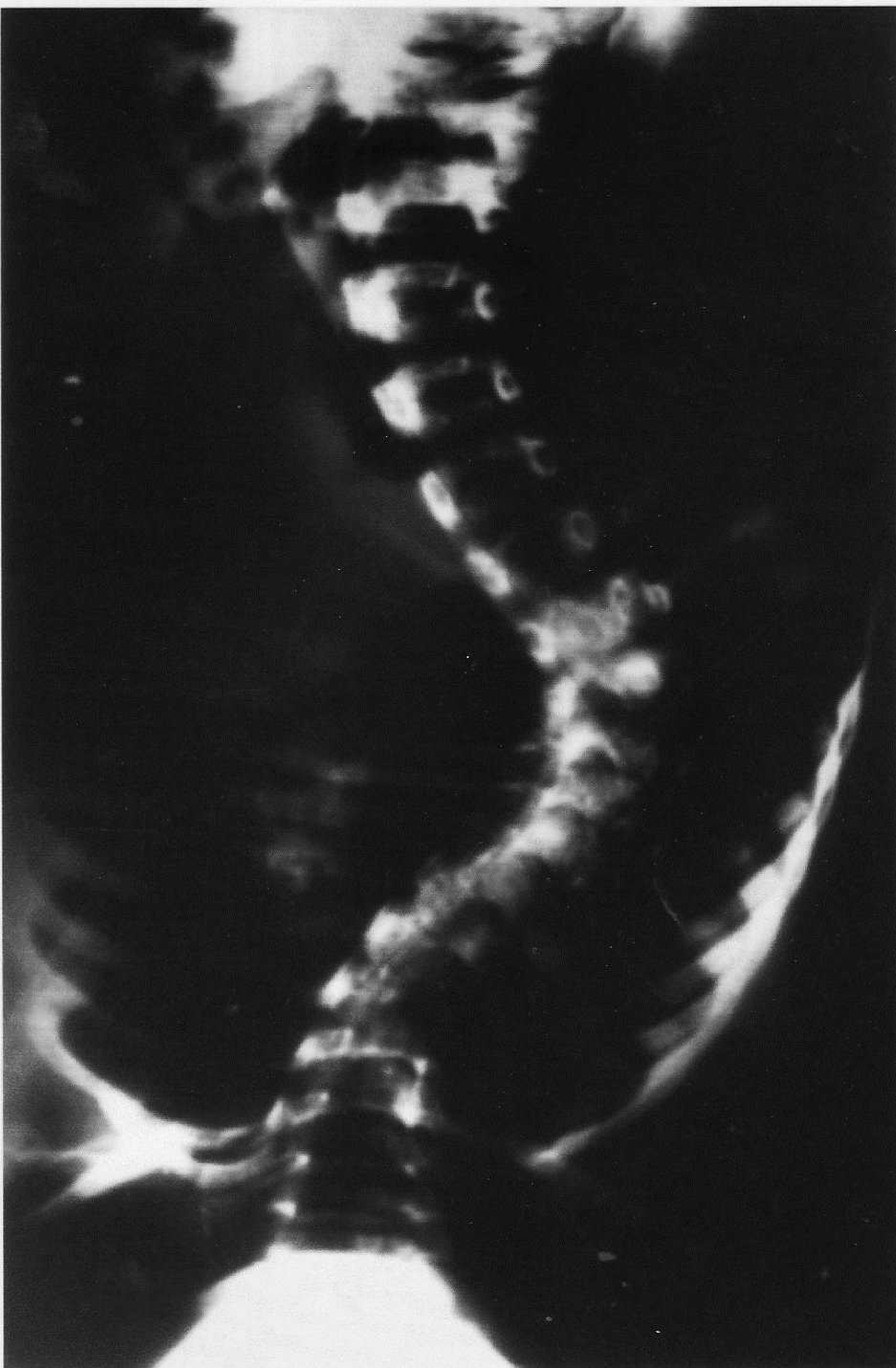
# BIOMECHANIKA KRĘGOSŁUPA



**Skolioza**

**czyli utrata stateczności?**











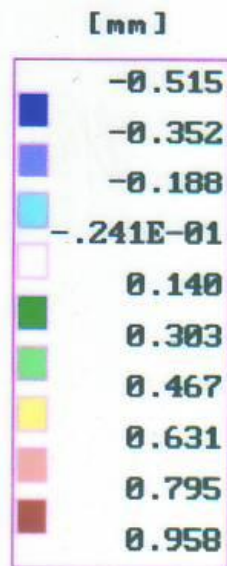
# Stateczność

In the technical systems the rods, or slender constructions similar to the rods, axially compressed shorten, but in the beginning they maintain the balance without the shape change. If the load exceeds the certain critical value, they loose the first, symmetrical form of stability and undergo the flexural deformation.

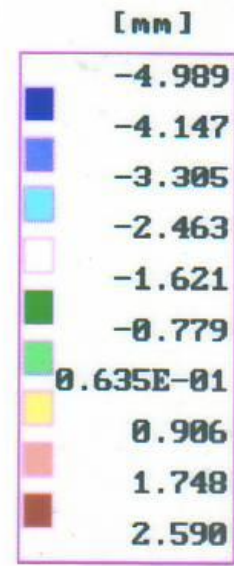


# Analiza liniowa

Linear analysis means that the non-linear equations are linearized for the considered spine position. Non-linear approach takes into account the material and geometrical non-linearities of the model. The geometrical non-linearity means that deformation caused by an external load changes the distribution of that load. Due to that the computation has to be carried out using step-by-step method (modified Newton-Raphson method). The external load has to be increased gradually, from zero up to the given value. The non-linear computation lasts usually about 20 times longer than linear one.



a)

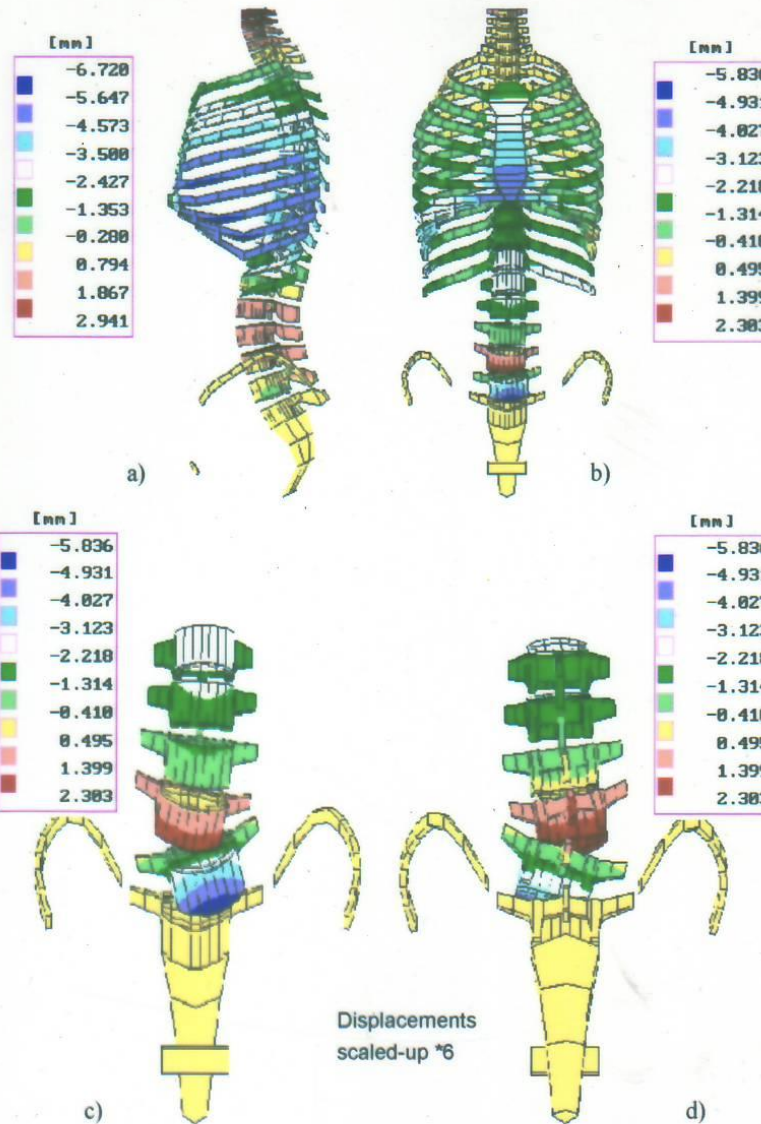


b)

Spine equilibrium in the first, symmetrical state of stability, side view.  
 Displacements in sagittal plane due to: a) body weight 300N, b) body weight and external load  $2 \times 191.5\text{N} = 383\text{N}$  held in hands.

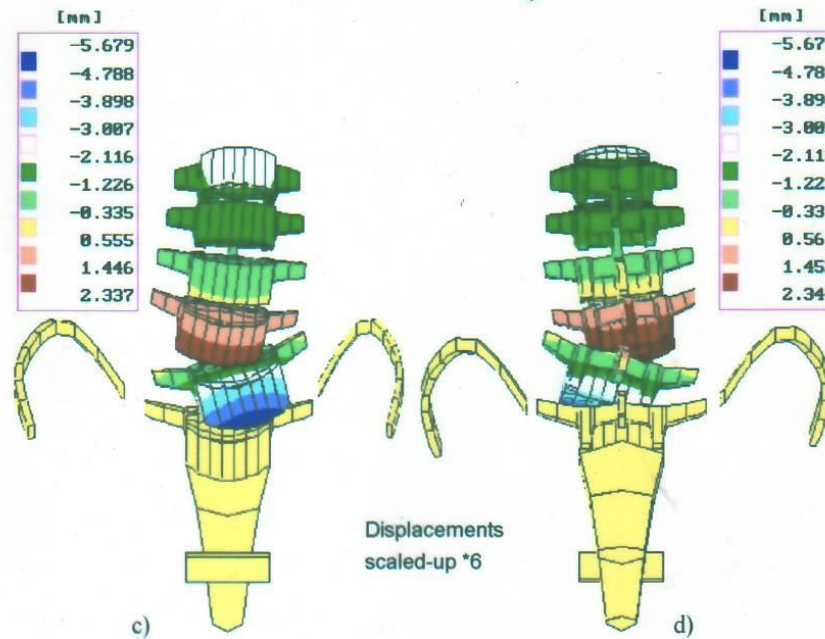
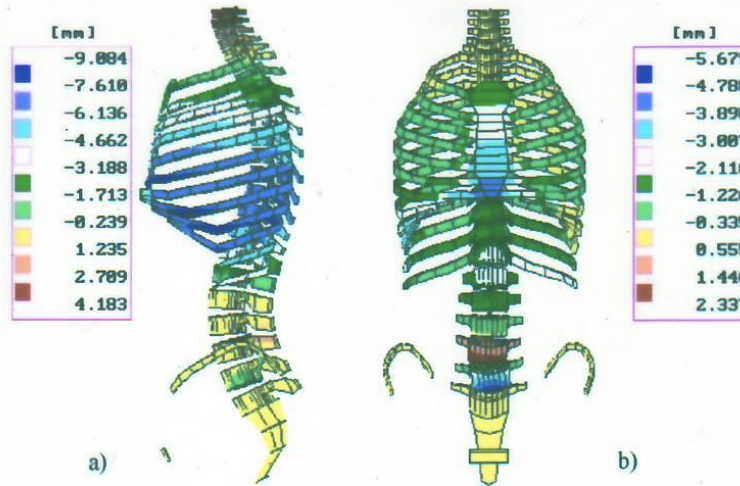
*(Non-linear analysis, energetic criterion, initial position of the body - straightened)*





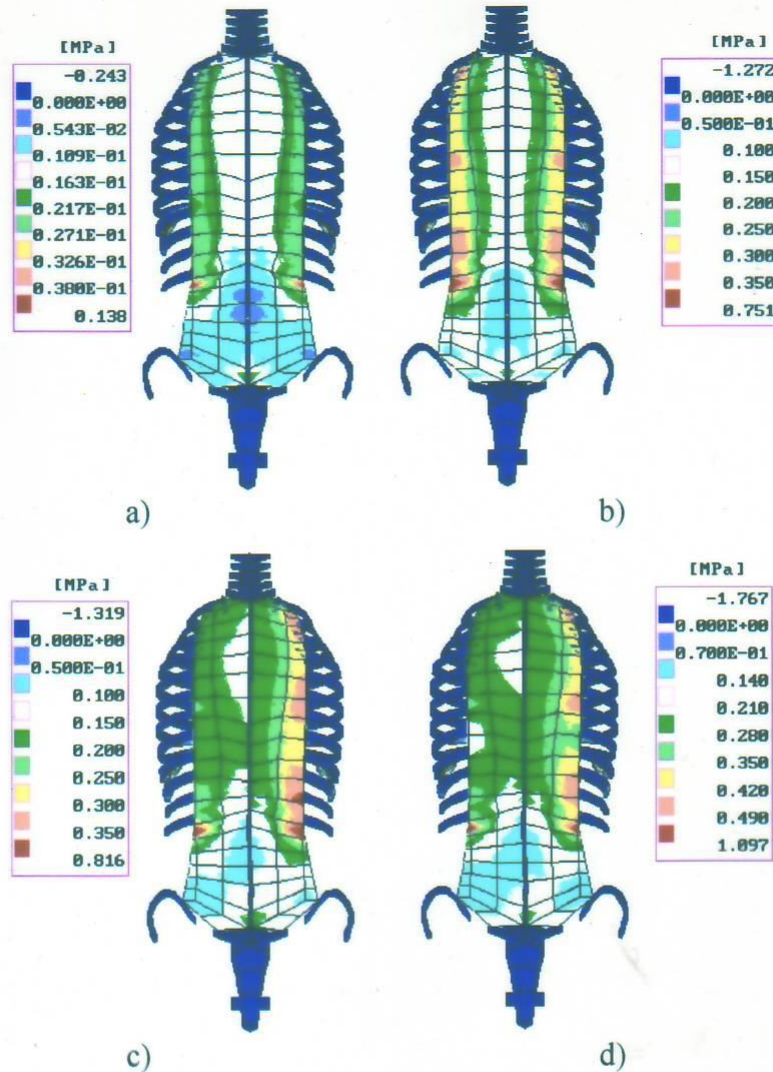
Spine equilibrium in the second, asymmetrical state of stability.  
 Displacements due to body weight 300N and external load  $2 \times 211.5\text{N} = 423\text{N}$   
 held in hands: a) in sagittal plane - side view, b) in frontal plane - front view,  
 c) in frontal plane - front view, d) in frontal plane - back view.

(Non-linear analysis, energetic criterion, initial position of the body -  
 straightened)



Spine equilibrium in the second, asymmetrical state of stability.  
 Displacements due to body weight 300N and external load  $2 \times 311.5\text{N} = 623\text{N}$   
 held in hands: a) in sagittal plane - side view, b) in frontal plane - front view,  
 c) in frontal plane - front view, d) in frontal plane - back view.

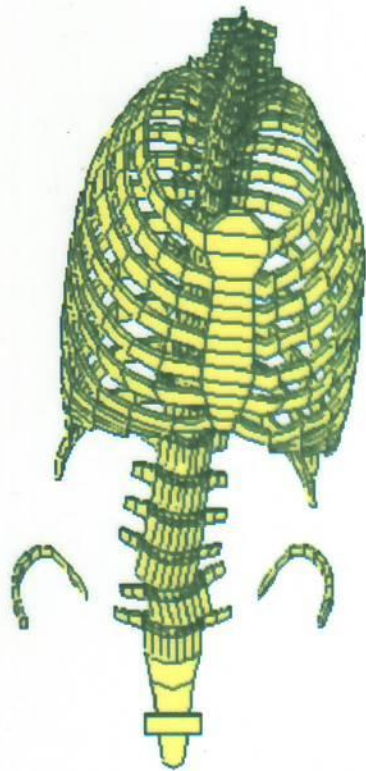
*(Non-linear analysis, energetic criterion, initial position of the body - straightened)*



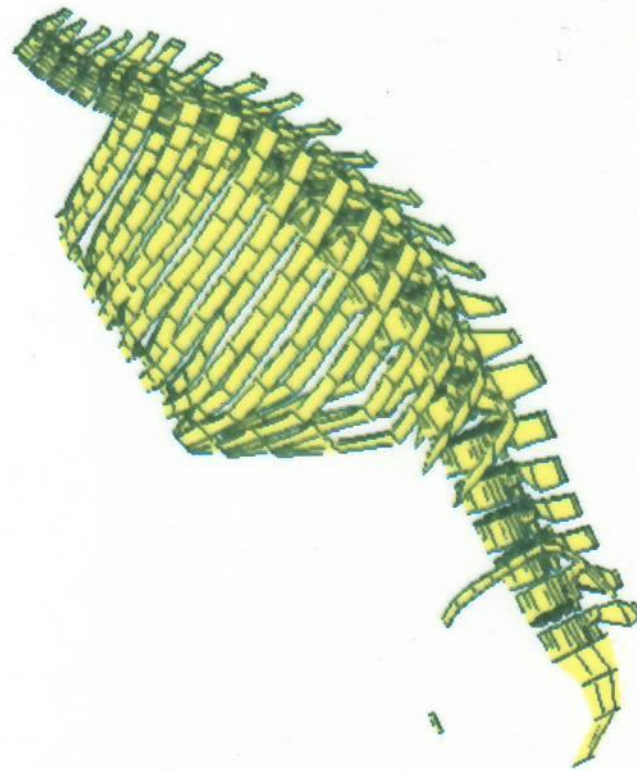
Tension distribution along muscle fibres in erector spinae, back view, due to:  
a) body weight 300N (symmetrical state of stability), b) body weight 300N and external load  $2 \times 191.5\text{N} = 383\text{N}$  held in hands (symmetrical state of stability),  
c) body weight 300N and external load  $2 \times 211.5\text{N} = 423\text{N}$  held in hands (asymmetrical state of stability) d) body weight 300N and external load  $2 \times 311.5\text{N} = 623\text{N}$  held in hands (asymmetrical state of stability).

*(Non-linear analysis, energetic criterion, initial position of the body - straightened)*





a)



b)

Form of deflection due to instability of the spine loaded with body weight 300N and external load  $2 \times 349\text{N} = 698\text{N}$  held in hands: a) front view, b) side view.

*(Non-linear analysis, energetic criterion, initial position of the body - straightened)*



# Wniosek

The cause of the idiopathic scoliosis may be the loss of stability of the spinal system due to incorrect operation of the muscular system. The operation is incorrect when some muscle groups are too weak in comparison with other groups. It may cause the loss of the first symmetrical form of stability at quite low external compressive load. The second asymmetrical state of stability can be fixed by remodelling of the bones, which leads to permanent deformation of the spine.

# BIOMECHANIKA KRĘGOSŁUPA

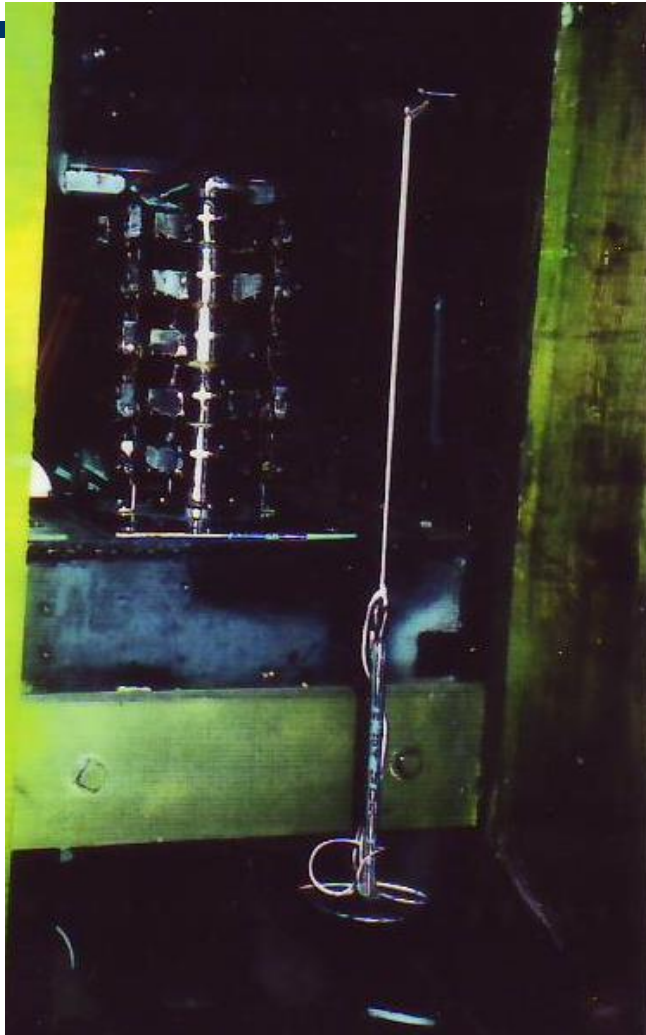
## Model materialny kręgosłupa lędźwiowego





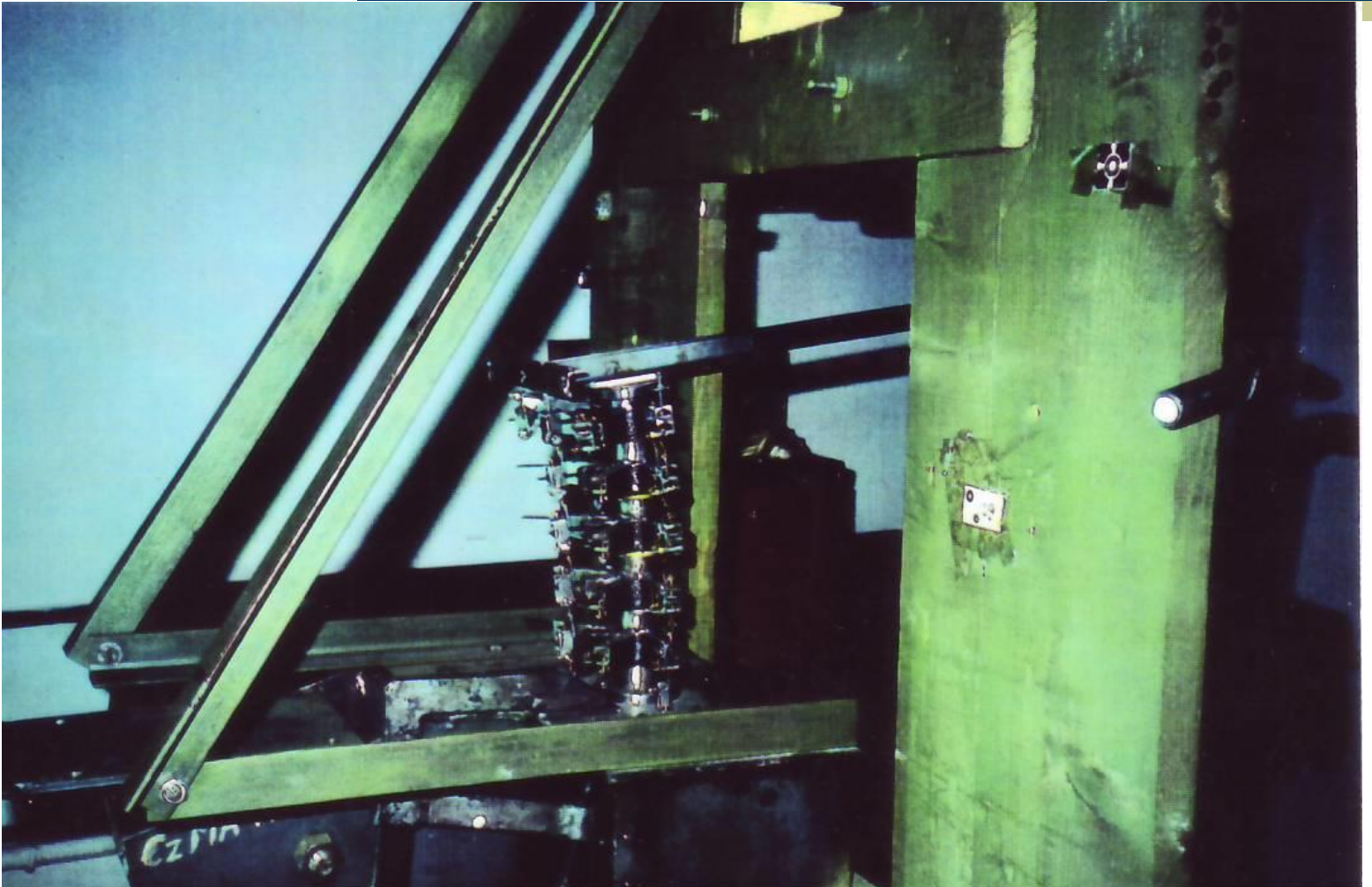


## Widok z przodu





## Widok z boku



# BIOMECHANIKA KRĘGOSŁUPA

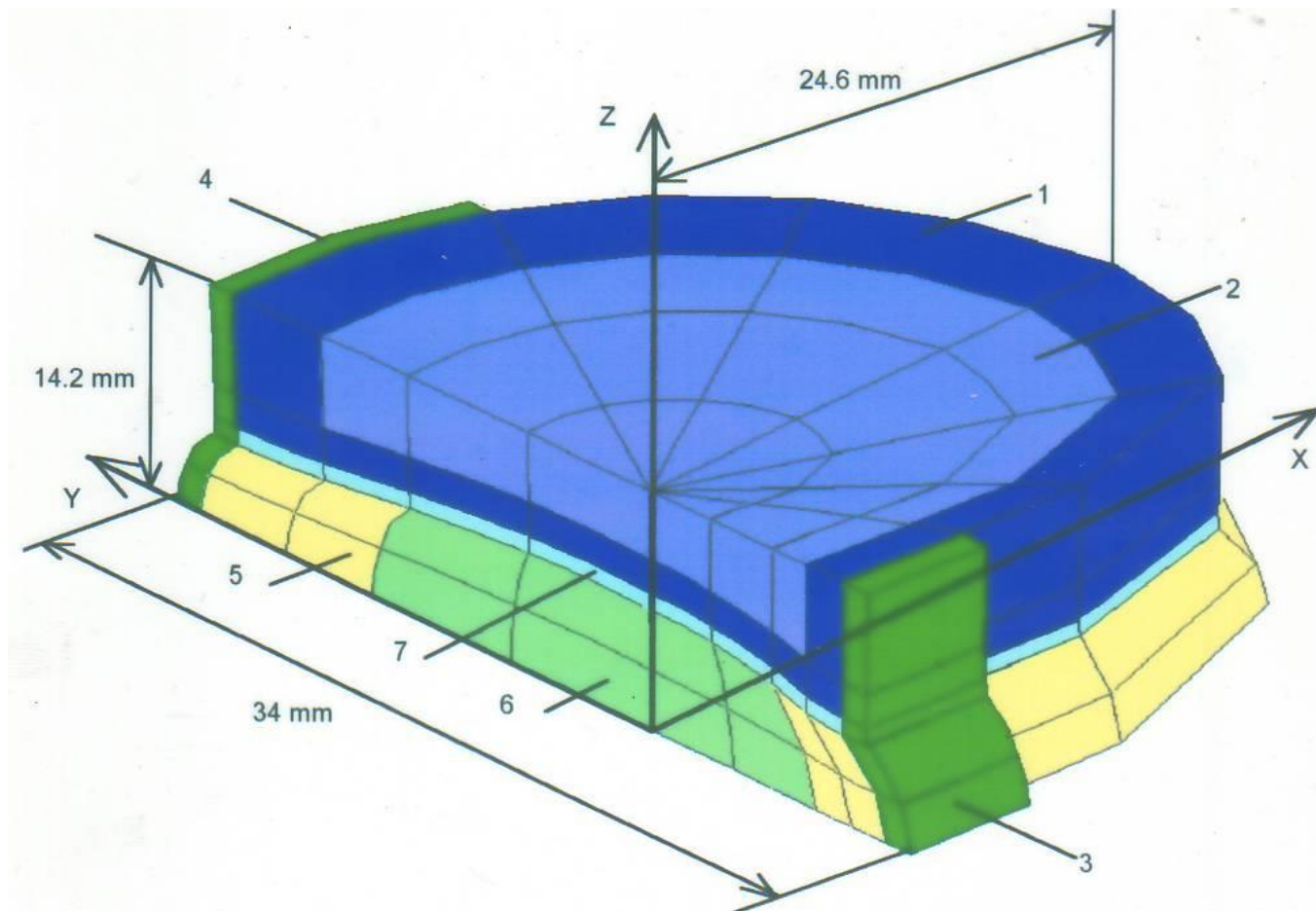
## Stateczność krążka międzykręgowego

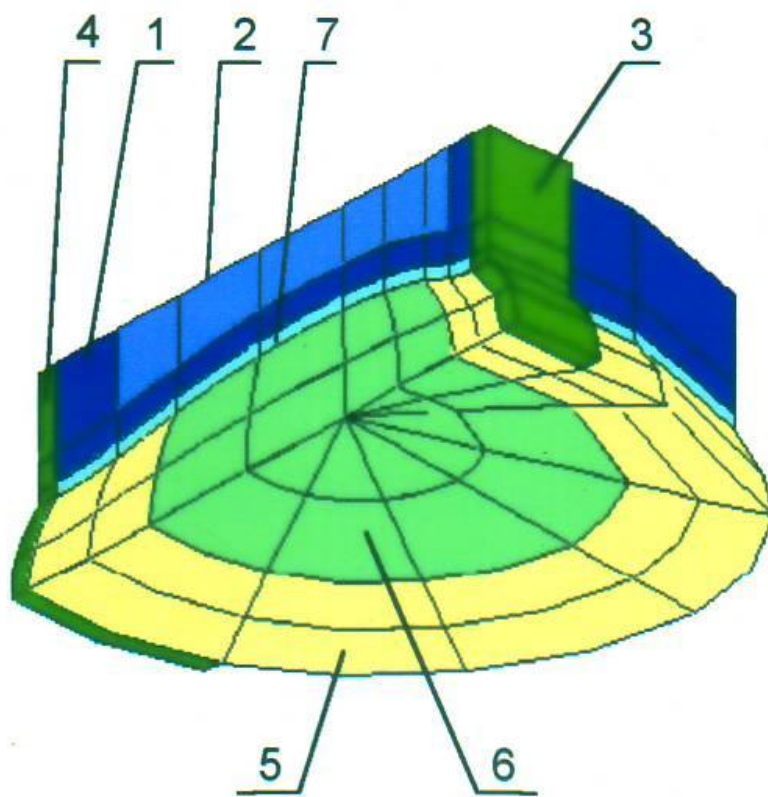




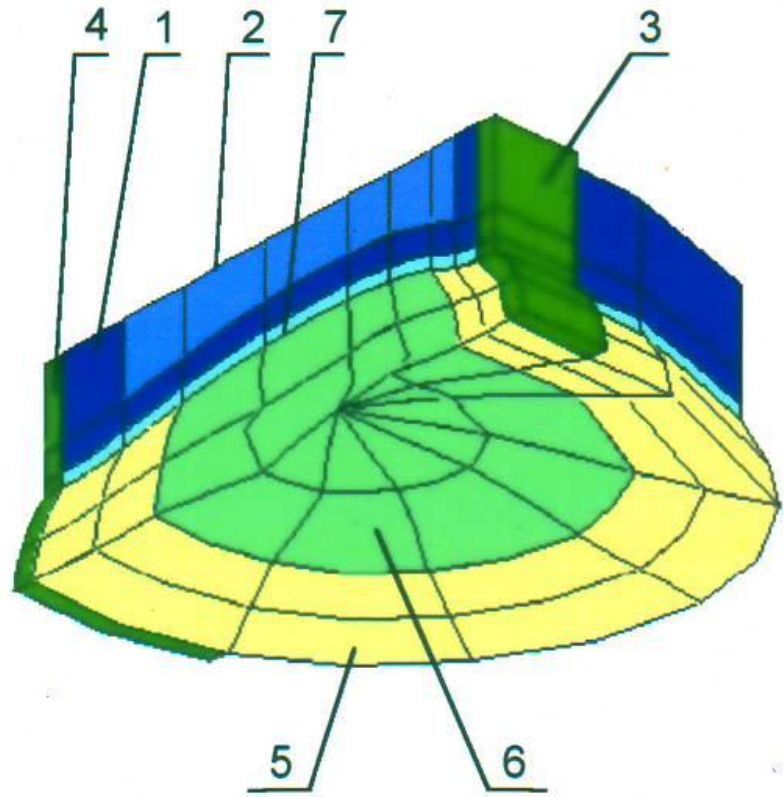


FEM mesh of truncated spine motion segment — one-fourth of a symmetric with respect to the horizontal and sagittal planes model: 1) cortical shell, 2) spongy core, 3) posterior and 4) anterior longitudinal ligaments, 5) annulus fibrosus, 6) nucleus pulposus, 7) endplate.





a)



b)

FEM mesh of the truncated spine motion segment - one fourth of a model symmetric in respect to the horizontal and sagittal planes: a) unloaded, b) first form of deformation due to instability under the compression load; 1) cortical shell, 2) spongy core, 3) posterior and 4) anterior longitudinal ligaments, 5) annulus fibrosus, 6) nucleus pulposus, 7) endplate.

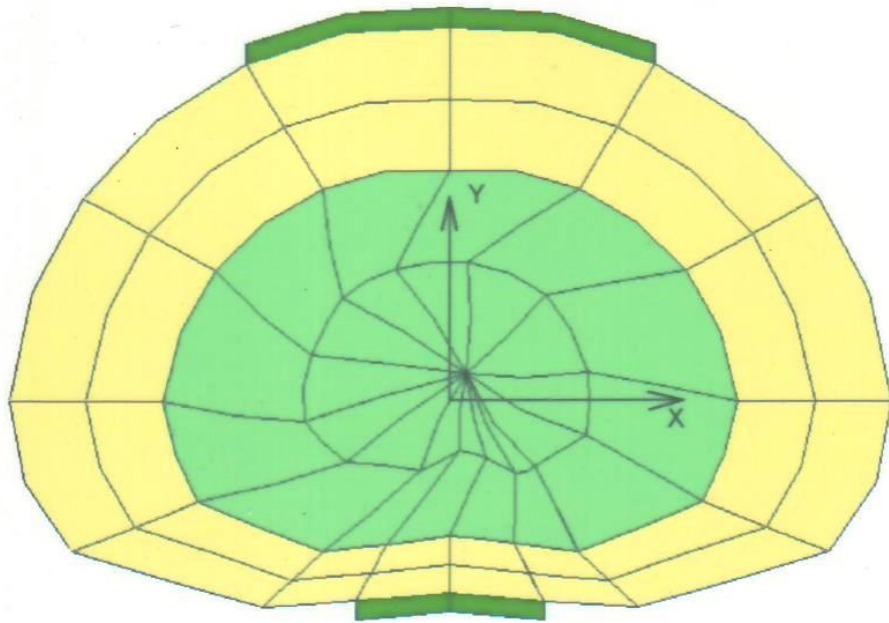
*(Non-linear analysis)*



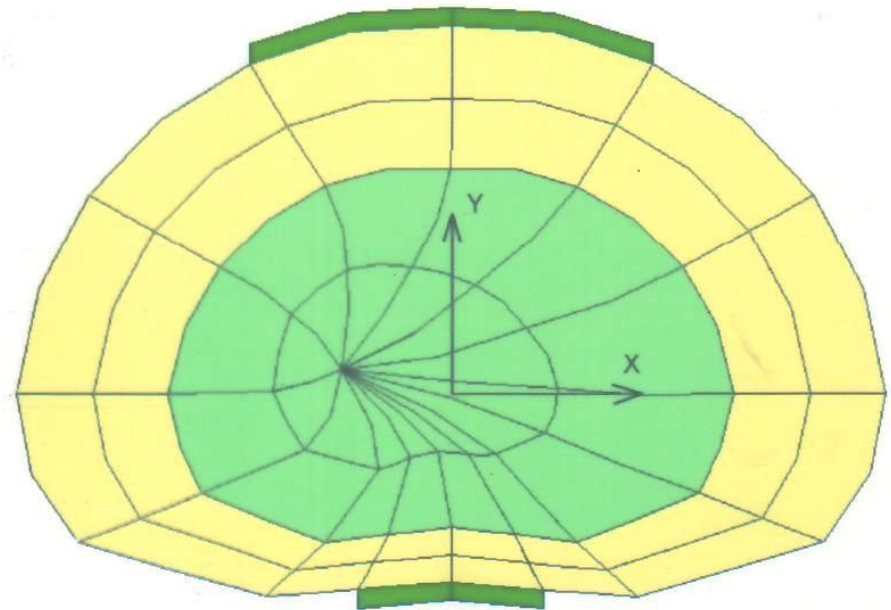
First (a) and second (b) forms of local stability; horizontal cross-sections in half-height of the disc.

*(Non-linear analysis)*

a)



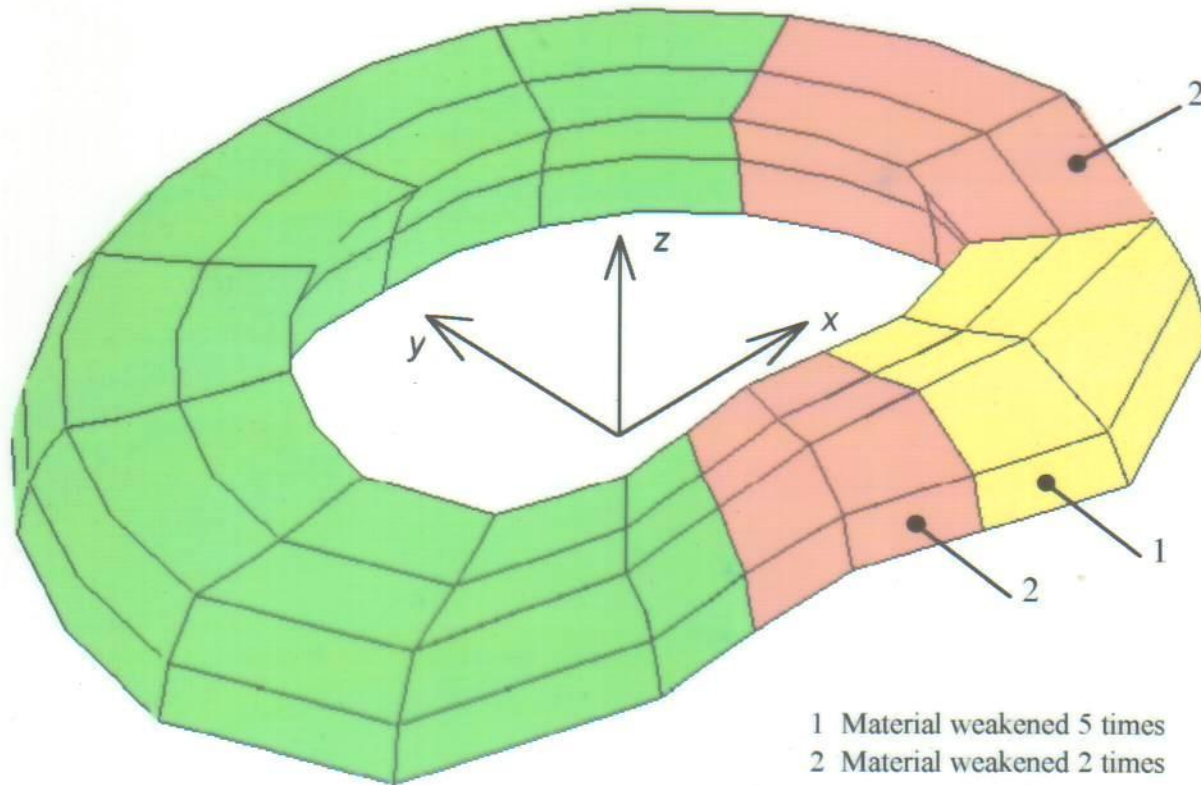
b)

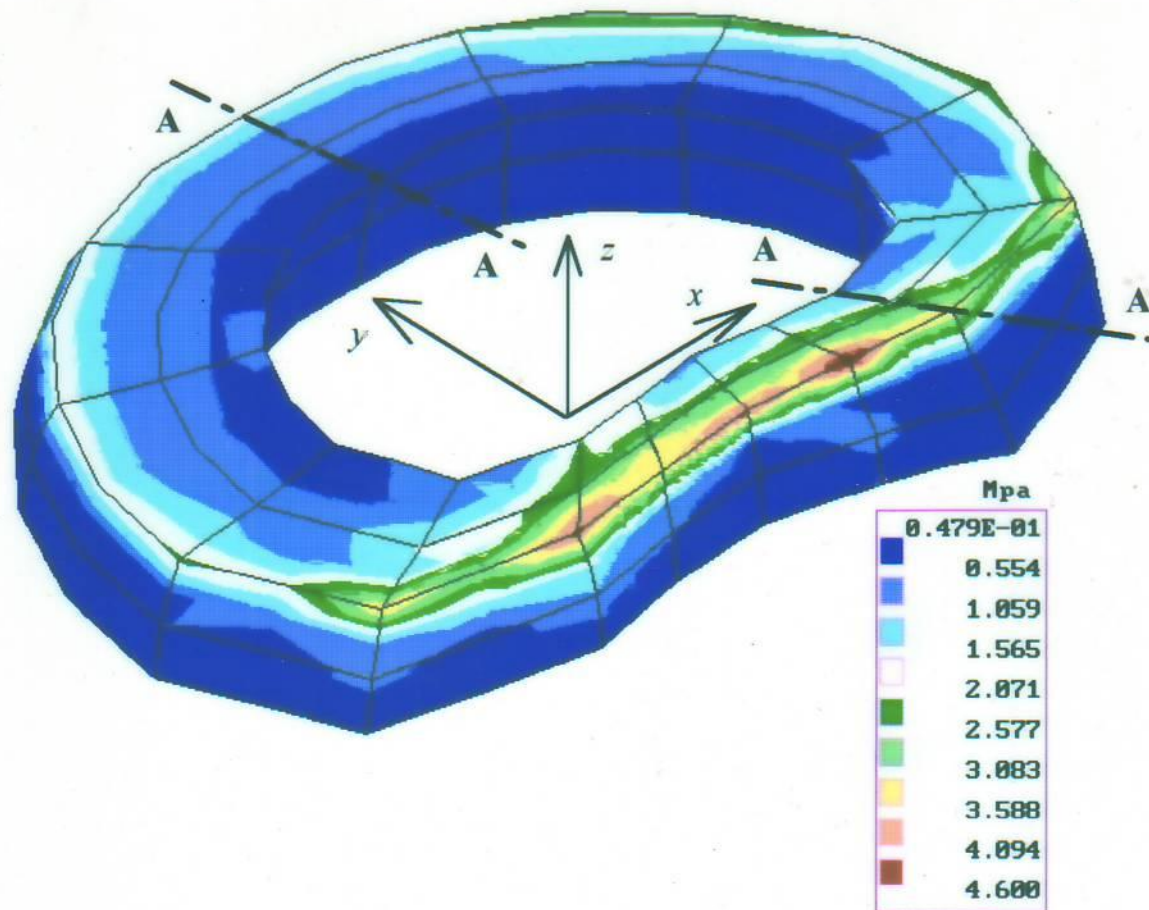




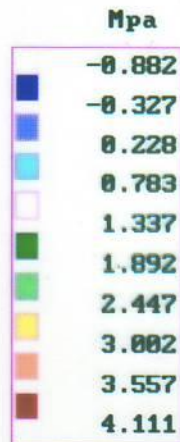
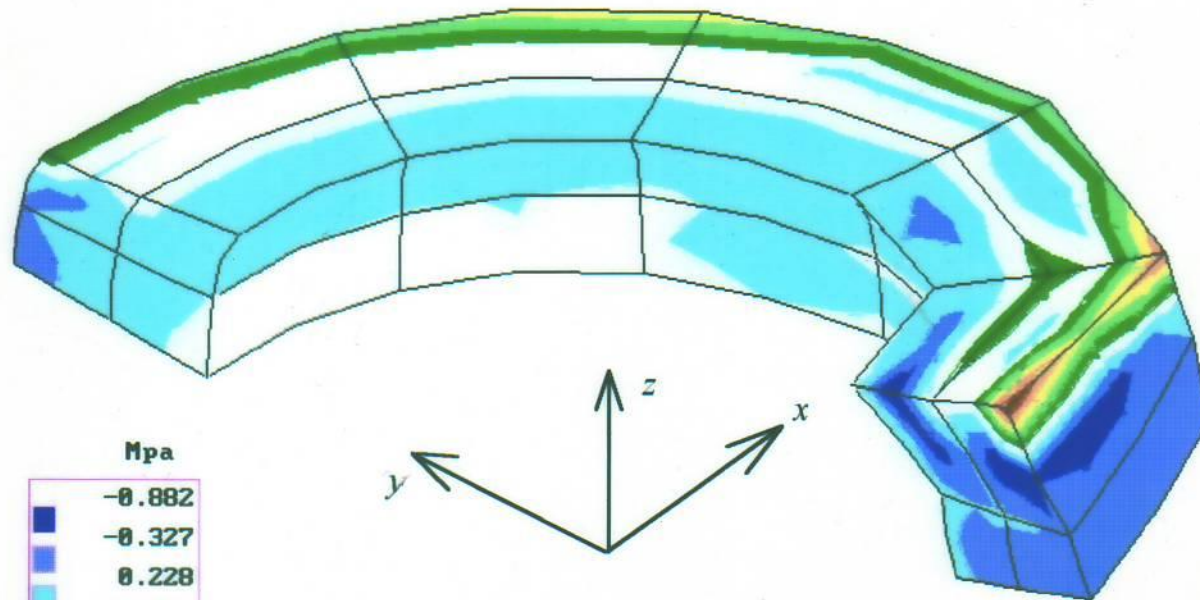


## Annulus fibrosus with hernia, with respect to the half-symmetric model in the horizontal plane



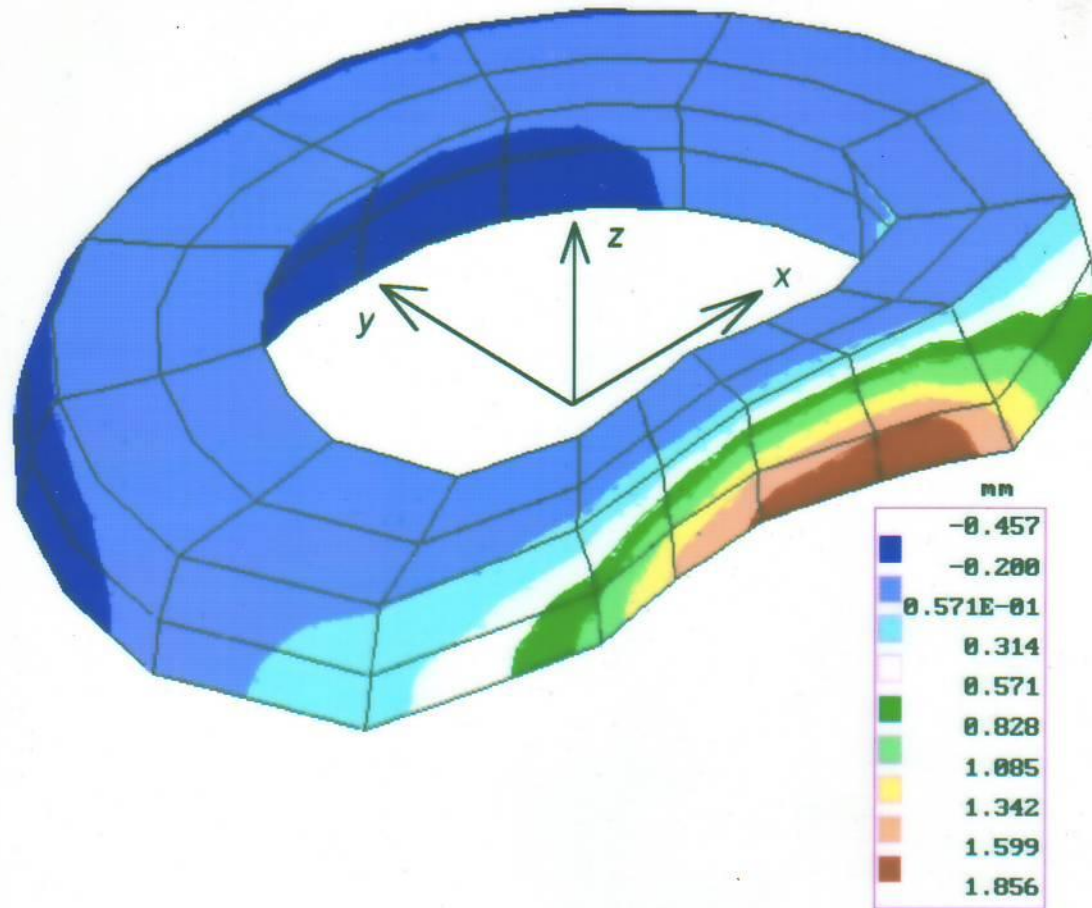


Isolines of reduced (according to the Huber-Mises hypothesis) stresses of the stretched disc with hernia, with respect to the half-symmetric model in the horizontal plane



Isolines of stresses in the  $z$  direction of the stretched disc with hernia: cross-section (marked AA in figure above) through the maximum bulge of hernia





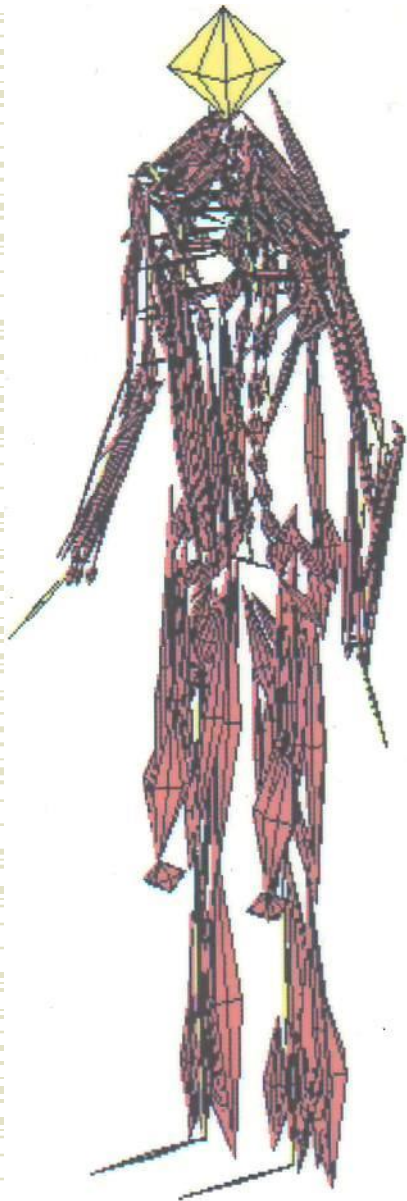
Isolines of dislocations of the stretched disc with hernia in the  $y$  direction, with respect to the half-symmetric model in the horizontal plane

# BIOMECHANIKA KRĘGOSŁUPA

## Model całego człowieka



# Model Człowieka



General view of the scheme of the human musculoskeletal system physical model.

Bones and muscle are marked on the scheme by means of two cones of common base. In the case of muscle the area of a cone base is proportional to the averaged physiological cross-section of a given muscle.

The elements of types spring - 6D, spring - 3D and beam - 3D, respectively, are not shown in the figure.





$$\mathbf{M}_0 \ddot{\mathbf{q}}_1 + \mathbf{C}_0 \dot{\mathbf{q}}_1 + \mathbf{R}_{E0} + \mathbf{K}_0 (\mathbf{q}_1 - \mathbf{q}_0) = \mathbf{P}_{E0} + \Delta \mathbf{P}_E + \mathbf{P}_{M0} + \Delta \mathbf{P}_M$$

$\mathbf{q}_1$  - vector  $\mathbf{q}$  of linear and angular generalised displacements of rigid bodies in local coordinate systems and generalised linear displacements of chosen points of the system, (e.g. markers) in global coordinate system at the instant  $t_1$ ,

$\mathbf{q}_0$  - vector  $\mathbf{q}$  of generalised displacements at the instant  $t_0$ ,

$\dot{\mathbf{q}}_1$  - vector  $\dot{\mathbf{q}}$  of generalised velocities at the instant  $t_1$ ,

$\ddot{\mathbf{q}}_1$  - vector  $\ddot{\mathbf{q}}$  of generalised accelerations at the instant  $t_1$ ,

$\mathbf{M}_0$  - mass matrix  $\mathbf{M}$  at the instant  $t_0$ ,

$\mathbf{C}_0$  - damping matrix  $\mathbf{C}$  at the instant  $t_0$ ,

$\mathbf{K}_0$  - tangent stiffness matrix at the instant  $t_0$ ,

$\mathbf{R}_{E0}$  - vector of internal generalised elastic forces (forces and moments)  $\mathbf{R}_E$  at the instant  $t_0$ ,

$\mathbf{P}_{E0}$  - vector of external generalised forces (forces and moments applied)  $\mathbf{P}_E$  at the instant  $t_0$ ,

$\Delta \mathbf{P}_E$  - increment of the vector  $\mathbf{P}_E$  in the time interval  $\Delta t = t_1 - t_0$ ,

$\mathbf{P}_{M0}$  - vector of generalised muscle forces  $\mathbf{P}_M$  at the instant  $t_0$ ,

$\Delta \mathbf{P}_M$  - increment (positive or negative) of the vector of generalised muscle forces in the time interval  $\Delta t$ .

# Widok z boku



$t = 0.00 \text{ s}$



$t = 0.25 \text{ s}$



$t = 0.50 \text{ s}$



$t = 0.75 \text{ s}$



$t = 1.00 \text{ s}$



$t = 1.25 \text{ s}$



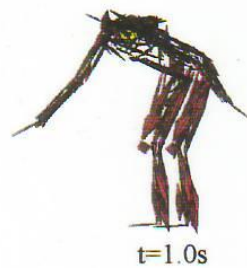
$t = 1.50 \text{ s}$



$t = 1.75 \text{ s}$



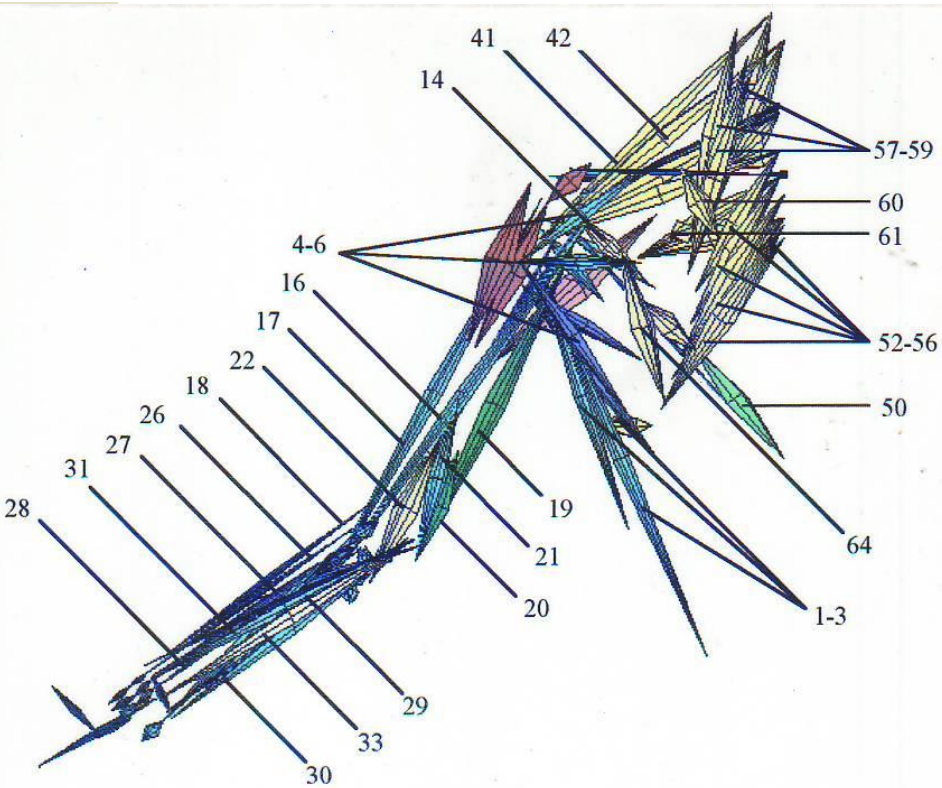
$t = 2.00 \text{ s}$







# Model kończyny górnej

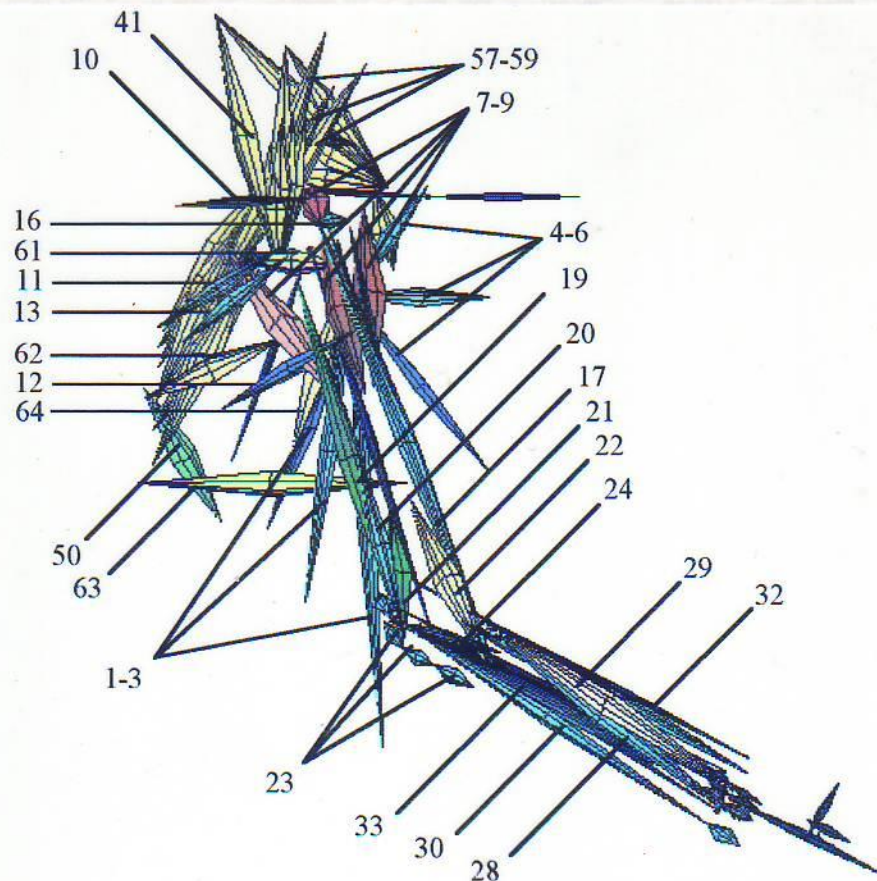


1. latissimus dorsi "1"
2. latissimus dorsi "2"
3. latissimus dorsi "3"
4. pectorialis major "1"
5. pectorialis major "2"
6. pectorialis major "3"
- \* 7. deltoideus "1"
- \* 8. deltoideus "2"
- \* 9. deltoideus "3"
- \* 10. supraspinatus
- \* 11. infraspinatus
- \* 12. teres major
- \* 13. teres minor
14. subskapularis
- \* 15. coracobrachialis
16. biceps brachi caput breve
17. biceps brachi caput longum
18. brachioradialis
19. triceps brachi caput longum
20. triceps brachi caput mediale
21. triceps brachi caput laterale
22. brachialis
- \* 23. anconeus
- \* 24. supinator
- \* 25. pronator teres
26. extensor carpi radialis longus
27. extensor carpi radialis brevis
28. extensor digitorum communis
29. extensor capri ulnaris
30. flexor capri ulnaris
- \* 31. flexor capri radialis
- \* 32. flexor pollicis longus

33. flexor digit sublimis
- \* 32. trapezius "1"
- \* 35. trapezius "2"
- \* 36. trapezius "3"
- \* 37. trapezius "4"
- \* 38. trapezius "5"
- \* 39. trapezius "6"
- \* 40. trapezius "7"
41. trapezius "8"
42. trapezius "9"
- \* 43. trapezius "10"
- \* 44. trapezius "11"
- \* 45. trapezius "12"
- \* 46. trapezius "13"
- \* 47. trapezius "14"
- \* 48. trapezius "15"
- \* 49. trapezius "16"
50. trapezius "17"
- \* 51. trapezius "18"
52. rhomboid "1"
53. rhomboid "2"
54. rhomboid "3"
55. rhomboid "4"
56. rhomboid "5"
57. levator scapulae "1"
58. levator scapulae "2"
59. levator scapulae "3"clavius
60. subclavius
61. serratus anterior "1"
- \* 62. serratus anterior "2"
- \* 63. serratus anterior "3"
64. pectorialis minor

\* ( not marked )

# Model kończyny górnej



- |                                      |                                  |
|--------------------------------------|----------------------------------|
| 1. latissimus dorsi "1"              | 33. flexor digit sublimis        |
| 2. latissimus dorsi "2"              | * 34. trapezius "1"              |
| 3. latissimus dorsi "3"              | * 35. trapezius "2"              |
| 4. pectorialis major "1"             | * 36. trapezius "3"              |
| 5. pectorialis major "2"             | * 37. trapezius "4"              |
| 6. pectorialis major "3"             | * 38. trapezius "5"              |
| * 7. deltoideus "1"                  | * 39. trapezius "6"              |
| * 8. deltoideus "2"                  | * 40. trapezius "7"              |
| * 9. deltoideus "3"                  | 41. trapezius "8"                |
| 10. supraspinatus                    | * 42. trapezius "9"              |
| 11. infraspinatus                    | * 43. trapezius "10"             |
| 12. teres major                      | * 44. trapezius "11"             |
| 13. teres minor                      | * 45. trapezius "12"             |
| * 14. subscapularis                  | * 46. trapezius "13"             |
| * 15. coracobrachialis               | * 47. trapezius "14"             |
| 16. biceps brachi caput breve        | * 48. trapezius "15"             |
| 17. biceps brachi caput longum       | * 49. trapezius "16"             |
| * 18. brachioradialis                | 50. trapezius "17"               |
| 19. triceps brachi caput longum      | * 51. trapezius "18"             |
| 20. triceps brachi caput mediale     | * 52. rhomboid "1"               |
| 21. triceps brachi caput laterale    | * 53. rhomboid "2"               |
| 22. brachialis                       | * 54. rhomboid "3"               |
| 23. anconeus                         | * 55. rhomboid "4"               |
| 24. supinator                        | * 56. rhomboid "5"               |
| * 25. pronator teres                 | 57. levator scapulae "1"         |
| * 26. extensor carpi radialis longus | 58. levator scapulae "2"         |
| * 27. extensor carpi radialis brevis | 59. levator scapulae "3" clavius |
| 28. extensor digitorum communis      | * 60. subclavius                 |
| 29. extensor capri ulnaris           | 61. serratus anterior "1"        |
| 30. flexor capri ulnaris             | 62. serratus anterior "2"        |
| * 31. flexor capri radialis          | 63. serratus anterior "3"        |
| 32. flexor pollicis longus           | 64. pectoralis minor             |

\*( not marked )